

# Ancillary Subunits Associated With Voltage-Dependent $K^+$ Channels

OLAF PONGS AND JÜRGEN R. SCHWARZ

*Institut für Neurale Signalverarbeitung, Zentrum für Molekulare Neurobiologie Hamburg,  
Universitätsklinikum Hamburg-Eppendorf, Universität Hamburg, Hamburg, Germany*

I. Introduction	756
II. $Kv\beta$ -Subunits	757
A. Structure of $Kv\beta$ -subunits	757
B. Structure of $Kv\alpha/Kv\beta$ channel complex	759
C. Interaction of $Kv\beta$ -subunits with cytoplasmic proteins	759
D. Functional in vitro studies	760
E. Influence of $K\beta$ -subunits on Kv channel surface expression	762
F. Function of $Kv\beta$ -subunits in vivo	762
III. KChIPs and DPPLs: Ancillary Subunits of $Kv4$ Channels	764
A. Structure of KChIPs	765
B. Function of KChIPs in vitro	766
C. Structure of DPPLs	768
D. Coexpression of KChIPs and DPPLs in vitro	770
E. Function of KChIPs in vivo (heart)	771
F. Function of KChIPs and DPPLs for native A-type currents in vivo (brain)	772
G. KChIP function unrelated to $K^+$ channel activity	774
IV. KCNEs (MinK and MiRPs)	774
A. Structural basis of KCNE-Kv7.1 interactions	774
B. Effects of KCNEs on Kv7.1 channels in vitro	775
C. Effects of KCNEs on HERG in vitro	778
D. Function of KCNEs in vivo	779
E. Effects of KCNEs on other Kv channels in vitro	781
V. Ancillary BK Channel Subunits	781
A. Structure of $BK\beta$ -subunits	782
B. Function of $BK\beta$ -subunits in vitro	783
C. $BK\beta1$ -subunits	783
D. $BK\beta2$ -subunits	783
E. $BK\beta3$ -subunits	784
F. $BK\beta4$ -subunits	785
G. Function of $BK\beta$ -subunits in vivo	785
VI. Concluding Remarks	787

**Pongs O, Schwarz JR.** Ancillary Subunits Associated With Voltage-Dependent  $K^+$  Channels. *Physiol Rev* 90: 755–796, 2010; doi:10.1152/physrev.00020.2009.—Since the first discovery of  $Kv\beta$ -subunits more than 15 years ago, many more ancillary Kv channel subunits were characterized, for example, KChIPs, KCNEs, and  $BK\beta$ -subunits. The ancillary subunits are often integral parts of native Kv channels, which, therefore, are mostly multiprotein complexes composed of voltage-sensing and pore-forming  $Kv\alpha$ -subunits and of ancillary or  $\beta$ -subunits. Apparently, Kv channels need the ancillary subunits to fulfill their many different cell physiological roles. This is reflected by the large structural diversity observed with ancillary subunit structures. They range from proteins with transmembrane segments and extracellular domains to purely cytoplasmic proteins. Ancillary subunits modulate Kv channel gating but can also have a great impact on channel assembly, on channel trafficking to and from the cellular surface, and on targeting Kv channels to different cellular compartments. The importance of the role of accessory subunits is further emphasized by the number of mutations that are associated in both humans and animals with diseases like hypertension, epilepsy, arrhythmogenesis, periodic paralysis, and hypothyroidism. Interestingly, several ancillary subunits have in vitro enzymatic activity; for example,  $Kv\beta$ -subunits are oxidoreductases, or modulate enzymatic activity, i.e., KChIP3 modulates presenilin activity. Thus different modes of  $\beta$ -subunit association and of functional

impact on Kv channels can be delineated, making it difficult to extract common principles underlying Kv $\alpha$ - and  $\beta$ -subunit interactions. We critically review present knowledge on the physiological role of ancillary Kv channel subunits and their effects on Kv channel properties.

## I. INTRODUCTION

Voltage-gated potassium (Kv) channels selectively catalyze the transport of K<sup>+</sup> across the plasma membrane. The channels are multisubunit complexes, being composed of membrane-integrated Kv $\alpha$ -subunits and of accessory subunits. Kv $\alpha$ -subunits form a tetrameric protein complex that assembles the core of a Kv channel consisting of a pore domain with activation (and inactivation) gate(s) and selectivity filter linked to peripheral voltage-sensor domains. In *in vitro* expression systems, most Kv $\alpha$ -subunits form functional Kv channels, reproducing basic Kv channel properties such as opening and closing (gating) of the pore in response to a change in the membrane electric field (60, 219, 283, 342). The activation process is well described by a sequential gating model, in which voltage-sensor movements in each Kv $\alpha$ -subunit are usually followed by a concerted pore opening step to permit passage of K<sup>+</sup>. The details of conformational changes associated with the electromechanical coupling-mechanism between voltage sensor and activation gate are presently under intense investigation (33, 153, 154, 282).

*In vivo*, Kv channels appear as heteromultimeric complexes coassembled with accessory subunits. Accessory subunits influence a wide range of Kv channel properties, which play important roles during Kv channel ontogeny and function, respectively. The importance of the role of accessory subunits is emphasized by the number of mutations that are associated in both humans and animals with diseases like hypertension, epilepsy, arrhythmogenesis, hypothyroidism, and periodic paralysis (1, 15, 37, 39, 240, 258). Notably, two of the early described excitability mutants were described in *Drosophila melanogaster*, with a leg shaking phenotype (105) resulting from mutation in a Kv $\alpha$ -subunit (*Shaker*; Refs. 122, 221, 262) and from mutation in a Kv $\beta$ -subunit (hyperkinetic; Ref. 52). What are the exact biological roles of the accessory subunits has been a matter of intense research. To determine cellular function(s), two major avenues were followed. The first one investigates modulatory influences of accessory subunits on various ion channel gating parameters including the aim to closely reproduce in heterologous expression systems electrophysiological and pharmacological Kv channel properties observed *in vivo*, e.g., in primary neurons in culture or in acute brain slices (11, 161). The second avenue studies potential roles of accessory subunits in Kv channel assembly and exit from the endoplasmic reticulum (ER), Kv channel trafficking to and from the plasma membrane, Kv channel sorting, and

regulation of Kv channel activity by posttranslational modifications (66). The results unveil common themes, although accessory subunits come in different flavors. One important theme is that the ancillary subunits link Kv channel activity both with extra- and intracellular signaling pathways and protein networks, respectively.

Accessory Kv channel subunits exhibit different protein structures reflecting their divergent biological roles. Some accessory subunits, e.g.,  $\beta$ -subunits of both BK (130, 203) and Kv7 (KCNQ) channels (23, 248), are integral membrane proteins with additional NH<sub>2</sub>- and/or COOH-terminal sequences extending into the extra- and/or intracellular space. Other accessory subunits are cytosolic proteins and bind to cytoplasmic domains of Kv channel  $\alpha$ -subunits, e.g., Kv $\beta$ -subunits of *Shaker* Kv channels (232) and KChIPs of Kv4 channels (13). To date, we are unaware of extracellular accessory  $\beta$ -subunits binding to Kv channels from an extracellular site. The first accessory Kv channel subunit cloned and functionally characterized was a Kv $\beta$ -(Kv $\beta$ 1.1) subunit (232, 265). Studies on the biological function of this subunit class have been very influential for our present understanding of heteromultimeric Kv channel complexes, yet results on the cellular function of Kv $\beta$ -subunits are inconclusive and major questions still remain unresolved. An important evolving concept is that auxiliary subunits have, in addition to their influence on Kv channel gating parameters, important roles in Kv channel sorting and trafficking to distinct cellular localizations.

Since the discovery of the auxiliary Kv $\beta$ -subunits, impressive progress has been made. Many more accessory subunits were discovered, and their properties were studied. Stable association between Kv $\alpha$  and accessory subunits made it possible to obtain crystal structures, for example, the auxiliary Kv $\beta$ -subunit in association with the entire Kv1.2 channel (153), and the ancillary subunit KChIP2 in association with a cytoplasmic Kv4 $\alpha$  tetramerization domain (215, 319). The structural models have many important implications for our understanding about mechanisms of interaction between Kv $\alpha$ -subunits and accessory subunits. For functional studies, mostly *in vitro* expression systems were used. They have been instrumental to analyze influences of accessory subunits on Kv channel gating. Observed influences are often quite remarkable, e.g., members of the Kv $\beta$ -subunit family confer rapid inactivation to delayed rectifier-type Kv channels, which otherwise do not inactivate (94–96, 232); the ancillary BK $\beta$ -subunits of BK channels dramatically increase Ca<sup>2+</sup> sensitivity of BK channel gating and also markedly affect their pharmacological properties (130, 247). How-

ever, transient heterologous expression systems are potentially controversial and prone to artifacts. Not surprisingly, *in vitro* studies have frequently yielded conflicting results on possible cellular functions of accessory subunits. This seems particularly true for studies on specificity and stoichiometry of subunit assembly and its impact on Kv channel trafficking.

Despite the critical importance for understanding biological functions of Kv $\beta$  as well as other accessory subunits for human physiology, detailed structure-function studies on the role of Kv $\beta$ -subunits in genetically modified mice are relatively scarce. Furthermore, a clear-cut structure-function relationship between mutated accessory subunit gene and mutant phenotype is difficult to reach in correlating genotype and phenotype of mutant mice. Thus we have so far limited insights into disease mechanisms and the underlying pathophysiology of mutations in ancillary subunit genes. More studies of this kind will certainly be helpful to sharpen our understanding of the biophysical and cellular basis of disease correlated with mutations in accessory Kv channel subunit genes.

## II. Kv $\beta$ -Subunits

### A. Structure of Kv $\beta$ -Subunits

In the early days of biochemical and molecular biological research on ion channels, Kv channels from bovine brain were successfully purified based on their property to bind the mamba snake venom polypeptide  $\alpha$ -dendrotoxin ( $\alpha$ -DTX) with high affinity (206, 230). The purified preparation consisted of glycosylated Kv $\alpha$ -subunits (~70–80 kDa in size) and Kv $\beta$ -subunits (~40 kDa in size) (264, 265). Biochemical analysis of the purified  $\alpha$ -DTX receptor (Kv channel) had the important implication that Kv $\alpha$ - and Kv $\beta$ -subunits are tightly associated with each other in a heteromultimeric complex. This is highlighted by the resilience of the heteromultimeric complex against high-salt treatment. Sedimentation analyses, using the buoyant density method, yielded a size of ~400 kDa and a Stokes' radius of 8.6 nm for the purified Kv channel preparation (207). The data indicated that native  $\alpha$ -DTX-sensitive Kv channels are isolated as tightly associated octameric structures in a stoichiometry of four  $\alpha$ - and four  $\beta$ -subunits. Sequencing of NH<sub>2</sub>-terminal Kv $\alpha$  peptide showed that the major Kv $\alpha$ -subunit in the Kv channel preparation was Kv1.2 (318). Determination of proteolytic Kv $\beta$  polypeptides yielded partial sequences of Kv $\beta$ 1 and Kv $\beta$ 2 protein (232, 265). The important information from this study was that Kv1.2/Kv $\beta$ 1, Kv $\beta$ 2 seems a predominant Kv1 $\alpha$ /Kv $\beta$ -subunit combination for bovine brain Kv1 channels.

The Kv $\beta$  sequence information served to clone the mammalian Kv $\beta$ -subunit family (220, 222). In the mammalian genome, three genes encode Kv $\beta$ -subunits: Kv $\beta$ 1,

Kv $\beta$ 2, and Kv $\beta$ 3 (Fig. 1) (96, 142, 222, 259). The Kv $\beta$ 1 gene gives rise to splice variants resulting in Kv $\beta$ 1 proteins with different NH<sub>2</sub>-terminal sequences (70–90 amino acids; Kv $\beta$ 1.1–1.3). Protein sequence alignment of Kv $\beta$  family members showed that Kv $\beta$  proteins generally display variant NH<sub>2</sub>-terminal sequences which are followed by a highly conserved protein core sequence (~330 amino acids) with more than 80% sequence identity. Inspection of Kv $\beta$  protein sequences revealed two important properties. First, Kv $\beta$ -subunits are members of an extended protein superfamily, the oxidoreductases (88, 172). Second, certain NH<sub>2</sub>-termini, e.g., of Kv $\beta$ , display a sequence that potentially confers rapid inactivation to otherwise noninactivating Kv channels (220, 232). The first property concurred with the observation that purified Kv $\beta$ -subunits bind with low micromolar affinity oxidoreductase cofactors, for example, NADPH and NADP<sup>+</sup> (Fig. 2A). Importantly, analysis of the Kv $\beta$ 2 crystal structure nicely confirmed the potential relationship of Kv $\beta$  protein to oxidoreductase enzymes (Fig. 2, B–D; Ref. 88). The second property implies that Kv $\beta$ -subunits can influence Kv channel gating properties, conferring rapid inactivation to otherwise noninactivating Kv channels. Electrophysiological investigations with Kv1.1 and Kv $\beta$ 1.1-subunits coexpressed in *Xenopus* oocytes confirmed that the NH<sub>2</sub> terminus of Kv $\beta$ 1.1 behaves like an inactivating domain that rapidly occludes the pore of activated Kv channels of the Kv1 family (Fig. 4A).

The structure of the conserved Kv $\beta$  core sequence was determined by X-ray crystallography of a truncated mammalian Kv $\beta$ 2 protein both alone and in complex with Kv1.2  $\alpha$ -subunits (69, 88, 153). Four  $\alpha$ -subunits assemble

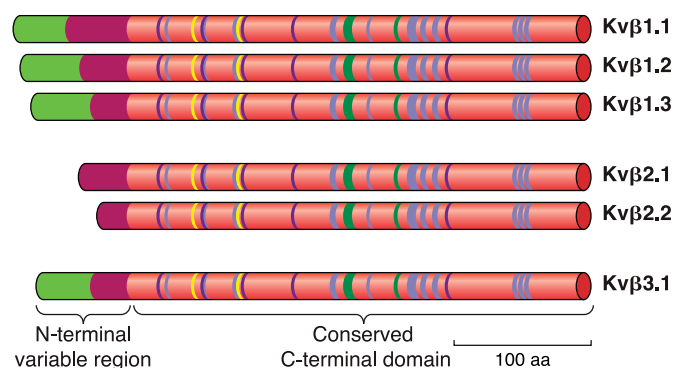


FIG. 1. Bar diagram of conserved domains in Kv $\beta$  protein family. The human KCNAB1 gene expresses Kv $\beta$ 1 proteins [Genbank (NCBI)]: NP\_751892 (Kv $\beta$ 1.1), NP\_003462 (Kv $\beta$ 1.2), NP\_751891 (Kv $\beta$ 1.3). The human KCNAB2 gene expresses Kv $\beta$ 2 proteins [Genbank (NCBI)]: NP\_003627 (Kv $\beta$ 2.1), NP\_742128 (Kv $\beta$ 2.2). The human KCNAB3 gene expresses Kv $\beta$ 3 protein [Genbank (NCBI)]: NP\_004723 (Kv $\beta$ 3.1). NH<sub>2</sub>-terminal variable region contains N-type inactivation domain (light green). Conserved COOH-terminal domain contains interface for assembly with tetramerization domain T1 of Kv $\alpha$ -subunit (boxed in dark green) and oxidoreductase active site. Catalytic residues are marked in yellow, substrate binding domains in violet, and cofactor binding domains in blue. [Modified from Bähring et al. (19).]

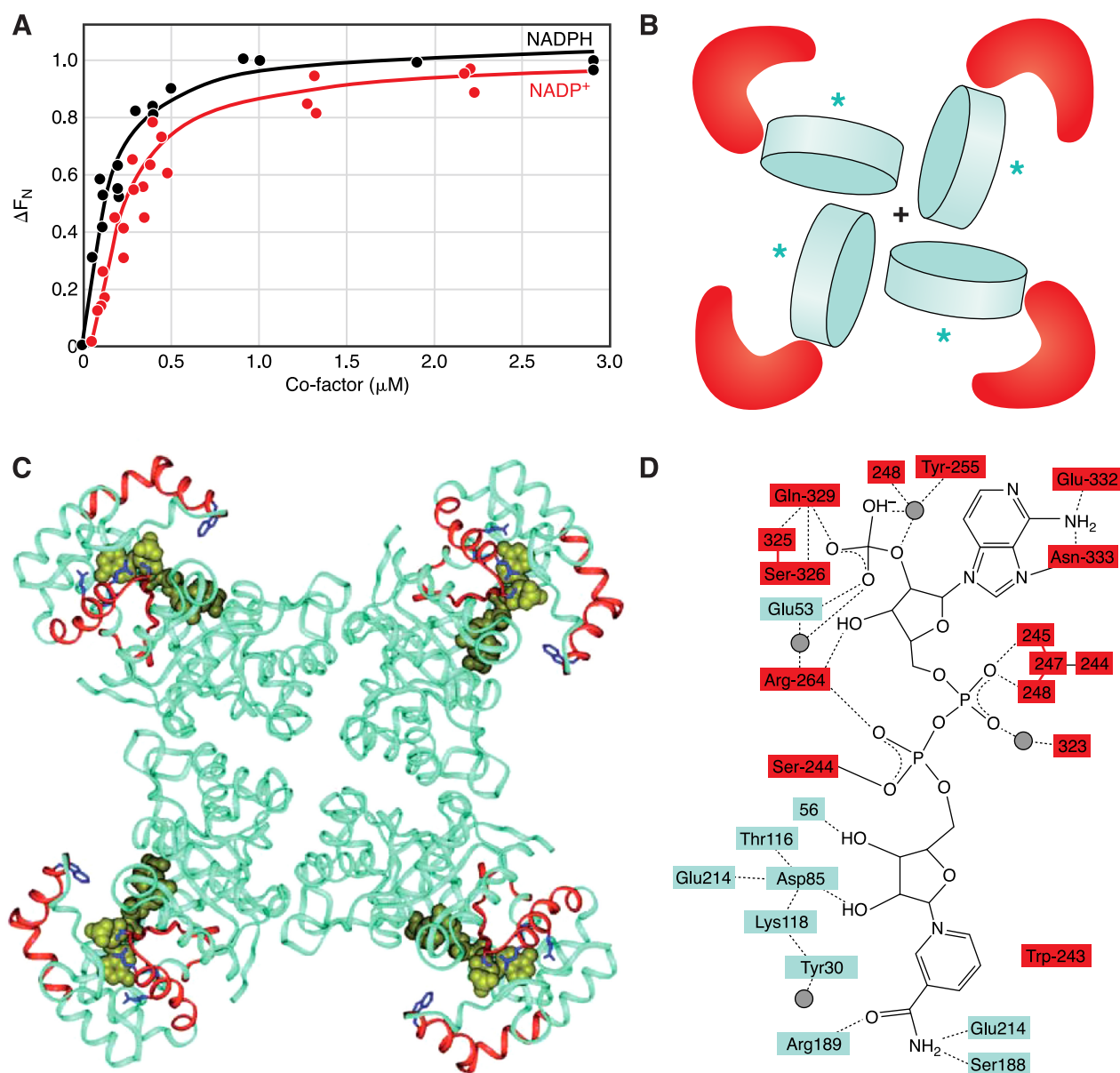


FIG. 2. Oxidoreductase properties of Kv $\beta$ -subunit. **A**: binding of NADPH and NADP<sup>+</sup> cofactor to Kv $\beta$ 2. Normalized decrease in Kv $\beta$ 2 fluorescence is plotted against cofactor concentration (I. Olmert and O. Pongs, unpublished results; see also Ref. 326). **B**: schematic structural organization of Kv $\beta$ 2 tetramer is shown (TIM barrel in light blue,  $\alpha$ -helical subdomain in red) with position of oxidoreductase active sites indicated by light blue asterisks. [Modified from Gulbis et al. (88).] **C**: ribbon representation of Kv $\beta$ 2 tetramer. Kv $\beta$  domains I and II (colored in red) provide amino acid residues to the Kv $\beta$  oxidoreductase active site and rescue inactivation failure of Kv $\beta$ 3.1. The NADPH cofactor bound to each Kv $\beta$ -subunit (green) is shown as a Corey-Pauling-Koltun model. Side chains are in stick representation and are magenta. [From Bähring et al. (19).] **D**: detailed illustration of selected interactions between cofactor and Kv $\beta$  amino acid residues. Residues of the Kv $\beta$ 2 TIM barrel surrounding NADP<sup>+</sup> are blue and those of Kv $\beta$ 2  $\alpha$ -helical subdomain are red. Contacts made solely with main chain atoms of the protein are denoted by amino acid numbering only, whereas those made with side chains are given full residue nomenclature. Water molecules are shown as gray circles. [Modified from Gulbis et al. (88).]

to form a functional K channel (Fig. 3A). The cytoplasmic T1 domains of each NH<sub>2</sub> terminus of the  $\alpha$ -subunits interact with each other, thereby generating an intracellular structure composed of four columns and a central platform called “hanging gondola” (277). The structural model revealed a tetrameric Kv $\beta$ -subunit assembly with a four-

fold symmetry matching the one seen in the structure of tetrameric K<sup>+</sup> channel  $\alpha$ -subunits (Fig. 2C). Each subunit disposes of a TIM barrel fold with typical  $\alpha_8\beta_8$  arrangement of  $\alpha$ -helices and  $\beta$ -strands. Oxidoreductases have a comparable TIM barrel fold with the active site located at the COOH-terminal edge of the  $\beta$ -strands. The Kv $\beta$ 2 TIM-



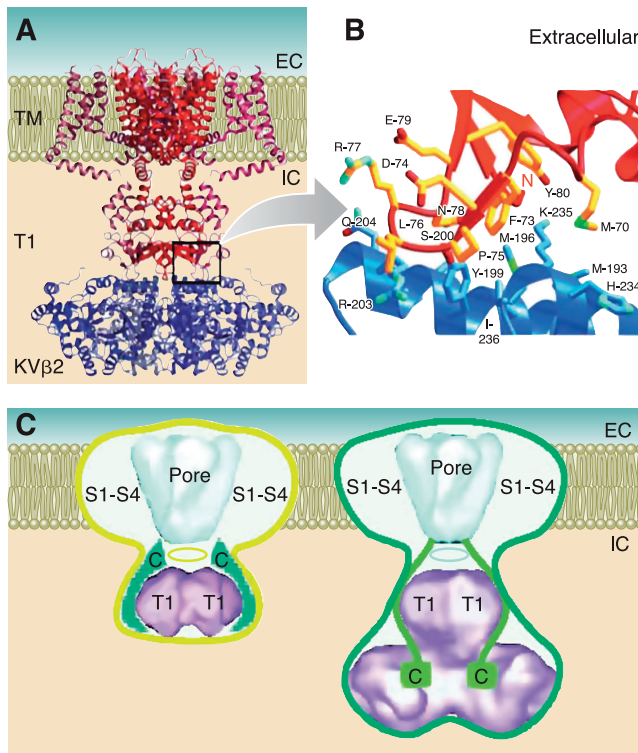


FIG. 3. Structural basis of Kv1.2-Kv $\beta$ 2 interaction. *A*: ribbon representation of the Kv1.2-Kv $\beta$ 2 subunit complex, viewed from the side. Each of the four Kv1.2 subunits is shown in a different color and consists of the transmembrane component TM and the tetramerization domain T1. Each of the four Kv $\beta$ 2-subunits is colored like the Kv1.2 subunit with which it interacts. The NADP<sup>+</sup> cofactor bound to each  $\beta$ -subunit is drawn as black sticks. [From Long et al. (153). Reprinted with permission from AAAS.] *B*: molecular details of the interface between Kv1.2 T1 domain (red) and  $\beta$ -subunit (blue). [From Gulbis et al. (89). Reprinted with permission from AAAS.] *C*: schematic drawing of the proposed conformational rearrangements of the *Shaker* COOH terminus on binding of Kv $\beta$ . *Left cartoon*: wild-type *Shaker* structure (yellow outline) with the KcsA structure (pore) [adapted from Doyle et al. (69)] and T1 domain (purple) [adapted from Kreusch et al. (133)]. The COOH termini occupy the space on the sides of the T1 domains. *Right cartoon*: wild-type *Shaker* Kv $\alpha$ -Kv $\beta$  complex (green outline) with low-resolution structures of KCsA in blue and T1 complex after binding of Kv $\beta$ 2 to T1 of Kv1.2 (purple). [Modified from Sokolova et al. (276).]

barrels are arranged in the tetramer end to side so that the back face of a barrel is wedged against the side of an adjacent barrel (Fig. 2*B*). This arrangement places the putative active Kv $\beta$  sites away from the fourfold axis. Each active Kv $\beta$ -site is composed of a substrate binding site, a NADP<sup>+</sup> (NADPH) cofactor binding pocket (Fig. 2*D*), and catalytic residues for hydride transfer reminiscent of those observed for bona-fide oxidoreductases. It, however, is still unclear whether Kv $\beta$ -subunits act *in vivo* as genuine oxidoreductase enzymes.

## B. Structure of Kv $\alpha$ /Kv $\beta$ Channel Complex

Recently, rat Kv $\alpha$ -subunit Kv1.2 and Kv $\beta$ -subunit Kv $\beta$ 2 were coexpressed in the yeast expression system

*Pichia pastoris*, purified, and crystallized (153). Throughout purification and crystallization procedures, it was necessary to have reducing and oxygen-free solutions, which may indicate an exquisite sensitivity of the Kv channel complex towards oxidation. This went unnoticed during the purification of native bovine Kv $\alpha$ /Kv $\beta$  channel complexes (207, 265, 271). The crystal structure (Fig. 3*A*) impressively confirmed the stoichiometry of the complex and allows unprecedented insight into Kv $\beta$  structure and its interaction with Kv $\alpha$ -subunits. The interaction site is formed by a contact loop between each Kv $\alpha$ - and Kv $\beta$ -subunit, which provides the docking surface engaging only a few amino acids of the Kv $\alpha$  tetramerization domain and the complementary Kv $\beta$  surface (Fig. 3*B*). The amino acid sequence of the contact loop is highly conserved among members of the Kv1 $\alpha$ -subunit family, providing a molecular explanation for the specificity of Kv1 $\alpha$ - and Kv $\beta$ -subunit interactions (89). Complex formation between Kv1 $\alpha$ - and Kv $\beta$ -subunits is only associated with a small tilt of the tetramerization domain in the NH<sub>2</sub> terminus of the Kv1 $\alpha$ -subunit with respect to the central four-fold axis of the channel (154). The important implication of this observation is that both Kv1 $\alpha$ - and Kv $\beta$ -subunits seem to associate with each other as preformed tetramers. Note the available crystal structures are uninformative about the distal NH<sub>2</sub> and the COOH terminus of the Kv channel. A structural study based on electron microscopic images indicated a conformational change at the Kv $\alpha$  COOH terminus upon Kv $\beta$ 2 subunit binding, during which a large part of the COOH terminus is shifted away from the Kv $\alpha$ -subunit membrane domain and into close contact with the  $\beta$ -subunit (Fig. 3*C*; Ref. 276).

## C. Interaction of Kv $\beta$ -Subunits With Cytoplasmic Proteins

The interaction of Kv1 channels with Kv $\beta$ -subunits extends the membrane-inserted pore domain and voltage sensor of the channel by  $\sim 100$  Å deep into the cytoplasm (Fig. 3*A*). Thus the Kv $\beta$ -subunit may provide a large surface for interaction with other proteins, e.g., protein kinases, protein phosphatases, and other signaling complexes, and also provides a potentially important link to the cytoskeleton. Two types of fishing approaches have been used to characterize potential binding partners of Kv $\beta$ -subunits. In the first approach, a yeast two-hybrid library made from rat hippocampal cDNA was screened (83). In the second approach, Kv1.1 channel complexes were isolated by immunoaffinity purification from plasma membrane-enriched protein fractions of rat brain (258). The yeast two-hybrid approach showed that ZIP1 and ZIP2 protein can bind to Kv $\beta$ 2 and to protein kinase C (PKC)- $\zeta$ , thereby acting as physical link in the assembly of

PKC- $\zeta$  with Kv1 channels. Whether this interaction also occurs in vivo and plays a role in fine tuning Kv1 channel activity remains to be shown. In the second approach, mass spectrometry (MS)-purified Kv1.1 channel protein complexes revealed in addition to the expected Kv1 $\alpha$ - and Kv $\beta$ -subunits a remarkable number of other proteins. Some of the proteins were members of the PSD95 (128) and neuroligin (218) families known to be involved in Kv1 channel clustering at the neuronal membrane. Other proteins seem to operate in the synaptic active zone or have no clear function. The MS/MS analysis of the purified Kv channel multiprotein complex suggests a multitude of possible Kv channel interacting proteins (258). Their interactions may be of permanent or transient nature. It is unclear whether axonal, presynaptic, or postsynaptic Kv channels have different protein compositions. This is an attractive hypothesis for explaining differential targeting and functions of the channel complexes.

Interestingly, Lgil has been copurified with Kv1.1 protein (258). In heterologous expression systems, Lgil interferes with Kv $\beta$ 1-conferred inactivation of Kv1 channels. This activity was not seen with Lgil mutants. The data suggest that Lgil can modulate gating properties of Kv1 channels. The molecular basis of the Lgil effect on Kv1 channel inactivation is presently unknown. Mutations in the Lgil gene are causatively associated with one form of epilepsy, the autosomal dominant lateral temporal lobe epilepsy (258). However, expression profiles of Kv1.1 and Lgil protein in adult rat brain are distinct and only partially overlapping, leaving room for alternative explanations to the cause of this type of epilepsy. The pathophysiological relevance of coassembly between mutant Lgil and Kv1.1 channels remains to be determined.

## D. Functional In Vitro Studies

The relative ease to assay Kv channel inactivation in vitro gave rise to a plethora of data reporting modulation of Kv1 channel inactivation properties (Table 1). Electrophysiological investigations with Kv1 $\alpha$ - and Kv $\beta$ 1.1-subunits coexpressed in *Xenopus* oocytes showed that the NH<sub>2</sub> terminus of Kv $\beta$ 1.1 behaves like an inactivating domain that rapidly occludes the open pore of Kv1.x channels (Table 1; Fig. 4A; Refs. 19, 95, 96, 232). A detailed analysis of the structural and functional interactions between Kv $\beta$ 1.2 and Kv1.2 provides a coherent picture of how Kv $\beta$ 1.2 in vitro modulates gating properties of the Kv1.2 channel. At depolarized potentials, the extent of open channel block by the Kv $\beta$ 1.2 inactivating domain (5, 6, 73, 329) progressively increases hindering the activation gate within the channel's conduction pathway to close. Thus Kv $\beta$ 1.2 directly slows deactivation and indirectly enhances slow inactivation as well as shifts Kv1.2 channel activation to more negative voltages (211).

Some published data, however, are equivocal, and it is not clear whether reported gating modulations are due to indirect or direct effects. Since the membrane provides a special environment for membrane proteins like ion channels to carry out their functions, changes in lipidic environment can have profound influences on Kv channel gating properties (255). For example, phosphoinositides remove N-type inactivation from A-type channels by immobilizing the inactivating domains. Conversely, arachidonic acid and its amide anandamide confer rapid voltage-dependent inactivation to a broad range of Kv channels that otherwise do not inactivate (200). Similarly, function of the voltage-dependent K<sup>+</sup> channel KvAP de-

TABLE 1. *Kv $\beta$  effects on heterologously expressed Kv channels*

Kv $\beta$ Subunit	Coexpressed With	Current Density	Activation $V_{1/2}$	N-Type Inactivation	Reference Nos.
Kv $\beta$ 1.1	Kv1.1–1.5	+	$\pm$	+	19, 94–96, 142, 232
	Kv1.6	+	$\pm$	$\pm$	
	Kv4.3	+	$\pm$	$\pm$	337
Kv $\beta$ 1.2	Kv1.2	+	Approximately –12 mV	+	5, 6, 142, 211, 272
	Kv1.5	$\pm$	$\pm$	+	
Kv $\beta$ 1.3	Kv1.5	–	Approximately –13 mV	+	62, 63, 72, 305
Kv $\beta$ 2.1	Kv1.1, 1.2	+	$\pm$	$\pm$	5, 6, 95, 96, 141, 170, 171, 173, 189, 272
	Kv1.3	+	$\pm$	$\pm$	
	Kv1.4	+	Approximately –10 mV	+	
	Kv1.5	–	Approximately –10 mV	$\pm$	
	Kv1.6	+	$\pm$	+	
	Kv4.3	+	$\pm$	$\pm$	321, 337
	Kv1.1, 1.5, Kv1.6	ND	$\pm^*$	$\pm^*$	19, 46, 95, 96, 182
Kv $\beta$ 3.1	Kv1.4	ND	$\pm^*$	$\pm^*$	
	Kv1.1	$\pm^\dagger$	Approximately –15 mV $^\dagger$	$\pm^\dagger$	20, 141
	Kv1.2, 1.4–1.6	$\pm^\dagger$	$\pm^\dagger$	$\pm^\dagger$	
	Kv1.3	$\pm^\dagger$	Approximately –7 mV $^\dagger$	$\pm^\dagger$	

+, Increase in parameter; –, decrease or shift to more negative potentials;  $\pm$ , no effect; ND, parameter was not determined.  $V_{1/2}$ , membrane potentials at which 50% of the channels are activated. Effects were measured in *Xenopus laevis* oocyte (\*) or in Chinese hamster ovary (CHO) cell expression system ( $^\dagger$ ).

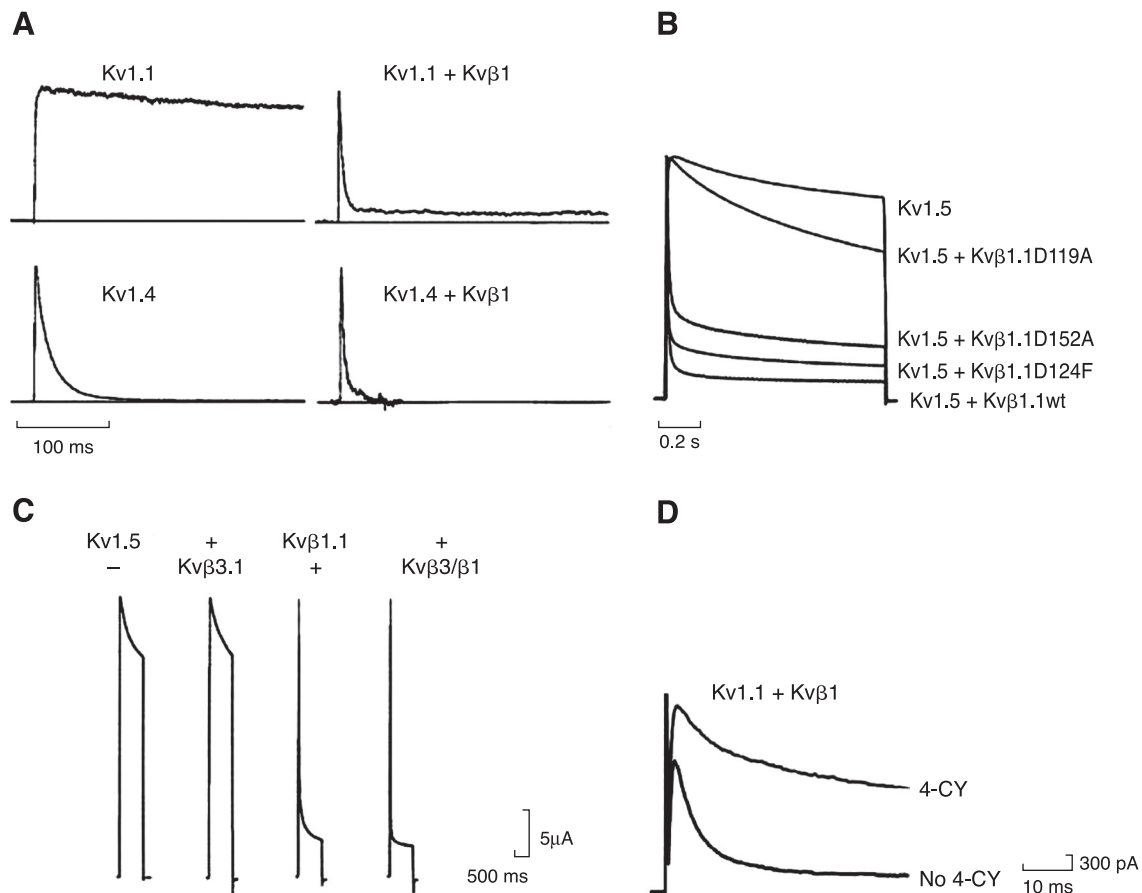


FIG. 4. Kv $\beta$  inactivating domain confers rapid inactivation to Kv1 channels. **A**: outward K currents recorded with potential steps to 50 mV from a holding potential of -100 mV from *Xenopus* oocytes injected with cRNA encoding Kv1.1, Kv1.1 + Kv $\beta$ 1, Kv1.4, or Kv1.4 + Kv $\beta$ 1. [Modified from Rettig et al. (232).] **B**: superimposed outward K currents recorded from *Xenopus* oocytes injected with Kv1.5 cRNA without or with wild-type and mutant Kv $\beta$ 1.1 cRNA as indicated. [Modified from Bähring et al. (19).] **C**: normalized outward currents recorded in *Xenopus* oocytes expressing Kv1.5 alone or in combination with wild-type Kv $\beta$ 1.1, Kv $\beta$ 3.1, or a chimeric Kv $\beta$ 3/ $\beta$ 1 construct as indicated. [Modified from Pongs et al. (222).] **D**: modulation of K channel inactivation by 4-cyanobenzaldehyde (4-CY). Outward membrane currents recorded from inside-out patches from *Xenopus* oocytes expressing Kv1.1 + Kv $\beta$ 1 before (black trace) and after bath perfusion with 5 mM 4-CY. [Modified from Pan et al. (204).]

depends on membrane lipid composition (254), and removal of phosphor-head groups of membrane lipids can have dramatic effects on voltage-dependent gating properties of Kv channels (229, 336). These observations have important implications and add a note of caution to many studies in the literature reporting effects on Kv channel inactivation. Potentially, overexpression of Kv channels in transient transfection systems can expose expressed channels to a lipidic environment that the channel does not normally see. Also, the overexpressed Kv channel may encounter interacting partners in membrane microdomains that the channel may not visit in vivo.

A combination of electrophysiological investigations and structure-based mutations suggests that oxidoreductase activity and inactivating domain activity of Kv $\beta$ -subunits are coupled (19, 204, 300, 326). In particular, amino acid substitutions of catalytic residues attenuated the activity of Kv $\beta$ 1.1 to confer inactivation to a noninactivating Kv1.5 channel (Fig. 4B). Kv $\beta$ 3.1 also contains an NH<sub>2</sub>-

terminal inactivating domain (Fig. 1). This domain, however, is ineffective when Kv $\beta$ 3.1 is coexpressed with the Kv1.5 channel in *Xenopus* oocytes (Fig. 4C). The failure of Kv $\beta$ 3.1 to confer rapid inactivation to the Kv1.5 channel was rescued replacing Kv $\beta$ 3.1 active site residues by those of Kv $\beta$ 1.1 (Fig. 4C) (19). Furthermore, catalytic activity of Kv $\beta$ 1 affects in a voltage-dependent manner the rate of Kv channel inactivation concomitant with an increase in outward current (Fig. 4D). Also, mutation of catalytic residues or substitution of NADPH by NADP<sup>+</sup> have apparently similar attenuating effects on Kv $\beta$ 1.1-mediated reduction of Kv channel activity (204, 300, 301, 326). The physiological relevance of these findings is presently unclear. Note that Kv $\beta$ 2, the major Kv $\beta$ -subunit in mammalian brain, does not have an NH<sub>2</sub>-terminal inactivating domain like Kv $\beta$ 1.1 and Kv $\beta$ 3.1 (Fig. 1). Yet, coexpression of the Kv1.4 channel with Kv $\beta$ 2 accelerates Kv1.4 N-type inactivation (171). Whether an important physiological role of Kv $\beta$ -subunits is to couple membrane excit-



ability to the redox status of the cell still awaits investigation in primary cells and tissue.

### E. Influence of K $\beta$ -Subunits on Kv Channel Surface Expression

The biochemical preparation of Kv1 $\alpha$ /Kv $\beta$ -channel complexes showed tight association of the subunits within an octameric complex (264, 265). Assembly of Kv1 $\alpha$ - and K $\beta$ -subunits appears as early biosynthetic event in Kv channel genesis. Yet, regulation of subunit coassembly and stoichiometry remains largely unexplored. Note Kv1 $\alpha$ /Kv $\beta$ -subunit coassembly is neither obligatory nor necessary for Kv1 channels to reach the cell surface. It, therefore, is unclear if all Kv1 channels represent Kv1 $\alpha$ /Kv $\beta$  heteromultimeric complexes in the plasma membrane. Also, Kv $\beta$ -subunits can assemble to tetramers in the absence of Kv1 $\alpha$ -subunits (88, 89, 310). Furthermore, synthesis of Kv1 $\alpha$ - and Kv $\beta$ -mRNA may be uncoordinated. For example, stimulation of lymphocytes with mitogen induces expression of Kv $\beta$ 1- and Kv $\beta$ 2-mRNA, but not of Kv1 $\alpha$ -mRNA (16, 54). Combining these data with the ones for Kv $\beta$  knockout mice tells us that expression of Kv1 $\alpha$ - and Kv $\beta$ -subunits can occur independently of each other. How the cell controls assembly of Kv $\alpha$ -subunits and Kv $\beta$ -subunits remains a mystery. In this context, a recent report about a reversible assembly and disassembly of Kv1 $\alpha$ - and Kv $\beta$ -subunits is revealing (204). Reversibility of Kv-subunit assembly and its physiological consequences appears an interesting field for future investigation on Kv channel heteromultimers.

Kv $\beta$  coexpression with Kv $\alpha$ -subunits can increase surface expression of Kv channels in heterologous expression systems. For example, coexpression of Kv1.2 and Kv $\beta$ 1.2-subunits in *Xenopus* oocytes resulted in a sixfold increase in current amplitude (Table 1) (5). Since Kv1.2 single-channel conductance was not altered by Kv $\beta$ , the observed current increase was most likely due to increased channel density at the plasma membrane. The data found further support in studies with Kv1.2 and Kv $\beta$ 1.2 coexpressed in tissue culture cells. This resulted in an increase in  $\alpha$ -DTX binding sites as well as in increased anti-Kv1.2 antibody binding to the cell surface. Therefore, it was suggested that stimulation of surface expression, unlike modulation of Kv channel gating, is a more general function of Kv $\beta$ -subunits (272).

However, the evidence that Kv $\beta$ -subunits generally function as chaperones is not compelling. Coexpression with Kv $\beta$ -subunits does not increase Kv1.5 surface expression (142). Thus Kv $\beta$ -subunits may either stimulate or attenuate Kv1 channel density in the plasma membrane (5). A recent report suggests an important role for Kv $\beta$ -subunits in targeting of Kv1 channels to axonal compartments (86). Transfection of cultured hippocampal neurons

with dye-labeled Kv1.2 $\alpha$  and Kv $\beta$ 2 constructs showed that Kv $\beta$ 2-subunits can independently target to the axon. Remarkably, Kv1.2 subunits were not targeted to the axon, unless Kv $\beta$ 2 was present. Next, it was shown that the microtubule (MT) plus-end tracking protein EB1 was crucial for Kv $\beta$ 2 axonal targeting. EB1 was found in coimmunoprecipitation experiments to associate with Kv1.2 and Kv $\beta$ 2. A possible scenario to explain the data is that Kv1.2 and Kv $\beta$ 2, after assembly in the endoplasmic reticulum (188), are sorted with EB1 into post-Golgi carrier vesicles which then travel down the axon utilizing the KIF3/kinesin II motor system to reach their final destination (86). The chaperone hypothesis incurs with data obtained with Kv $\beta$  knockout mice. Both Kv $\beta$ 2 knockout and Kv $\beta$ 1/Kv $\beta$ 2 double knockout mice displayed an apparently similar expression of Kv1.1 and Kv1.2 channels at the surface of cerebellar neurons and peripheral nerve (56, 170). In summary, Kv $\beta$ -subunits may play a role in trafficking Kv channels to distinct cellular sites. However, this is still a controversial issue and needs further investigation.

### F. Function of Kv $\beta$ -Subunits In Vivo

Kv1 channels and Kv $\beta$  subunits are widely expressed in the mammalian brain, having distinct as well as overlapping expression patterns (234, 311). Kv $\beta$ 2 is the predominant ancillary Kv $\beta$  subunit in the brain and exhibits a similar expression pattern as Kv1.1 and Kv1.2 (234–236). Kv $\beta$ 1 also codistributes extensively with Kv1.1 and Kv1.4 (236). It is unclear whether the same Kv channel complex contains both Kv $\beta$ 1 and Kv $\beta$ 2 (or Kv $\beta$ 3) subunits. Possibly, the different Kv $\beta$  subunits are associated with localizing the Kv channel to distinct cellular subsites. This, however, needs to be explored. In the axolemma of myelinated nerve fibers, Kv1.1 and Kv1.2 are coexpressed in the juxtaparanodes, together with Kv $\beta$ 2 most likely representing a heteromeric Kv channel complex (234–236). Since in the nodal axolemma of mammalian myelinated nerve fibers this channel complex is absent (199, 242), application of TEA does not increase the duration of the action potential in these fibers (260, 261). Its main function in myelinated nerve fibers seems to be the inhibition of reexcitation following an action potential. The axon initial segment (AIS) of cortical and hippocampal pyramidal neurons also expresses a channel complex composed of Kv1.1, Kv1.2 (Fig. 5), and presumably also of Kv $\beta$ 2. In the AIS of mitral cells of the olfactory bulb, only Kv1.2 channels are expressed, whereas in the AIS of Purkinje neurons, Kv1.1 and Kv1.2 are absent (Fig. 5). The density of the Kv1.1/Kv1.2 channel complex increases toward the distal part of the AIS of cortical pyramidal neurons. The Kv1.1 channel is strategically positioned to play a dynamic role in shaping the orthodromic action



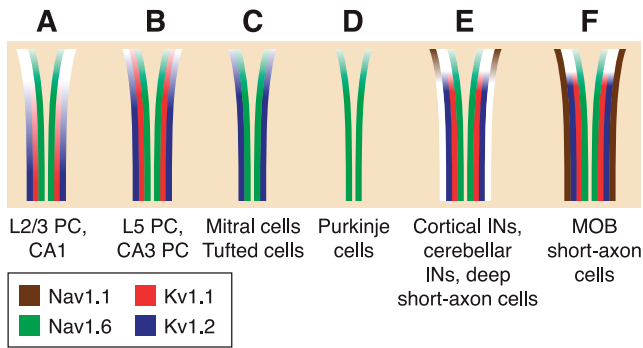


FIG. 5. Schematic diagram illustrating the molecular composition of the axon initial segments (AIS) of distinct types of nerve cells. A: in layer 2/3 and CA1 pyramidal cells, Kv1.1 and Kv1.2 subunits are localized at more distal parts of the AIS, and their density gradually increases towards the end of the AIS. B: in layer 5 and CA3 pyramidal cells, the Kv1.1 and Kv1.2 subunits have a relatively uniform distribution at high densities along the AIS. C: in mitral/tufted cells of the olfactory bulb, only Kv1.2 subunits are localized along the whole length of the AIS. D: in cerebellar Purkinje cells, there are no Kv1.1 and Kv1.2 subunits. E and F: GABAergic interneurons in the neocortex, hippocampus, cerebellum, and olfactory bulb express Kv1.1 and Kv1.2 at high densities in their AISs. In addition, the distribution of Nav1.1 and Nav1.6 is shown. [From Lorincz and Nusser (156).]

potential and to integrate slow subthreshold signals to provide control of presynaptic action potential wave form and synaptic coupling in local cortical circuits (131). Note Kv1.1 subunits also occur in dendrites (226) due to a local synthesis from dendritic Kv1.1 mRNA. Whether dendritic Kv1.1 channels are assembled with Kv $\beta$ -subunits is presently unknown.

The association of Kv1 channels with Kv $\beta$ 2 has a marked influence on the threshold potential of action potentials (shift of the activation curve to more negative membrane potentials; Table 1). Also, they are involved in regulation of action potential duration. This is especially true for Kv1.4 channels that are primarily located in pre-

synaptic terminals. Kv1.4 channels are characterized by slow recovery from inactivation. This property has not only been observed in homomeric Kv1.4 channels (246), but it also occurs in heteromeric Kv1.1/Kv1.2/Kv1.4 channels or channels consisting of Kv1.x, Kv $\beta$ 1, and Kv $\beta$ 2 subunits (232, 236). A functional consequence of slow recovery from inactivation is frequency-dependent broadening of action potentials which has been observed in presynaptic terminals and in nerve endings of the posterior pituitary (112). Simultaneous recordings of Ca<sup>2+</sup> currents from presynaptic terminals of hippocampal mossy fiber boutons and postsynaptic excitatory postsynaptic currents (EPSCs) showed that spike broadening led to an increase in Ca<sup>2+</sup> influx into the presynaptic terminal and to an increase in the EPSCs, indicating an increase in the synaptic strength upon spike broadening (81). In line with this, the reported properties of Kv1.4/Kv $\beta$ 1/Kv $\beta$ 2 channel complexes and the occurrence of the Kv subunits in mossy fibers support the idea that Kv1.4 channel complexes play a role in regulating action potential duration in the hippocampal mossy fiber system of the mouse.

The phenotype of Kv $\beta$ 1 knockout (Kv $\beta$ 1<sup>-/-</sup>) mice show deficits in learning and memory as tested with the Morris water maze (Table 2; Refs. 82, 190). Kv $\beta$ 2 knockout (Kv $\beta$ 2<sup>-/-</sup>) and Kv $\beta$ 1/Kv $\beta$ 2 double-knockout (Kv $\beta$ 1<sup>-/-</sup>/Kv $\beta$ 2<sup>-/-</sup>) mice (56) are characterized by a reduced life span, an increased neuronal excitability, occasional seizures, and cold swim-induced tremors (Table 2). Although surface expression of Kv1.1/Kv1.2 channels appears normal in these mice, it is unclear whether this applies to all Kv1.x subunits in all neurons and neuronal compartments, respectively. Electrophysiological recordings from CA1 neurons of Kv $\beta$ 1<sup>-/-</sup> mice showed a decrease in A-type current and an increase in sustained outward K<sup>+</sup> current amplitude. Also, frequency-dependent spike broadening and reduced afterhyperpolarization amplitude was

TABLE 2. Kv $\beta$  knockout mice

Genetic Background	Phenotype	Electrophysiology, Molecular Biology	Reference Nos.
Kv $\beta$ 1 <sup>-/-</sup>	3-Mo-old mice: impairment in learning and memory (water maze, food preference task); rescue: enriched environment, aging	CA1 neurons: $I_A$ decreased, $I_{so}$ increased, less broadening of frequency-dependent AP, decreased slow AHP, no change in Kv1.1, Kv1.2, Kv1.4 density.	82, 190
	Aged mutants (12 mo): enhanced learning (Morris water maze) $\uparrow$	LTP more readily induced than in WT control	185
Kv $\beta$ 1 <sup>-/-</sup> (targeted to heart)	Normal ECG	Ventricular myocytes: $I_{to,f}$ (Kv4.3) decreased, $I_{K,slow}$ (Kv2.1) increased, no change in Kv1.4, Kv1.5, no change in AP shape	8
Kv $\beta$ 2 <sup>-/-</sup>	Life span reduced, occasional seizures and cold swim-temperature-induced tremors	Normal Kv1.1, Kv1.2 density and localization in cerebellar basket cell terminals and juxtaparanodes of myelinated nerve fibers	56, 170
Kv $\beta$ 1 <sup>-/-</sup> ; Kv $\beta$ 2 <sup>-/-</sup>	Increased mortality, cold-induced tremor	No change in Kv1.2 density in cerebellar basket cells	56

ECG, electrocardiogram;  $I_A$ , A-type current;  $I_{to,f}$ , fast component of transient outward K current;  $I_{K,slow}$ , sustained component of outward-rectifying K current;  $I_{K,slow}$ , slow component of the outward-rectifying K current; AP, action potential; AHP, afterhyperpolarization; LTP, long-term potentiation.

observed for hippocampal neurons of the knockout mice compared with controls (82). Mice with a targeted deletion of  $Kv\beta 1$  in the heart were used to analyze the role of  $Kv\beta 1$  in the generation of ventricular  $Kv$  currents in the mouse (8). Wild-type and  $Kv\beta 1^{-/-}$  cardiomyocytes isolated from the left ventricular apex displayed similar action potential wave forms and a similar peak  $Kv$  current density. The contribution of individual  $Kv$  channels to  $Kv$  current density, however, differed between wild-type and  $Kv\beta 1^{-/-}$  ventricular cardiomyocytes. Notably,  $Kv4.3$  channel expression was decreased and  $Kv2.1$  expression was increased in  $Kv\beta 1^{-/-}$  ventricular cardiomyocytes compared with wild type. The density of  $Kv1$  channels ( $Kv1.1$ ,  $Kv1.2$ ,  $Kv1.4$ ) was not changed, similar to the finding in CA1 neurons of a general knockout of  $Kv\beta 1$  (82) and  $Kv\beta 2$  (no change in  $Kv1.4$ ,  $Kv1.5$ ; Refs. 56, 170). The data indicate that a loss of ancillary subunit expression may not be a simple matter and may give rise to complex compensatory mechanisms at the transcriptional as well as translational and posttranslational level of  $Kv$  channel. Presently, it is unclear by which cellular mechanism(s) loss of  $Kv\beta 1$  leads to modulation of  $Kv4.3$  and  $Kv2.1$  channel density at the cell surface. An as yet unexplored possibility in this context is the influence of  $Kv\beta 1$  on the oxygen sensitivity of cardiac  $Kv$  channels, which reportedly affects their activity (55, 208, 210). In summary, *in vitro* and *in vivo* studies on the function of  $Kv\beta$ -subunits have provided important insights into their role to confer inactivation on  $Kv1$  channels. However,  $Kv\beta$ -subunits most likely also have other functions. For example, all  $Kv\beta$ -subunits contain an oxidoreductase active site, but why this is so still remains a mystery. Detailed electrophysiological and biochemical studies on intact cells in which  $Kv\beta$  subunit function is specifically being manipulated may shed more light into the physiological role(s) of auxiliary  $Kv\beta$  subunits.

### III. KChIPs AND DPPLs: ANCILLARY SUBUNITS OF $Kv4$ CHANNELS

$K^+$  channel interacting proteins (KChIPs) represent another family of ancillary subunits (Fig. 6). They specifically interact with cytoplasmic domains of  $Kv4$   $\alpha$ -subunits, which form rapidly inactivating A-type  $K^+$  channels exhibiting a broad variability in both time course and voltage dependence of activation and inactivation. The variant gating properties of  $Kv4$  channels appear to be mainly due to complex formation of  $Kv4$  channels with different KChIPs (36, 117) as well as transmembrane dipeptidyl aminopeptidase-like proteins (DPPL) (117, 161, 187). These two types of ancillary subunits may either separately or jointly associate with  $Kv4$  subunits to multiprotein complexes modulating trafficking, targeting to the plasma membrane, as well as turnover and endocyto-

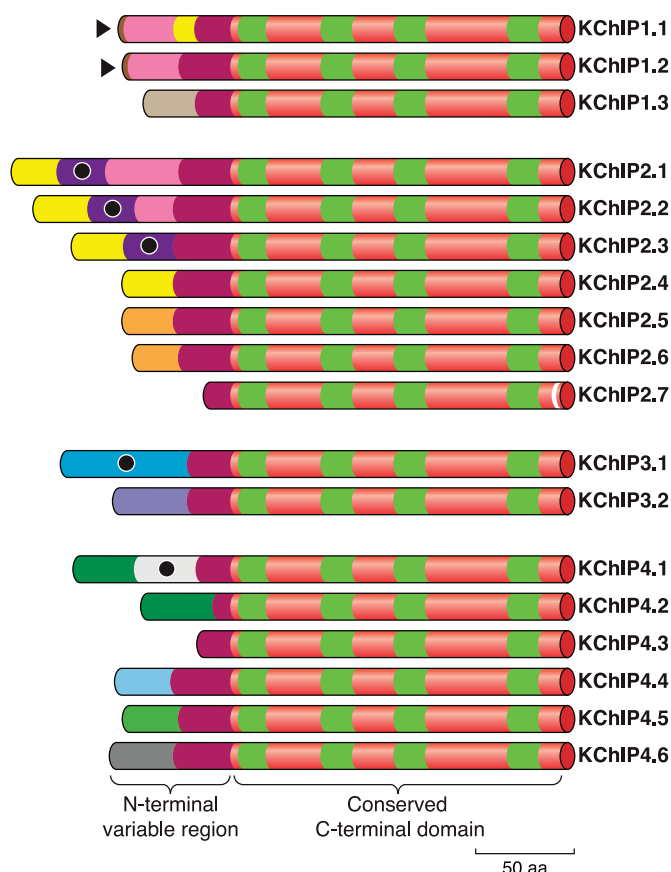


FIG. 6. Bar diagram of KChIP protein family. Alternative splicing of the four human KChIP genes generates a large number of isoforms (KChIP1–4) with a variant NH<sub>2</sub>-terminal region and a conserved COOH-terminal domain containing four EF hands (boxed in light green). Human KCNIP1 gene generates three KChIP1 isoforms. Genbank (NCBI) accession numbers are as follows: NP\_001030009 (KChIP1.1), NP\_055407 (KChIP1.2), NP\_001030010 (KChIP1.3). Human KCNIP2 generates seven KChIP2 isoforms. Genbank (NCBI) accession numbers are as follows: NP\_055406 (KChIP2.1), NP\_775283 (KChIP2.2), NP\_775284 (KChIP2.3), NP\_775285 (KChIP2.4), NP\_775286 (KChIP2.5), NP\_775287 (KChIP2.6), NP\_775289 (KChIP2.7). Human KCNIP3 gene generates two KChIP3 isoforms. Genbank (NCBI) accession numbers are as follows: AAH12850 (KChIP3.1), NP\_001030086 (KChIP3.2). The human KCNIP4 generates six KChIP4 isoforms. Genbank (NCBI) accession numbers are as follows: NP\_079497 (KChIP4.1), NP\_671710 (KChIP4.2), NP\_001030176 (KChIP4.3), NP\_671712 (KChIP4.4), NP\_001030175 (KChIP4.5), NP\_AA277809 (KChIP4.6). Functional domains are indicated by different colors or symbols, e.g., EF hands (green), myristoylation sites (▶), palmitoylation sites (●), KIS domain (light blue). [Modified from Burgoyne (40).]

sis of  $Kv4$  channels. Importantly,  $Kv4$  multiprotein complexes represent the molecular correlate to neuronal somatodendritic A-type  $K$  current ( $I_{SA}$ ) and cardiac transient outward current ( $I_{to}$ ) (161, 193, 266).  $I_{SA}$  plays a considerable role in neuronal excitability, for example, in timing and frequency, and in backpropagation of action potentials into dendrites of hippocampal neurons (100).  $I_{to}$  contributes to the regulation of cardiac action potential repolarization in ventricular muscle (193). Thus two distinct types of ancillary subunits significantly modulate  $Kv4$  channel gating properties, notably regulating  $Kv4$

channel activity near or below the threshold potential of action potential firing.

### A. Structure of KChIPs

Members of the KChIP family were biochemically not purified from brain lysates like Kv $\beta$  subunits but were identified in yeast two-hybrid screens using the NH<sub>2</sub> terminus of Kv4 $\alpha$ -subunits and, respectively, the COOH terminus of presenilin 2 as bait (13, 184). The first screen yielded KChIP1–3. Incidentally, KChIP3 was already known as calsenilin (43) and as DREAM (downstream regulatory element antagonistic modulator) (45). The second screen resulted in the characterization of neuronal Ca<sup>2+</sup> sensor protein CALP (calsenilin-like peptide), which is identical to KChIP4. Altogether, four KChIP genes (KChIP1–4) are known, giving rise to a large number of alternatively spliced isoforms. This makes the KChIP protein family the most diverse of the ancillary Kv-channel subunit families (Fig. 6). As for Kv $\beta$ -subunits, KChIP isoforms all contain a conserved COOH-terminal core region of ~180 amino acids, but distinct NH<sub>2</sub> termini variable in sequence and length (13, 117, 286). Unlike Kv $\beta$  subunits, which form tetramers, purified KChIP proteins come as homomers. KChIPs are Ca<sup>2+</sup> binding proteins belonging to the neuronal calcium-sensor (NCS) superfamily (40). Similar to other NCS proteins, KChIPs contain four EF-hand Ca<sup>2+</sup>-binding motifs within their conserved COOH terminus (Fig. 6) with Ca<sup>2+</sup> bound to the third and fourth EF-hand (Fig. 7C). According to the crystal structural analysis of a

KChIP1 preparation, EF-1 and EF-2 form the N lobe, and EF-3 and EF-4 the C lobe. Each of the two lobes consists of five  $\alpha$ -helices (127, 251, 351). It has been shown that point mutations of highly conserved amino acids in EF-hands 2, 3, and 4 attenuate Ca<sup>2+</sup> binding to KChIP1. The mutant KChIPs were still capable of binding to the Kv4 channel, but apparently had lost their capacity to modulate Kv4-channel inactivation (13). This result suggested that Ca<sup>2+</sup> may affect Kv4 channel kinetics by binding to KChIP EF-hands. A direct effect of Ca<sup>2+</sup>, however, remains to be shown. Thus the functional significance of Ca<sup>2+</sup> binding to KChIP EF-hands is still unclear.

Based on an electron microscopical analysis of purified Kv4.2-KChIP2 complexes (127), they represent octameric structures in a stoichiometry of four KChIP2 and four Kv4 $\alpha$ -subunits. But unlike Kv $\beta$  tetramers, which are docked vertically to the bottom of the Kv1-assembly (T1) domain, KChIPs bind laterally to the Kv4 T1 domain (Fig. 7). Note that the overall three-dimensional structures of Kv1 and Kv4 T1 domains are very similar, yet the Kv $\alpha$ /Kv $\beta$  binding interfaces are quite different. Literally, the tetrameric T1 domains look like a gondola hanging beneath the membrane-inserted pore domain of Kv channels (277). Then the four bound KChIP molecules, which are rotated by 45° against the central T1 axis, form a circle and, thereby, markedly increase the area of the central platform of the gondola (127). Since the platform of the hanging gondola has no ion-permeable pore in its center, ions have to travel along the outer KChIP surface and subsequently pass the “ropes” of the gondola to

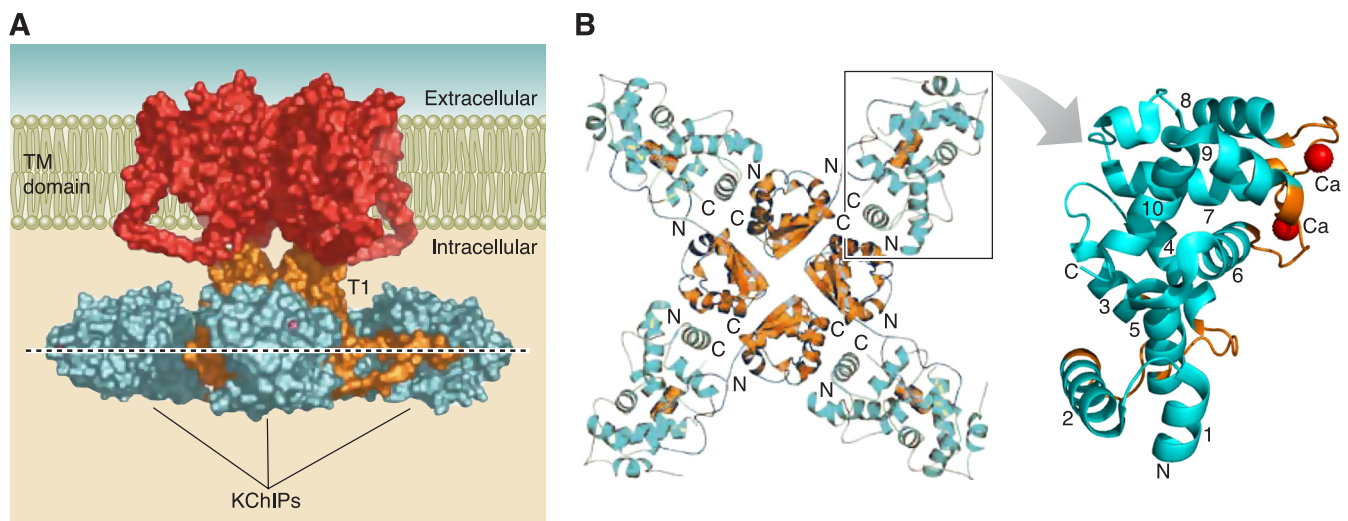


FIG. 7. Model of Kv4.3-KChIP1 channel complex. The model from Pioletti et al. (215) was constructed by docking KChIP1 to the cytoplasmic NH<sub>2</sub> terminus of a Kv channel structure, which is based on the Kv1.2 crystal structure (153). A: side view of the channel complex. Transmembrane (TM) domains are shown in dark red, tetramerization (T1) domains in orange, and KChIPs in blue. Ca<sup>2+</sup> are in magenta. [From Pioletti et al. (215). Reprinted with permission from Macmillan Publishers Ltd.] B: view of the channel complex from the cytoplasmic side. KChIPs (blue) and Kv4.3 components (orange) are shown as ribbons. On the right, an enlarged view of KChIP1 (boxed area) is shown. EF hands are highlighted in orange and the two Ca<sup>2+</sup> binding to EF-hand 3 and 4 in red. NH<sub>2</sub>-terminal (1–5) and COOH-terminal (6–10)  $\alpha$ -helices are numbered. KChIP1 structure was taken from a protein databank (1S1E). [From Wang et al. (319). Reprinted with permission from Macmillan Publishers Ltd.]



approach and finally enter the channel pore from the cytoplasmic side.

In contrast to the small contact sites between Kv1 $\alpha$ - and Kv $\beta$ -subunits, the interaction of Kv4 $\alpha$ -subunits with KChIP appears more complex, involving several, spatially separated sites. This conclusion is derived from extensive studies employing targeted deletions and site-directed mutagenesis of the Kv4 NH<sub>2</sub> terminus combined with Kv4 current recordings in heterologous expression systems and with crystallography analyses. The data suggest that a proximal (residues 7–11) and distal (residues 71–90) domain of the NH<sub>2</sub> terminus of Kv4.2 are important for binding KChIP1 (13, 17, 44, 251). The proximal NH<sub>2</sub>-terminal Kv4 domain contains an  $\alpha$ -helical stretch of hydrophobic amino acid residues. Presumably, it binds to a hydrophobic pocket of KChIP1, thereby forming a stable complex. This view is strongly supported by the crystal structure of KChIP1 in complex with the proximal Kv4.2 NH<sub>2</sub> terminus (amino acids 1–30). The structure shows the  $\alpha$ -helix of the Kv4.2 NH<sub>2</sub> terminus in close contact with KChIP amino acid residues within a hydrophobic groove of the KChIP1 molecule (251). Mutagenesis of the distal NH<sub>2</sub>-terminal Kv4.2 domain indicated that this domain is essential for binding KChIPs (44). This hypothesis found strong support by an elegant experiment, where this domain was inserted into the NH<sub>2</sub> terminus of Kv1.2. The insertion conferred to the Kv1.2 channel binding to KChIP1, which otherwise does not interact with Kv1.2 (251).

Recently, the structure of cocrystals between the human Kv4.3 NH<sub>2</sub> terminus (residues 6–145) and KChIP1 (residues 38–217) were solved at a resolution of 3.2 Å (319). The crystal structure provides a detailed picture of an octameric KChIP-Kv4.2 complex, in which four KChIPs are symmetrically arranged around the four  $\alpha$ -subunits (Fig. 7B). Importantly, the structure shows each KChIP molecule in contact with two neighboring Kv4.3 NH<sub>2</sub> termini (215, 319). Note formation of two interfaces between a Ca<sup>2+</sup>-binding protein and a cytoplasmic K<sup>+</sup>-channel domain is also seen in the crystal structure of a complex between calmodulin and a small-conductance (SK) K<sup>+</sup> channel (10, 168). But in detail, the two complexes are quite different. An elongated groove formed by the displacement of the helix 10 on the surface of KChIP1 is the first interface with the proximal NH<sub>2</sub>-terminal Kv4.3 binding domain. The second interface involves helix 2 of the same KChIP molecule, which contacts the T1 assembly domain of the neighboring Kv4.3 $\alpha$ -subunit. It is likely that this interaction clamps two Kv4 $\alpha$ -subunits together to stabilize the octameric Kv4-KChIP channel complex (215, 319). This hypothesis is supported by the observation that KChIPs are capable of rescuing assembly-defective Kv4 subunits. Point mutations in the Kv4 NH<sub>2</sub> terminus, which affect the Zn<sup>2+</sup> binding sites in the T1 domain (251), disrupt Kv4 $\alpha$ -subunit tetramerization and trap Kv4 pro-

tein in the ER (135). When coexpressed with KChIPs, the mutant subunits, however, assemble together and form tetramers (135, 319).

Unfortunately, available Kv-channel crystal structures are uninformative on the contribution or role of COOH-terminal Kv-channel domains to binding ancillary subunits like Kv $\beta$  or KChIP. Mutagenesis studies imply that the cytoplasmic Kv4 COOH terminus contains a third KChIP-interaction site. Mutations in this COOH-terminal Kv4 domain similarly to those in the NH<sub>2</sub>-terminal Kv4 domains seem to influence surface expression as well as Kv4 channel gating (44, 92). Clearly, additional structural data are needed to understand whether the observed mutational effects are based on direct or indirect effects on KChIP binding to the Kv4 channel.

## B. Function of KChIPs In Vitro

Coexpression of KChIPs with Kv4 in heterologous expression system may lead to two effects. The first one is seen as an increase in Kv4 current density, presumably because the density of Kv4 channels is increased in the plasma membrane. The second one concerns Kv4-channel kinetics of inactivation and recovery from inactivation. Both are altered by KChIP binding to the channel (Table 3). The effect on current density differs greatly for the various KChIP isoforms. In fact, some KChIP variants, for example, KChIP4, have almost no effect, and others stimulate current density 10- to 100-fold (13, 17). In this case, KChIPs seem to facilitate Kv4 channel assembly in the ER and Kv4 trafficking to the plasma membrane. The molecular mechanisms underlying these different steps are unclear (13, 101, 135, 274).

The variant NH<sub>2</sub> termini of the different KChIP isoforms display remarkably distinct sets of consensus sequences for myristoylation and palmitoylation (40, 286). As proposed for other members of the NCS protein family, myristoylation and palmitoylation of KChIPs may be important for membrane localization (197). In some NCS proteins, like recoverin, the translocation from the cytosol to the membrane-bound form is Ca<sup>2+</sup> dependent, because the myristoyl group is only exposed after binding of Ca<sup>2+</sup> (40). KChIPs appear to have a permanently exposed myristoyl or palmitoyl group, insensitive to Ca<sup>2+</sup> binding. Thus KChIPs are membrane-associated proteins; only KChIP isoforms like most of the KChIP4 isoforms (Fig. 6), which lack a myristoyl or palmitoyl group, are cytosolic proteins. They bind to the plasma membrane only after association with Kv4 channel  $\alpha$ -subunits (40). Interestingly, the effect of KChIP2.2 (KChIP2.b) and KChIP3 on current density was eliminated by mutation of an NH<sub>2</sub>-terminal double cysteine motif for palmitoylation to alanine. Note the effect of the mutant KChIPs on Kv4.2 channel kinetics was like that of wild-type KChIPs (286).



TABLE 3. *Effects of KChIPs and/or DPPLs on Kv4 channels in heterologous expression systems*

Subunit	Coexpressed With	Increase in Surface Expression	Activation $V_{1/2}$	Inactivation $V_{1/2}$	Inactivation Kinetics	Recovery From Inactivation	Reference Nos.
KChIP1	Kv4.1	+	+12 mV	+	+	+, 4-fold	24, 189
	Kv4.2	~14-fold	-20, -40 mV	-5 mV	-, 4-fold	+, 3-fold	11, 13, 101, 102, 187, 189
	Kv4.3	2-fold	-3 mV	+5 mV	-, 2- to 3-fold	+, 2- to 10-fold	13, 24, 101, 102, 187
KChIP2	Kv4.1	>100-fold	Approximately +15 mV	Approximately +30 mV	-, ~7-fold	+, ~7-fold	17, 18
	Kv4.2	9- to 55-fold	+, 9, -30 mV	Approximately +16 mV	-, ~3-fold	+, ~6-fold	13, 17, 18, 209
	Kv4.3	10-fold	+14 mV	+16 mV	-, 3-fold	+, 4.5-fold	17, 18, 145
KChIP3	Kv4.2	6- to 14-fold	Approximately -40 mV	Approximately +5 mV	-, ~2-fold	+, 2- to 3-fold	13, 114, 116, 135
	Kv4.2	1.5-fold	Approximately +10 mV	Approximately +5 mV	-, ~2-fold	$\pm$	115, 116
KChIP4	Kv4.3	-	Approximately +10 mV	$\pm$	-, ~10-fold	ND	101, 263
	Kv4.2	11- to 20-fold	-20, -30 mV	Approximately -15 mV	+, 2- to 3-fold	+, 3-fold	11, 114, 125, 186, 187, 275, 346
DPPX-S (DPP6)	Kv4.3	3-fold	-15, -30 mV	-8 mV	+, ~2-fold	+, ~3-fold	125, 187, 231
	Kv4.2	7-fold	-10, -30 mV	-8-16 mV	+, ~8-fold	+, ~3-fold	114, 115, 145, 346
	Kv4.3	+	-10 mV	-17 mV	+, ~3-fold	+, ~2-fold	145
DPPX-S + KChIP1	Kv4.2	+	Approximately -15 mV	-8 mV	U-shaped	+, 3-fold	11
+KChIP2	Kv4.2	ND	-12 mV	$\pm$	ND	+, 11-fold	275
+KChIP4	Kv4.2	ND	-18 mV	-5 mV	+, 2-fold	+, ~2-fold	115
	Kv4.3	+		-10 mV	+	+, 4-fold	145
DPP10 + KChIP2	Kv4.2	twofold	Approximately -20 mV	-4 mV	U-shaped	+, ~8-fold	114, 115
+KChIP3	Kv4.3	ND	$\pm$	-10 mV	+, 2-fold	+, 4-fold	145
+KChIP4	Kv4.2	$\pm$	-10 mV	-9 mV	+, ~5-fold	+, 2.5-fold	115

+, Increase in parameter or shift to more positive potentials; -, decrease or shift to more negative potentials;  $\pm$ , no effect; ND, parameter was not determined.  $V_{1/2}$ , membrane potentials at which 50% of the channels are activated or inactivated.

The data suggest that the variant KChIP NH<sub>2</sub> termini specifically affect Kv4 channel trafficking and membrane targeting. Possibly, distinct posttranslational KChIP modifications influence Kv4-channel targeting to distinct microdomains of the plasma membrane. Potentially, KChIPs may also play an important role in modulating membrane mobility and endocytosis of the Kv4 channel. This aspect of Kv4 channel trafficking remains largely unexplored. Clearly, further studies are needed to understand the specific roles of KChIP NH<sub>2</sub> termini in Kv4 channel assembly, trafficking, and endocytosis.

An important aspect of KChIP activity is that they markedly affect Kv4 channel gating (Table 3; Fig. 10, A and B). The Kv4 channel expresses a rapidly inactivating current; inactivation is fast and voltage dependent. In contrast to *Shaker*-type channels, which enter the inactivated state from the open state(s), the Kv4 channel mostly inactivates from closed state (17, 22, 118). Closed-state inactivation, which is a hallmark of Kv4 channels, has intensely been investigated, and detailed kinetic models have been developed to explain this type of inactivation (11, 117, 124). Steady-state inactivation of Kv4 channels is high at a resting membrane potential of about -60 mV, but recovery from Kv4 inactivation at more negative membrane potentials is very fast. Thus closed-state inactivation

in Kv4 channels represents an effective mechanism to regulate Kv4-channel availability at subthreshold membrane potentials. For example, brief conditioning hyperpolarization, such as a hyperpolarizing afterpotential, which follows an action potential, will rapidly recruit inactive Kv4 channels.

KChIPs induce large changes in time- and voltage-dependent properties of Kv4 current and, therefore, are probably important regulators of Kv4 channel activity in excitable cells. For example, KChIP2s slow the time course of Kv4.1-current inactivation ~7-fold and increase the rate of recovery from inactivation 2- to 10-fold. In contrast, KChIP1 accelerates the time course of Kv4.1-current inactivation (189; Table 3). Furthermore, the voltage dependence of Kv4.2 activation is shifted to more negative membrane potentials by 30 to 40 mV (Table 3; Refs. 11, 13, 24, 101, 187). KChIP1-3 accelerate Kv4.2 and Kv4.3 current inactivation at depolarizing potentials from -40 to -20 or 0 mV. At more positive potentials, however, the time course of Kv4 current inactivation becomes slower again, inducing a U-shaped voltage dependence. This type of voltage dependence has also been observed in native A-type currents, e.g., in cerebellar granule cells (11) and hippocampal pyramidal neurons of the CA1 region (100). In addition, modulatory effects of cAMP-de-

pendent protein kinase and arachidonic acid on current density and kinetics of Kv4 currents require KChIP presence (102).

In addition to closed-state inactivation, the Kv4 channel may undergo an N-type inactivation in which the distal part of the NH<sub>2</sub> terminus of the Kv4 channel moves towards the cytoplasmic pore of the channel and occludes it in its open state (11, 17, 80). A characteristic of this type of voltage-dependent inactivation is that it becomes monotonically faster with more positive membrane potentials (11). Interestingly, binding of KChIP1–3 to the Kv4 NH<sub>2</sub> terminus sequesters and immobilizes the NH<sub>2</sub>-terminal Kv4 inactivating domain. The KChIP1–3-Kv4 interaction prevents N-type but not closed-state inactivation, which is the predominant type of Kv4 channel inactivation (215, 319).

KChIP4.4 represents a special case and demonstrates the enormous variability of KChIP effects on Kv4 channel activity. KChIP4.4 suppresses fast inactivation of the Kv4.3 and Kv4.2 channel, converting the fast transient A-type Kv4 current into a slowly inactivating outward current. The KChIP4.4 channel inactivation suppressor (KIS) domain is located within the first 34 amino acids of the KChIP4 NH<sub>2</sub> terminus (101). The KIS domain forms an extended  $\alpha$ -helix that folds back onto the KChIP core region, where it binds to the same hydrophobic surface pocket recently shown to harbor the NH<sub>2</sub>-terminal  $\alpha$ -helix of Kv4.3 in a KChIP1-Kv4.3 T1 complex (Fig. 7; Refs. 215, 263, 319). Functionally, this interaction abolishes the increased surface expression mediated by the KChIP-core domain (101). The observation provides a coherent picture of KChIP effects on Kv4 channel surface expression. During assembly of Kv4 channel complexes in ER and Golgi compartments, the Kv4 NH<sub>2</sub> terminus will be exposed on the surface and interacts with a retention apparatus in ER and Golgi compartments. KChIP binding to the Kv4 NH<sub>2</sub> terminus then will relieve retention and stimulate anterograde trafficking to the plasma membrane. In contrast, any KChIP4.4 subunit associating with Kv4 channel will expose a Kv4 NH<sub>2</sub> terminus and, thus, impair surface expression of the Kv4 channel (263).

### C. Structure of DPPLs

Comparison of current properties mediated by heterologously expressed KChIP/Kv4 channel complexes with those measured in primary cells showed significant kinetic differences, in particular in the inactivation time course (Fig. 10, *B* and *D*). This led to the hypothesis that Kv4 channel complexes contain an additional subunit. Indeed, analysis of immunopurified Kv4 channel complexes showed that they consisted of three main Kv4 channel types of protein: Kv4, KChIP, and an unidentified 115-kDa protein. The protein was purified and sequenced

by tandem mass spectrometry. This led to the discovery of a novel Kv4 channel-associated protein. This new subunit (DPP6 or DPPX) exhibited sequence similarity to dipeptidyl aminopeptidase protein (DPP), an integral membrane protein with serine-protease activity. Coexpression of DPP6 with the Kv4 channel leads to a great increase in surface expression and to a significant acceleration of the inactivation time course of the Kv4 channel (Table 3; Ref. 187). Importantly, assembly of the Kv4/KChIP/DPP-channel complex in *in vitro* expression systems yielded inactivating outward currents indistinguishable from those observed as  $I_{SA}$  in primary neurons (Fig. 10, *C* and *D*; Refs. 114, 115, 145, 161, 263). The data concur with the idea that native Kv4 channels are multiprotein complexes assembled from Kv4, KChIP, and/or DPP-like subunits (Fig. 8).

DPPL Kv4 channel subunits carry mutations of the highly conserved serine residue in the catalytic site of the DPP serine proteases. Most likely, this is the reason why DPPL subunits of Kv4-channel complexes do not exert dipeptidyl aminopeptidase activity (225, 281). Two DPPL families have been described, DPP6 (DPPX) and DPP10 (DPPY) (Fig. 9) (114, 187, 346). The general topology reveals a relatively short cytoplasmic NH<sub>2</sub> terminus, a

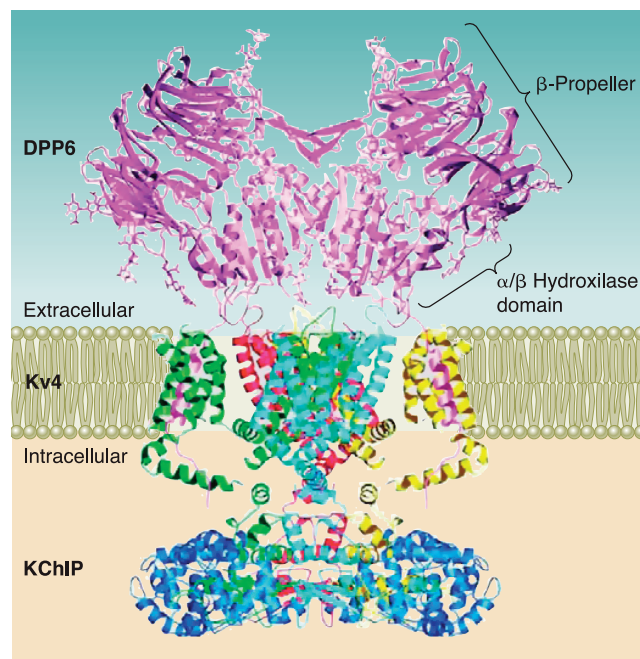


FIG. 8. Structural model of Kv4.3-KChIP1-DPP6 channel complex. DPP6 structure is derived from the crystal structure of the extracellular DPP6 domain (281). The model of the Kv4.3-KChIP1 complex is as described in Figure 6. The four Kv4 $\alpha$ -subunits are shown in different colors (green, yellow, red, and light green). KChIP is shown in blue. The DPP6 transmembrane domain is proposed to interact with the Kv4 $\alpha$  voltage sensor domain. For clarity, only two of four DPP6 subunits are shown. Each contains an  $\alpha/\beta$  hydroxylase domain and a  $\beta$ -propeller as indicated by brackets. The two DPP6 subunits interact to form a dimer. [From Maffei and Rudy (161), with permission from John Wiley and Sons.]

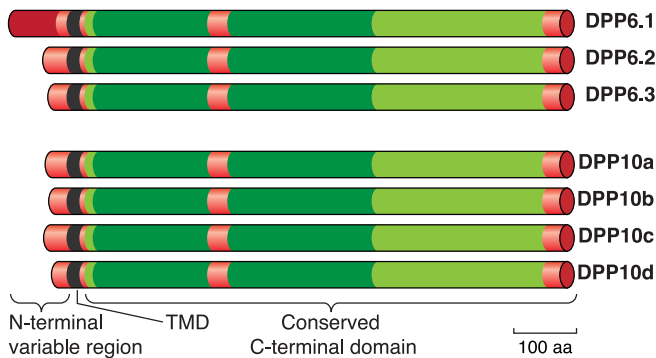


FIG. 9. Bar diagram of DPPL protein family. Human DPP6 (DPPX) gene generates three isoforms. Genbank (NCBI) accession numbers are as follows: NP\_570629 (DPP6.1, DPP6 isoform 1, DPP6-L, long isoform), NP\_001927 (DPP6.2, DPP6 isoform 2, DPP6-S, short isoform), NP\_001034439 (DPP6.3, DPP6 isoform 3). Human DPP10 (DPPY) gene generates four isoforms. Genbank (NCBI) accession numbers are as follows: NP\_065919 (DPP10 variant a, long isoform), ABI16085 (DPP10 variant b), ABI16086 (DPP10 variant c), ABI16087 (DPP10 variant d, short isoform). Transmembrane domain (TMD) is boxed in black,  $\beta$ -proteobacter domain is dark green, and  $\alpha/\beta$ -hydroxylase is light green.

single transmembrane segment, and a large extracellular COOH terminus, which displays a glycosylation domain, a cysteine-rich domain, and an aminopeptidase-like domain. DPP6 protein is related to the dipeptidyl aminopeptidase CD-26. This serine-protease mediates several important functions through its extracellular catalytic and cysteine-rich domain in cell adhesion, cell migration, and T-cell activation. The latter domain binds to components of the extracellular matrix. It is likely that the extracellular domain of DPPL subunits comparably interacts with extracellular matrix proteins (187, 281). Possibly, this interaction provides a molecular basis for the observed large increase in Kv4 channel surface expression upon coexpression with DPPL subunits. Potentially, they could fix the Kv4 channel in the plasma membrane making the channel more resistant to endocytotic turnover. It is attractive to speculate that interaction with extracellular matrix aids Kv4 channel clustering at hippocampal synaptic spines.

Whereas the extracellular domain(s) of the DPPL subunits may interact with extracellular matrix components, it has been proposed that the single DPPL-transmembrane domain binds to the voltage sensors of the Kv4 channel (231). This binding could explain observed DPPL effects on voltage-dependent Kv4 channel gating (68, 346). If the DPPL NH<sub>2</sub> terminus interacts with a cytoplasmic domain of the Kv4 channel remains to be explored. Also, it is uncertain how many DPPL molecules bind to the tetrameric Kv4 channel. DPP6 is more stable as a dimer than as a monomer (281). Most likely, the Kv4 channel complex contains four DPP6 molecules (two dimers) (275). DPPL subunits can form *in vitro* homo- as well as heterodimers (281). Consider the possibility that Kv4 channel multiprotein complexes assemble heterodimeric

DPPL subunits and different KChIP isoforms. This enables almost unlimited combinatorial possibilities for Kv4 channel multiprotein complexes in neuronal membranes. How extensively heteromultimerization contributes to Kv4 channel diversity in excitable cells is uncertain and needs to be explored.

The human DPP6 gene expresses three isoforms (DPP6.1–3) (Fig. 9). As with other Kv-channel ancillary subunits, DPP6 isoforms have a conserved COOH-terminal domain and a variable NH<sub>2</sub>-terminal cytoplasmic domain differing in length and sequence (106, 161). In the mouse, one embryonic isoform (DPP6-E) and four adult isoforms DPP6-L (long), DPP6-S (short), DPP6-K, and DPP6-D have been detected (115, 186, 285). DPP6-L is expressed almost exclusively in the brain; DPP6-S is also found in other organs, e.g., in heart (227). DPP6-L, DPP6-S, and DPP6-K have distinct but partially overlapping expression profiles in the brain (114, 160, 186, 346). DPP6-S and DPP6-K showed a wide-spread expression, whereas DPP6-E and DPP6-L showed a more restricted expression profile. The human DPP10 (DPPY) gene expresses four isoforms (DPP10.1–4, slice variants a-d; Refs. 115, 186).

The expression pattern of DPP6, DPP10, and KChIP isoforms overlaps with those of Kv4.2 and Kv4.3 in somatodendritic localizations throughout the rodent brain, e.g., in cortex, hippocampus, and cerebellum (114, 160, 187, 233, 346). The overlapping expression patterns support the notion that Kv4 channels represent heteromultimeric multiprotein complexes assembled from Kv4, KChIP, and DPPL. This observation found strong support by results obtained with coimmunoprecipitation experiments, using anti-Kv4, anti-KChIP, and anti-DPPL specific antibodies in tissue from heterologous expression systems and from solubilized membrane extracts of rat cortex, cerebellum, and hippocampus (11, 114, 115, 161, 187). However, in addition to the distinct neuronal expression patterns of KChIP isoforms, expression levels of DPPL subunits can substantially differ from one brain region to another. For example, DPP6 expression in hippocampus is markedly stronger than that of DPP10, whereas both subunits have a similar expression level in neurons of neocortical layers (114). How the different expression levels reflect variant heteromultimerizations to binary and ternary Kv4 channel complexes is presently unclear. Intuitively, however, distinct differences in subunit protein levels provide a reasonable explanation for the different biophysical properties of native A-type currents. In conclusion, Kv4-channel protein complexes containing different members of the KChIP and DPPL subunit families most likely reflect differences in A-type currents observed in various types of neurons.

Yet another turn in the complexity of Kv4 channel assembly with KChIP and DPPL is that DPPL isoforms, like KChIP, appear to have additional cellular functions unrelated to Kv4 channel activity. Thus, with the use of a



conditional DPP6 knockout mouse, it was shown that DPP6 occurs at high density in hippocampal mossy fibers where Kv4 channels are absent (53), and single nucleotide polymorphisms in the DPP10 gene have been shown to be associated with asthma (231). It is unknown whether these activities cross-talk with the ones associated with Kv4 channel activity. Possibly, reversible association with the Kv4 channel is connected with channel-unrelated functions of ancillary Kv4 subunits. Mutations in DPP6 have also been associated with human diseases, like amyotrophic lateral sclerosis (58, 309) and autism (163). It is not known in which way the mutated DPP6 is associated with these diseases.

#### D. Coexpression of KChIPs and DPPLs In Vitro

Heterologous coexpression of Kv4 channels with DPPL and KChIP subunits reveals two kind of general effects. The first alters the gating behavior of the Kv4 channel. The second one significantly increases surface expression of the Kv4 channel in the plasma membrane. Coexpression of DPP6-S with Kv4.2 in *Xenopus* oocytes induces large negative shifts in voltage dependence of steady-state activation ( $-30$  mV) and inactivation ( $-15$  mV) of the Kv4.2 current. Also, it significantly accelerates the time course of activation, inactivation, and recovery from inactivation (Table 3) (187). Detailed kinetic analysis showed that the presence of DPP6-S increases severalfold the rate of closed-state Kv4.2-channel inactivation, i.e., the main DPP6-S effect on Kv4-channel gating is to enhance preopen-closed state inactivation of the channel (117). Coexpression of DPP6-S with Kv4.2 yields A-type currents that inactivate faster with more positive membrane potentials. In contrast, coexpression of Kv4.2, KChIP1, and DPP6-S yields A-type currents that inactivate increasingly slower at higher positive membrane potentials, resulting in an U-shaped voltage dependence (11). Cerebellar granule cells express a combination of DPP6-S, KChIP1, and Kv4.2. Coexpression of DPP6-S together with KChIP1 and Kv4.2 indeed yields Kv4.2 currents faithfully displaying the characteristic properties of A-type currents recorded from cerebellar granule neurons (Fig. 10) (11, 161). This resemblance to native A-type currents was not observed when Kv4.2 was coexpressed with either ancillary subunit alone (187). Another example, where in vitro expressed A-type current properties match well to native A-type current, represents the coexpression of Kv4.2 and DPP6-E. This binary subunit combination generates A-type currents that inactivate increasingly faster with more positive membrane potentials. The results can provide a handy explanation for the voltage dependence of the time course of A-type current inactivation recorded from layer V neocortical neurons (25, 26, 132).

Differential effects on Kv4.2 current inactivation are also seen upon coexpression of Kv4.2 with members of

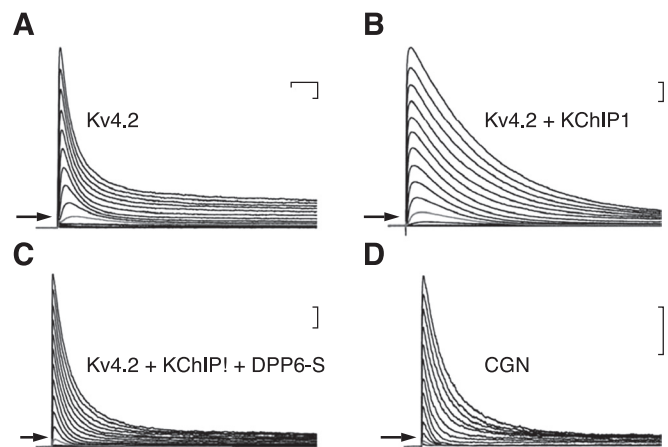


FIG. 10. Influence of ancillary subunits on Kv4 current properties. Families of membrane currents recorded with potential steps from  $-90$  to  $60$  mV in increments of  $10$  mV from a holding potential of  $-90$  mV on HEK293 cells. Cells were transfected with Kv4.2, KChIP1, and DPP6-S cDNA as indicated (A–C). A-type current recorded on cerebellar granule neuron (CGN) is shown in D for comparison. The currents closely resemble those shown in C (Kv4.2 + KChIP1 + DPP6-S). Arrows indicate current traces elicited by depolarizations to  $-30$  mV in A, to  $-40$  mV in B, and to  $-50$  mV in C and D. Horizontal scale bar,  $50$  ms; vertical scale bars,  $1$  nA for HEK293 cells (A–C) and  $0.5$  nA for CGN (D). [From Maffie and Rudy (161), with permission from John Wiley and Sons.]

the DPP10 subunit family, which consists of four isoforms (DPP variant a–d). Coexpression of Kv4.2 with DPP10a induces Kv4 currents exhibiting strong acceleration of inactivation with more positive membrane potentials, whereas inactivation of the Kv4 currents recorded after coexpression of Kv4.2 with DPP10c or DPP10d accelerates only slowly with more positive potentials (115). Interestingly, coexpression of DPP10c or DPP10d with KChIP3 and Kv4.2 induced a U-shaped voltage dependence of the time constants of Kv4 current inactivation. In contrast, coexpression of DPP10a with KChIP3 and Kv4.2 induced an A-type current inactivation which became monotonically faster with more positive potentials (115). Taken together, the in vitro expression data show that the biophysical properties of native A-type currents can satisfactorily be reproduced in vitro by choosing the right subunit combination (11, 114, 115, 161, 187). Note biophysical Kv4 current properties are also sensitive to decreasing or increasing relative amounts of subunit cRNA or cDNA (114).

Another aspect of DPPL subunits, which may be independent of their effects on Kv4 channel gating, is their influence on Kv4 channel surface expression. Coexpression of Kv4.2 with DPP6-S or DPP6-L in CHO cells results in a  $\sim 20$ -fold increase in the surface-exposed channel protein as measured by a surface protein biotinylation assay (Table 3) (187). This increase in surface expression of the Kv4.2 protein correlates with a similar current increase following coexpression of Kv4.2 with DPP6-S in CHO cells. The data indicate that binding of



DPP6 to Kv4 channels leads to a dramatic increase of Kv4 channels resident in the plasma membrane (187). It is possible that both ancillary subunits exert their effects on surface expression by different mechanisms. KChIPs have been proposed to facilitate anterograde trafficking of the Kv4.2 channel to the plasma membrane (see above). Conversely, DPPL subunits may slow retrograde trafficking by stimulating Kv4 channel retention in the plasma membrane by binding to components of the extracellular matrix. This hypothesis predicts that both ancillary subunits cooperatively stimulate cell surface expression of the Kv4 channel. Future studies will shed light onto the mechanisms that regulate cell surface expression of the Kv4 channel and the specific roles of Kv4 ancillary subunits in trafficking.

### E. Function of KChIPs In Vivo (Heart)

In mice, the  $I_{to}$  consists of a fast component ( $I_{to,f}$ ) characterized by fast activation, inactivation, and fast recovery from inactivation.  $I_{to,f}$  is mediated by Kv4.2 and Kv4.3 channels. The slow component of  $I_{to}$  ( $I_{to,s}$ ) is mediated by Kv1.4 channels. In addition, a slow K current ( $I_{K,slow}$ ) mediated by Kv1.5 and Kv2.1 channels and a steady-state K current component ( $I_{ss}$ ), possibly mediated by TASK1 channels, have been distinguished (193). In the mouse,  $I_{to,f}$  is important for fast action potential repolarization and may be responsible for the triangular action potential shape. Because binding of KChIP2 to Kv4.2/Kv4.3 accelerates recovery from inactivation, the mouse  $I_{to,f}$  is equipped with the important property to maintain

the high resting heart rate of the mouse ( $\sim 700$  beats/min).  $I_{to}$  has also been found in the heart of many other mammals. However, the relative subunit compositions and contributions of  $I_{to,f}$  and  $I_{to,s}$  to  $I_{to}$  vary within the different regions of the heart and from species to species (193, 209). In human and canine heart,  $I_{to}$  mediates the early phase of repolarization (phase 1) and sets the initial plateau potential (phase 2).

Whereas KChIP1–4 are expressed in the brain (13, 184), only KChIP2 is expressed in cardiac tissue (245), where it has been shown to interact with Kv4.2 and Kv4.3 to form  $I_{to,f}$  (193, 196). This is fortunate as it greatly simplifies investigations on the in vivo function of a particular KChIP isoform by choosing cardiac tissue for study. In canine and human ventricles, the density of KChIP2 mRNA and protein increases from endo- to epicardium, whereas Kv4.3 mRNA is uniformly expressed within a gradient of Kv4.3 protein (243, 245). It is assumed that the KChIP2 gradient regulates the Kv4.3 protein gradient, which then mediates the  $I_{to,f}$  gradient. Although in mouse ventricles there is a small transmural KChIP2 gradient, the transmural gradient of  $I_{to,f}$  is presumably caused by graded expression of Kv4.2 (244, 292). In vitro, KChIP2 increases Kv4-encoded K currents, slows inactivation, and accelerates recovery from inactivation (13, 65).

The functional importance of KChIP2 for  $I_{to}$  expression was clearly demonstrated in KChIP2 knockout mice (Table 4). The heart of these mice completely lacks  $I_{to,f}$  (136), whereas the amplitude of  $I_{K,slow}$  mediated by Kv1.5 is increased to an extent that the maximal peak K current in KChIP2 knockout mice is not changed. Although Kv4.2

TABLE 4. *KChIP and DPPX knockout mice*

Genetic Background	Behavioral Tests	Electrophysiology, Molecular Biology	Reference Nos.
KChIP1 <sup>-/-</sup>	Normal life expectancy, increased susceptibility to PTZ-induced seizures		334
KChIP2 <sup>-/-</sup>	Highly susceptible to arrhythmias, otherwise normal structure and function of the heart	AP duration prolonged, cardiac $I_{to}$ (Kv4.2/Kv4.3) absent, $I_{K,slow}$ increased; Kv1.5 mRNA increased, Kv1.4 and Kv2.1 mRNA unchanged	136, 295
KChIP3 / Calsenilin / DREAM <sup>-/-</sup>	No obvious movement disorders	A-type current decreased, LTP enhanced in dentate gyrus; CREB-dependent transcription during learning facilitated	9, 47, 50, 78, 147
	Enhanced learning and synaptic plasticity: shorter escape latencies (Morris water maze); fear conditioning: memory 24 h after training significantly enhanced	A $\beta$ amyloid peptide concentration levels reduced	
	8-Mo-old dream <sup>-/-</sup> mice display learning and memory capacities similar to young mice	Prodynorphin mRNA and dynorphin A peptides in the spinal cord increased	
	Marked analgesia in models of acute and chronic pain: latency in tail-flick assay prolonged, shock sensitivity increased	Cortical progenitor cells fail to express GFAP in response to PACAP: number of astrocytes reduced, number of neurons increased	
dppx <sup>-/-</sup>	Mice viable, no gross anatomical changes, possibly impairments in social interaction and learning	$I_A$ activation and inactivation shifted to more positive potentials, recovery from inactivation slowed, LTP increased	345

$I_{to}$ , transient outward K current;  $I_{K,slow}$ , sustained component of outward rectifying K current, LTP, long-term potentiation.

and Kv4.3 are still transcribed, in KChIP2<sup>-/-</sup> mice no  $I_{to}$  could be measured (295). Interestingly, in Kv4.2<sup>-/-</sup> mice, an upregulated  $I_{K,s}$  and increased transcription of Kv1.4 has been found (90). Although KChIP2 and Kv4 expression in the mouse heart seem to influence each other, the data also indicate that the compensatory mechanisms differ in Kv4.2<sup>-/-</sup> and KChIP2<sup>-/-</sup> mice. As a result of the abolished  $I_{to,f}$  the cardiac action potential is prolonged, making KChIP2 knockout mice susceptible to ventricular tachycardia (136). Hitherto, mutants in the human KChIP gene as a cause of a hereditary cardiac arrhythmia have not been described. Comparably to KChIP2, differences in  $I_{to}$  density are correlated with variations in cardiac Kv4.2 protein expression. Also, deletion of Kv4.2 eliminates  $I_{to}$  (90, 196). Note Kv4.3 is expressed in cardiac tissue as well. Remarkably, Kv4.3 mRNA expression is essentially the same in different heart regions and does not display a concentration gradient between endo- and epicardium like KChIP2 and Kv4.2 (245). Furthermore, loss of cardiac Kv4.3 expression in the mouse leaves  $I_{to}$  density unaffected. Thus Kv4.3 protein is unimportant for mediating  $I_{to}$  in the mouse (196). Its significance for cardiac K<sup>+</sup> channel expression is uncertain.

The effects of KChIP2 are not restricted to Kv4 channels. In addition to its binding to Kv4.2/Kv4.3 channels, KChIP2 impairs trafficking and cell surface expression of Kv1.5 channels in transiently transfected HEK293 cells (144). This important observation may explain the increased density of Kv1.5 channels in cardiomyocytes in KChIP2 knockout mice. Other examples support the notion that KChIP2 is a multifunctional Kv channel accessory subunit. Silencing of KChIP2 eliminates the Na<sup>+</sup> current in neonatal myocytes (65), and in KChIP2 knockout mice the L-type Ca<sup>2+</sup> current is decreased by 30% (296), suggesting that KChIP2 may have a chaperone function for Ca<sup>2+</sup> channels to increase cell surface expression. These data indicate that in vivo KChIP2 modulates Kv4 channel gating properties and is involved in regulating surface expression of different types of ion channels (Kv1.5, Kv4, Na<sup>+</sup>, and Ca<sup>2+</sup> channels). DPPLs are also expressed in the human heart. Since coexpression of Kv4.3 with KChIP2 does not satisfactorily reproduce the characteristic fast kinetics of inactivation and recovery from inactivation of human cardiac  $I_{to,f}$ , it was found that a heterologously expressed ternary complex of Kv4.3, KChIP2 and DPPX produced current kinetics very similar to  $I_{to,f}$  in human cardiomyocytes (227). Like KChIPs, DPPL function may go beyond an interaction with Kv4 channels. DPP10 affects Kv1.4 channel properties comparably to Kv4 channels, accelerating the time course of Kv1.4 current activation and shifting the voltage dependence of activation and inactivation to more negative membrane potentials. However, in contrast to its effect on Kv4 channels, DPP10 slows recovery from inactivation of Kv1.4 channels (144).

## F. Function of KChIPs and DPPLs for Native A-type Currents In Vivo (Brain)

Based on in vitro expression experiments, one may expect that the Kv4 channel associates with KChIPs and DPPLs to form large heteromeric protein complexes. Indeed, KChIP and Kv4 channel protein are coimmunoprecipitated from brain lysates, demonstrating association of the two types of ancillary subunits with native Kv4 channel (13, 101, 227, 245). However, one can only but speculate how many different Kv4 multiprotein complexes are expressed in the brain and what the underlying physiological basis is. Using specific anti-KChIP1–4 and anti-Kv4.2 or -Kv4.3 antibodies, Kv4 channel complexes were localized to neuronal somata and dendrites in immunohistochemical investigations on rodent brain slices (233). Apparently, the Kv4 channel complexes are being concentrated towards distal dendritic compartments of hippocampal pyramidal neurons and contain both types of ancillary subunits. This observation is supported by a combination of electrophysiological experiments showing higher  $I_{SA}$  density at distal than at proximal dendrites in these cells (100, 119) and by siRNA experiments knocking down DPP6 expression in hippocampal CA1 neurons through viral infection of an organotypic hippocampal slice preparation (126). The results indicated that Kv4 channels need DPP6 in CA1 neurons to steer precision of onset in action potential firing (126, 161). On the basis of data from heterologous expression studies (see above), it was predicted that knockdown of DPP6 would decrease Kv4 channel activity and, thereby, enhance excitability of CA1 pyramidal neurons. In contrast, the results from somatic recordings showed that siDPPX expression caused a decrease in subthreshold excitability of CA1 pyramidal neurons. The authors offer two alternative explanations to explain their unanticipated findings. First, DPP6 knockdown leaves more Kv4 channels available at rest and increases the window, where A-type current persists at steady state near the membrane resting potential. The increased window current induced an increase in the resting conductance leading to delayed onset of action potential firing upon depolarizing current injection. Second, DPP6 knockdown shallows the voltage dependence of Kv4 channel activation, which may significantly delay action potential onset times. Note the data add a cautious note to linear extrapolations between results obtained from studies using in vitro expression systems and transient channel subunit expression and those obtained by manipulating primary neurons.

The single-channel conductance ( $\gamma$ ) of neuronal somatodendritic A-type K<sup>+</sup> channels is about twofold larger than that of Kv4 channels expressed in heterologous cells. Association of DPP6-S with the Kv4 channel seems responsible for the observed  $\gamma$  difference between native and heterologously expressed Kv4 channels (125). Coex-

pression of the Kv4.2 channel with DPP6-S was sufficient to match the single-channel conductance of native Kv4 channel measured on cerebellar granule (CGN) neurons. On the other hand, CGN Kv4 channels from *dpp6* knockout mice showed a  $\gamma$ -like heterologously expressed Kv4 channel. Note KChIPs have no influence on  $\gamma$  of the Kv4 channel (24, 101). In summary, DPP6-S has several favorable effects on crucial aspects of Kv4 channel function. It promotes trafficking to the plasma membrane, accelerates recovery from inactivation, shifts the voltage dependence of activation to more negative voltages, and enhances single-channel conductance. Preliminary work reports that loss of DPP6-S in knockout mice affects LTP, learning, and social behavior (Table 4) (345). Furthermore, recent reports indicate that *dpp6* may belong to the susceptibility genes for amyotrophic lateral sclerosis (ALS) and autism (163, 309). To dissect the different effects of DPPLs on native Kv4 channels and how they contribute to functional and behavioral phenotypes in the mouse will be a challenging and important undertaking in the future.

Both the expression of KChIPs and their assembly with Kv4 protein displays a distinct pattern in different regions (or neurons) of the rodent brain. KChIP1 is colocalized with Kv4.3 in cerebellar Purkinje cells, and with Kv4.2 and Kv4.3 in hippocampal interneurons, cerebellar granule cells, and neurons of the thalamus. KChIP2 colocalizes with both Kv4 channels in apical and basal dendrites of hippocampal and neocortical pyramidal cells, whereas KChIP3 is predominantly expressed together with Kv4.2/Kv4.3 in neocortical layer VI, dentate gyrus of the hippocampus, and cerebellar granule and Purkinje cells. The differential expression of KChIPs may suggest that they have some nonoverlapping functions in the nervous system. This point of view is supported by the observation of noncompensated phenotypes in KChIP2 and KChIP3 knockout mice (50, 136, 147). KChIP4 was detected in all neocortical layers, the hippocampal CA1 region, the thalamus, and Purkinje cells (13, 114, 233). The data suggest that certain neurons appear to specifically express only one particular isoform, whereas other neurons, for example, the Purkinje cells, express more than one KChIP isoform. Potentially, KChIP4, which does not promote surface expression of Kv4.2, may competitively antagonize binding of other KChIPs to Kv4.2 (274). Whether these observations implicate that one Kv4 channel associates in a generic fashion with different KChIPs in heteromultimeric protein complexes or, alternatively, the formation of distinct subsets, each containing only one type of KChIP, is presently not known. To further our present understanding of KChIP expression patterns, it would be important to directly and quantitatively probe the functioning of KChIPs on ionic currents in intact neurons. Note a lack of investigations on a  $\text{Ca}^{2+}$ -dependent regulation of Kv4 channel activity by KChIPs, although knowl-

edge about the sensitivity of dendritic KChIP/Kv4 channel activity towards changes in cytoplasmic  $\text{Ca}^{2+}$  contraction might be of particular interest. Intuitively, a  $\text{Ca}^{2+}$ -binding protein such as KChIP would have the potential to confer  $\text{Ca}^{2+}$  sensitivity to Kv4 channel activity. This would be of high functional importance in dendritic boutons where transient increases in  $[\text{Ca}^{2+}]_i$  during synaptic transmission could induce transient changes in the binding affinity of KChIPs to Kv4 channels.

Although much is known about the regional and neuronal specificity of KChIP isoform expression, it is unclear how this affects the Kv4 channel in terms of localization to different neuronal compartments, trafficking, lifetime in the plasma membrane, endocytosis, and proteasomal degradation. Studies with Kv4.2 and KChIP-knockout mice have revealed very complex relationships between Kv4 channel and KChIP expression in the nervous system. Kv4.2 knockout mice exhibit a marked region-specific decrease in the expression of specific KChIP isoforms. For example, KChIP2 and KChIP3 expression is decreased in hippocampus, that of KChIP2 in striatum, and that of KChIP1 and KChIP3 in cerebellum (180). Conversely, KChIP1 and KChIP2 expression are unaffected in visual cortex, whereas KChIP3 protein expression is drastically reduced (192). Clearly, the data indicate a cross-talk between Kv4.2 and KChIP expression. Yet, regulation of this cross-talk seemingly differs among different brain regions or neurons. The mechanisms leading to such a complex subtype- and neuron-specific regulation of KChIP expression remain to be investigated. Also, the possible involvement of DPPL in this cross-talk is an important aspect of Kv4 channel activities in future investigations.

Astonishingly, Kv4.2 knockout mice apparently have a relatively normal phenotype and behavior. Also, there is no compensatory upregulation or redistribution of Kv4.3 channels (108). Conversely, loss of KChIP3 expression in KChIP3 knockout mice leads to a decrease in A-type current density in those neurons which strongly express KChIP3 and Kv4.2/Kv4.3 in the wild-type mouse (Table 4) (147). In particular, the decrease in Kv4 current amplitude in granule cells of the dentate gyrus appears associated with enhanced long-term potentiation (LTP) in the hippocampus. An attractive explanation for enhanced LTP in the KChIP3 knockout mice provides the proposed role of Kv4 channels as dendritic shock absorbers (100). It follows that a loss in Kv4 channel activity would lead to a more effective or unfiltered transmission of synaptic input. In conclusion, specific knockout of a KChIP isoform displays a defined decrease in Kv4.2 channel affecting LTP in distinct areas of the rodent brain. In contrast, the general loss of Kv4.2 expression leads to turmoil in KChIP isoform expression in the brain.



### G. KChIP Function Unrelated to K<sup>+</sup> Channel Activity

Multifunctionality seems a relatively widespread phenomenon for auxiliary proteins that is also relevant for those of ion channels. Here gephyrin presents a striking example as it is required for synaptic clustering of glycine channels in neurons of the spinal cord as well as for molybdoenzyme activity in nonneuronal tissue (74). Also KChIP isoforms have in addition to the common interaction with Kv4 channels other cellular activities. Thus observed phenotypical and cellular physiological changes in KChIP knockout mice might not solely originate from loss of KChIP function as ancillary Kv4 channel subunit. A very interesting aspect of KChIP physiology is that KChIP3 and KChIP4 interact with the presenilins and affect the processing of amyloid precursor protein (43, 184). KChIP3 isoforms have been characterized as calsenilin (43) and, respectively, as DREAM (45), even before recognizing KChIP3 as an ancillary Kv4 channel subunit. Calsenilin binds to presenilin, an important component of the  $\gamma$ -secretase, which is mainly localized to the ER and Golgi apparatus. Ca<sup>2+</sup>-dependent binding of calsenilin to presenilin-1 activates  $\gamma$ -cleavage of the  $\beta$ -amyloid precursor protein ( $\beta$ APP). Thus calsenilin stimulates in a Ca<sup>2+</sup>-dependent manner production of  $\beta$ -amyloid peptide, a crucial molecule in the pathophysiology of Alzheimer disease (147). In KChIP3 knockout mice, there is a decreased  $\beta$ -amyloid peptide concentration especially in cerebellum and cortex, which concurs with the hypothesis that calsenilin in vivo stimulates  $\gamma$ -secretase activity. The expression pattern of calsenilin (KChIP3) overlaps both that of presenilin and of the Kv4 channel (147).

The KChIP3 gene encodes an isoform (KChIP3.1) that acts as a Ca<sup>2+</sup>-regulated nuclear transcription factor and is denoted DREAM. DREAM activity of KChIP3 refers to its ability to act as a repressor of transcription when it is Ca<sup>2+</sup> free but not Ca<sup>2+</sup> bound (45). Compared with calsenilin (KChIP3.2), DREAM displays 30 additional residues at the NH<sub>2</sub> terminus (280). In fact, isoforms of all four KChIPs have been shown to have DREAM activity (149). The very different functions and cellular localizations of calsenilin and DREAM emphasize the importance of the variant NH<sub>2</sub> termini for cellular KChIP isoform function. At low intracellular Ca<sup>2+</sup> concentrations, DREAM represses transcription of the prodynorphin gene and the *c-fos* gene by binding downstream of the transcription start site to a conserved DNA sequence element, dubbed downstream regulatory element (DRE). Binding of Ca<sup>2+</sup> to DREAM attenuates DREAM repressor activity and elevates DREAM binding to its DRE binding site (43, 45). In line with DREAM function as a repressor of dynorphin-gene transcription, DREAM (KChIP3) knockout mice contain an increased concentration of dynorphin-A peptide in the spinal cord (Table 4). The knockout mice show a remarkable decrease in pain sensi-

tivity (50). It is likely that increased dynorphin-A binding to  $\kappa$ -opiate receptors is the molecular basis of reduced pain sensitivity.

Potentially, the different activities of KChIP3 may jointly play an important role in learning and memory of the mouse (Table 4), consistent with the observation that hippocampus LTP at perforant path-dentate granule cell synapses is enhanced (147). A recent study evaluated the role of KChIP3 in a hippocampus-dependent memory task, contextual fear conditioning. KChIP3 knockout mice showed in this task a significantly enhanced memory (9). Possibly, an increase in *c-fos* activity can be associated with enhanced LTP observed in the dentate gyrus of the KChIP3<sup>-/-</sup> hippocampus (147). The reported enhancing effect of KChIP3 on Ca<sup>2+</sup>-regulated secretion in PC12 cells may add other facets to a role of KChIP3 in cellular excitability (312). Importantly, studies with wild-type mice showed a marked redistribution of KChIP3 protein during fear conditioning training. It was observed in the data that membrane association and interaction with Kv4.2 of KChIP3 protein was significantly decreased, and nuclear KChIP3 (DREAM) expression was increased 6 h after the conditioning paradigm with no significant change in KChIP3 mRNA. Furthermore, prodynorphin mRNA expression was significantly decreased after training in wild-type but not in KChIP3<sup>-/-</sup> animals (9). These data suggest an intricate mechanism coupling neuronal excitability and gene transcription by redistributing KChIP3 between membrane and cell nucleus in consolidation of contextual fear conditioning memories.

## IV. KCNEs (MinK AND MiRPs)

### A. Structural Basis of KCNE-Kv7.1 Interactions

MinK (KCNE1) and MinK-related peptides MiRP1–4 (KCNE2–5) are small ancillary subunits (14–20 kDa or 103–177 residues) with one membrane-spanning domain (Fig. 11). KCNEs generally interact with members of the Kv7 (KCNQ) channel family and markedly modify their gating (174). KCNE1, also named IsK or MinK (minimal K channel protein), was initially reported to represent the minimal or smallest protein that could form a K channel (287). Subsequent in vitro studies showed that KCNE1 acts as ancillary  $\beta$ -subunit of the Kv7.1 channel (23, 248). Compared with Kv $\beta$ -, KChIP-, or DPPL-subunits, KCNEs distinguish themselves by several remarkable features.

First, KCNEs stand out as  $\beta$ -subunits because mutations in KCNE genes are associated with hereditary, especially cardiac diseases. For example, the Kv7.1/KCNE1 channel complex represents the molecular basis of  $I_{Ks}$ , the slow component of the delayed rectifier K current in cardiac ventricle (23, 248). Mutations in KCNE1 (or Kv7.1) are associated with a life-threatening cardiac arrhythmia,



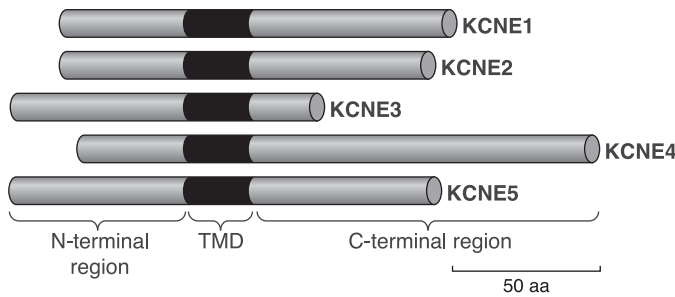


FIG. 11. Bar diagram of KCNE protein family. Each human KCNE gene expresses one subunit (KCNE1–5). Genebank (NCBI) accession numbers are as follows: CAG46556 (KCNE1), NP\_751951 (KCNE2), CAG33490 (KCNE3), NP\_542402 (KCNE4), ABQ08564 (KCNE5). Transmembrane domain (TMD) is indicated by a black box.

the long QT syndrome (LQT) (248). The other KCNE family members (KCNE2–5) have also been associated with inherited cardiac arrhythmias (34, 111, 159, 279, 309, 341). The KCNE5 gene is one of at least four genes deleted in the human AMME contiguous gene syndrome (Alport syndrome predominantly characterized by a chronic kidney disease and deafness, mental retardation, midface hypoplasia, and the erythrocyte abnormality elliptocytosis) (214). In which way the KCNE5 gene deletion is involved, e.g., in the neurological symptoms of this syndrome, is unclear.

Second, each KCNE is separately encoded by one gene, and splice variants are not known. Unlike Kv $\beta$ , KChIP- and DPPL-subunits, KCNE subunit sequences are relatively uninformative with respect to functional conserved domains. The sequences do not reveal a conserved COOH-terminal core region preceded by a variant NH<sub>2</sub>-terminal sequence. Sequence variations encompass the entire KCNE molecule. KCNEs contain one transmembrane domain like DPPLs but have a contrasting topology with the NH<sub>2</sub> terminus on the extracellular and the COOH terminus on the intracellular side of the membrane. As yet, a KCNE high-resolution structure is missing.

Third, stoichiometry and specificity of KCNE/Kv channel complexes are a matter of conjecture. Recent data indicate that two KCNE molecules bind to one tetrameric Kv7.1 channel (183). The 0.5:1 stoichiometry differs from the 1:1

stoichiometry of Kv $\beta$ -Kv1 and, respectively, KChIP-Kv4 channel complexes. Assembly of KCNE1 and Kv7.1 subunits apparently occurs at early stages in channel maturation promoting transport of the Kv7.1 channel to the plasma membrane and Kv7.1 current density (98, 134, 269).

Fourth, although most significant changes have been reported for KCNE effects on Kv7.1 channel gating (Table 5; Fig. 13), KCNE interaction with Kv channels seems promiscuous. Importantly, a modulation of cardiac HERG channel activity by KCNEs has been reported, suggesting multimeric HERG/KCNE channel complexes underlying  $I_{Kr}$  in cardiac cells.  $I_{Kr}$  represents an important repolarizing current for cardiac action potentials. Mutations in the HERG gene are also associated with an LQT syndrome (61, 249). In addition, a considerable number of ion channels have been reported to be modulated by KCNE1–5, e.g., Kv1, Kv2, Kv3, Kv4, and HCN channels (174, 291). This leaves us with a blurred picture of KCNE-ion channel interaction specificity. Possibly, some of the reported modulations are only observable in *in vitro* expression systems, which are notorious for artefacts caused by protein overexpression. Yet, it is quite remarkable that so many different ion channels are sensitive to the presence of KCNEs.

## B. Effects of KCNEs on Kv7.1 Channels In Vitro

Most studies were carried out coexpressing KCNE1 or KCNE3 together with Kv7.1 in heterologous expression systems (Table 5). By itself, the Kv7.1 channel distinguishes itself by two important features from other Kv channels, for example, the *Shaker* channel. First, the Kv7 channel disposes of a relatively short NH<sub>2</sub> terminus and a long COOH terminus. The latter contains tetramerization domain(s) determining the specificity of Kv7-subunit assembly as well as calmodulin binding sites and two coiled-coiled domains (91, 107, 256, 330). The crystal structure of part of the COOH terminus including the coiled-coiled domains has recently been solved (107). Second, the differences in topological organization of *Shaker* and Kv7.1 channel likely reflect significant differences in Kv7.1 channel gating that is both voltage and Ca<sup>2+</sup> sensitive (98, 269,

TABLE 5. KCNE effects on KCNQ1 channels in heterologous expression systems

KCNQ1	Increase in Surface Expression	Activation Kinetics	Activation $V_{1/2}$	Deactivation	Reference Nos.
+KCNE1 (Mink)	2- to 10-fold	–	Approximately +20 mV	±	14, 23, 41, 223, 248, 257, 303, 320
+KCNE2 (MiRP1)	–	+	+	+	64, 298
+KCNE3 (MiRP2)	2- to 10-fold	+	+	+	3, 257
+KCNE4 (MiRP3)	±	–	+, 50 mV	+	14, 27
+KCNE5 (MiRP4)	±	–	+, >140 mV	+	14, 27

+, Increase in parameter or shift to more positive potentials; –, decrease or shift to more negative potentials; ±, no effect.  $V_{1/2}$ , membrane potentials at which 50% of the channels are activated.

270). Thus, under certain conditions, the Kv7.1 channel shows a voltage-independent as well as a voltage-dependent conductance (223, 248, 303).

Coexpression of KCNE1 or KCNE3 with the Kv7.1 channel elicits dramatic and opposing effects on Kv7.1 channel gating behavior. Association of KCNE1 with Kv7.1 apparently stabilizes a closed conformation of the Kv7.1 channel, whereas the one of KCNE3 with Kv7.1 seems to destabilize the closed (or conversely stabilize the opened) Kv7.1 channel. Main features of KCNE1 effects on Kv7.1 channel gating are a marked slowing of the activation time course, a voltage-conductance relation shifted by  $\sim 20$  mV to more positive potentials, suppression of inactivation, and four- to sevenfold increase in single-channel conductance (23, 223, 248, 268, 279, 340). Potential effects of KCNE1 on  $\text{Ca}^{2+}$ -dependent gating of the Kv7.1 channel are still unexplored. In contrast, association of KCNE3 with Kv7.1 generates voltage-independent channels (Fig. 13D). The complete loss in voltage-dependent gating is accompanied by an  $\sim 10$ -fold increase in current density (3, 27, 257). Gating properties of the KCNE3/Kv7.1 channel resemble those of a  $\text{K}^+$  channel found in crypt cells of small intestine and colon. This  $\text{K}^+$  channel is open at the membrane resting potential and plays an important role in  $\text{K}^+$  recycling by crypt cells. In summary, heterologous expression of KCNEs with Kv7.1 can generate both voltage-dependent and voltage-independent  $\text{K}^+$  channels that resemble important  $\text{K}^+$  channels in native tissue (Fig. 13).

In addition to Kv7.1 channel trafficking and gating behavior, KCNEs affect Kv7.1 channel pharmacology. It is likely that the many and diverse KCNE effects reflect considerable conformational changes associated with KCNE-Kv7.1 interaction. It distinguishes KCNE from Kv $\beta$  and KChIP subunits, whose binding to Kv channels leaves their conformation relatively undisturbed. Indeed, mutagenesis studies have implicated the extracellular  $\text{NH}_2$  terminus, transmembrane spanning region, as well as cytoplasmic COOH terminus of the KCNE subunit in its various modulatory actions. A solution NMR study investigating the interaction between KCNE1 and Kv7.1 proposed that KCNE1 interacts with pore helix (S5-P-S6) residues (Fig. 12A) and that the single transmembrane domain of the KCNE1 protein is located in a cleft between voltage sensor domain of one Kv7.1 subunit and the pore helix of a neighboring subunit (Fig. 12B) (123). Tryptophan-scanning mutagenesis suggests that KCNE1 and KCNE3 reside in slightly different positions close to the Kv7.1 pore, thereby differently perturbing the S6 domain (205). Recent tryptophan and cysteine mutagenesis studies suggest that KCNE1 lodges between S1, S4, and S6 of three separate Kv7.1 subunits (269, 335). However, the models based on indirect data are tentative and use the Kv1.2 crystal structure as a template. The models await validation by crystallographical analysis of the KCNE1/Kv7.1 channel complex.

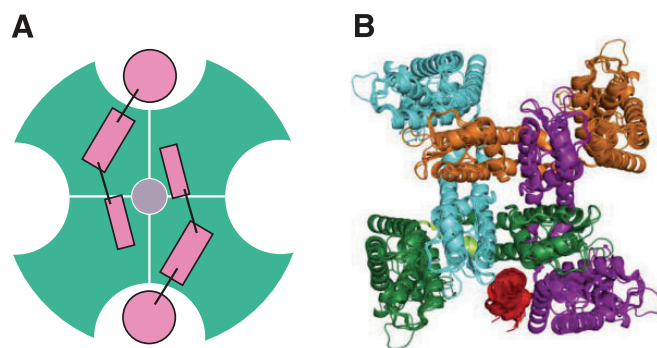


FIG. 12. Model of Kv7.1-KCNE1 channel protein complex. A: schematic presentation of the complex viewed from the extracellular top side. Model is based on the reported 2:4 stoichiometry of the KCNQ1-KCNE1 complex. KCNQ1 tetramer is illustrated by the green shapes. KCNE1 is in pink. The  $\alpha$ -helical transmembrane domain of KCNE1 is diagrammed as a circle, and the connecting lines and the pink rectangles indicate hypothetical locations of  $\text{NH}_2$ - and/or COOH-KCNE1 termini. B: ribbon diagram of Kv7.1-KCNE1 channel in the opened state. The model only shows one transmembrane domain of KCNE1 (residues 45–71), which is in red. The four Kv7.1 subunits are based on the Kv1.2 crystal structure. Subunits are green, magenta, light blue, and brown. [From Kang et al. (123).]

All three KCNE domains, extracellular  $\text{NH}_2$  terminus, transmembrane region, and cytoplasmic COOH terminus, are apparently engaged in some kind of interaction with the Kv7.1 channel. Association of KCNE1 with Kv7.1 reduces the sensitivity of the Kv7.1 channel to the specific Kv7-channel blocker XE991 14-fold (320) and increases the sensitivity to blockers like chromanol 293B or azimilide (41). The effect of KCNE1 on Kv7.1-channel pharmacology depends on the extracellular KCNE1  $\text{NH}_2$  terminus (256). A recently described contact in the extracellular KCNE1 and Kv7.1 domains (335) tentatively suggests that both domains jointly form a receptor site for antagonist binding to the extracellular side of the Kv7.1 channel pore. Effects on Kv7.1 pharmacology are not specific for KCNE1. Like KCNE1, KCNE2 and KCNE3 increase Kv7.1 sensitivity to block by chromanol 293B (298).

Apparently, the KCNE transmembrane region dominates the opposing effects of KCNE1 and KCNE3 on Kv7.1 gating. Swapping a short stretch of three amino acid residues within the transmembrane region of KCNE1 and KCNE3 (FTL 57–59 of KCNE1, TVG 71–73 of KCNE3) can confer to KCNE1 KCNE3-like effects on Kv7.1 channel gating and, vice versa, to KCNE3 KCNE1-like activity (178, 179). The data are in good agreement with mutagenesis studies suggesting an engagement of KCNE1 in interactions with Kv7.1 transmembrane segments S1, S4, and S6 (269, 335).

The KCNE1 COOH terminus binds to a Kv7.1 COOH-terminal domain which includes both coiled-coiled structures (91). This is in contrast to *Shaker* channels whose  $\text{NH}_2$ -terminal T1 tetramerization domain serves as a platform for a localized attachment of the Kv $\beta$  subunit (89). Both pulldown and immunoprecipitation experiments

demonstrated direct interaction between the COOH termini of KCNE1 and Kv7.1 (91). Note several LQT mutations are caused by mutations of amino acid residues in the KCNE1 COOH terminus. For example, a KCNE1 LQT-mutant (D76N), which alters the sequence of a conserved region within the proximal COOH terminus, seems to play a role in determining single-channel conductance and current density (59, 179). Presumably, the D76N mutation disturbs a correct positioning of KCNE1 within the KCNE1/Kv7.1 channel complex leading to a marked reduction in  $I_{Ks}$  amplitude (268). Another KCNE1 LQT mutant (L51H) is unable to traffic to the plasma membrane at the cell surface, underlining the importance of KCNE1/Kv7.1 assembly for normal Kv7.1 channel trafficking (34). On the other hand, association of KCNE1 with Kv7.1 appears insensitive to a deletion of the KCNE1 COOH terminus. The deletion, however, greatly impairs KCNE1 modulation of the Kv7.1 channel (289). The specific contributions of the three KCNE domains to the observed KCNE effects on Kv7.1 trafficking and gating need to be further unraveled in future studies. Clearly, both transmembrane and COOH-terminal KCNE domains affect the gating behavior of the Kv7.1 channel. Whether the domains function synergistically or independently of each other, as suggested by a "bipartite" model (79, 238), is still a matter of conjecture.

Comparably to KCNE3, coexpression of KCNE2 and Kv7.1 in COS cells yields constitutively open K<sup>+</sup> channels. KCNE2/Kv7.1-mediated currents almost instantaneously activate upon depolarization and rapidly deactivate upon repolarization, displaying an essentially linear voltage-current relation (298). Interestingly, the KCNE2/Kv7.1 channel exhibits a lower K<sup>+</sup> selectivity than the Kv7.1 channel (48 vs. 58 mV change upon a 10-fold change in extracellular K<sup>+</sup> concentration). Possibly, the KCNE2/Kv7.1 channel contributes to maintenance of the resting potential, e.g., in epithelial cells of stomach or intestine (97). Note mutations in the KCNE2 gene are also correlated with the LQT syndrome. However, the consequences of KCNE2 mutations for cardiac K<sup>+</sup> channel activity are unclear because in vitro both KCNE2 and KCNE3 can interact with at least four different cardiac Kv channels (Kv1.5, Kv4.2, Kv7.1, and HERG) (174).

KCNE4 (MiRP3) is unique among KCNE subunits. Coexpression of KCNE4 and Kv7.1 suppresses Kv7.1 current, whereas other Kv channels, e.g., Kv7.2-Kv7.5 and HERG, are insensitive to KCNE4 inhibition. Large depolarizations (>50 mV), however, slowly activate KCNE4/Kv7.1 currents, indicating that KCNE4 shifts Kv7.1 activation curve to even more positive (unphysiological) membrane potentials than KCNE1 (85). As for KCNE1 and KCNE3, KCNE4 transmembrane domain and COOH terminus are important for KCNE4 activity (162). A physiological function of the KCNE4/Kv7.1 channel complex is not known. The inhibitory action of KCNE4 is, however, not confined to Kv7.1, as KCNE4 reportedly also sup-

presses Kv1.3 currents in leukocytes by modulating trafficking, surface expression, and Kv1.3 channel gating (278). KCNE5 (MiRP4) also interacts with Kv7.1, shifting its activation curve by more than 140 mV to more positive potentials. KCNE5 is expressed in the heart, but whether it is also part of the Kv7.1 channel complex is not known (14). In Figure 13, *E* and *F*, activating membrane currents were only recorded at large positive potentials (up to 90 mV).

For a full reproduction of KCNE1/Kv7.1 channel properties, the complex has to be supplemented with yotiao, a protein kinase A (PKA) anchoring protein (AKAP). Yotiao binds to the Kv7.1 COOH terminus. Binding involves NH<sub>2</sub>- and COOH-terminal yotiao-binding domains and a COOH-terminal Kv7.1 leucine zipper motif. Yotiao acts as a scaffolding protein to position regulatory and catalytic PKA subunits as well as the phosphatase protein phosphatase 1 (PP1) close to the Kv7.1 channel, thereby controlling the state of Kv7.1 channel phosphorylation at an NH<sub>2</sub>-terminal serine residue (Ser-27) (167, 195). This is physiologically

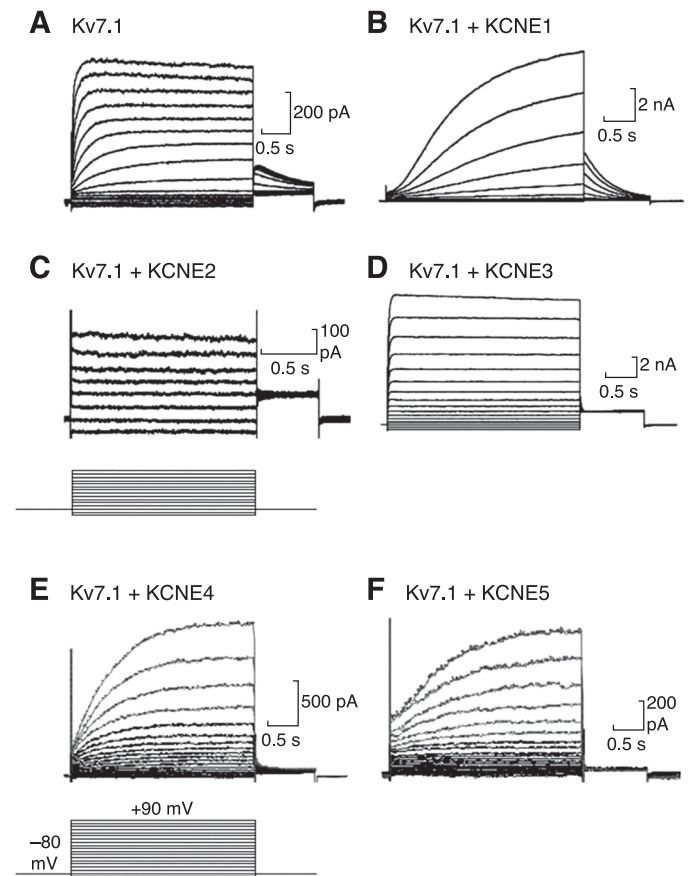


FIG. 13. Influence of KCNE subunits on Kv7.1 currents. After transfection of COS-7 cells with Kv7.1 cDNA alone (*A*) or together with KCNE1 (*B*), KCNE2 (*C*), KCNE3 (*D*), KCNE4 (*E*), and KCNE5 (*F*), currents were recorded in the whole cell patch-clamp configuration. Holding potential was  $-80$  mV. Currents were elicited at test potentials ranging from  $-100$  to  $40$  mV in increments of  $10$  mV (*A–D*) and from  $-100$  to  $90$  mV (*E* and *F*). [From Bendahhou et al. (27), by permission of Oxford University Press.]



very important because a read-out of  $\beta$ -adrenergic signaling in cardiomyocytes is associated with Kv7.1 phosphorylation. This leads to an increase in  $I_{Ks}$  amplitude concomitant with accelerated action potential repolarization. A comparable stimulation of Kv7.1 current by PKA phosphorylation is only observed in vitro if Kv7.1 is coexpressed together with KCNE1 and yotiao. Apparently, assembly of quite a large multiprotein complex is required to reproduce all facets of  $I_{Ks}$  properties (138). Interestingly, a mutation in the human Kv7.1 gene (G589D), which disturbs assembly of the Kv7.1/KCNE1/yotiao multiprotein complex, renders the Kv7.1 channel insensitive to PKA phosphorylation. This mutation is correlated with LQT syndrome emphasizing yotiao binding as an important component for physiological Kv7.1 activity and its response to  $\beta$ -adrenergic signaling (138, 167).

### C. Effects of KCNEs on HERG In Vitro

A potentially physiologically important example for KCNE promiscuity is the finding that KCNE1 and KCNE2 can interact in in vitro expression systems with the HERG (human ether-à-go-go-related gene) channel (4, 111, 158, 174, 175, 307). Upon depolarization, the HERG channel very slowly activates and rapidly inactivates, endowing the HERG channel with inwardly rectifying properties (250, 273, 304). The HERG channel mediates  $I_{Kr}$ , the rapidly activating  $K^+$  current component of repolarizing current in cardiac action potentials (249). Biophysical properties of  $I_{Kr}$  can be fairly well reproduced by coexpressing two HERG isoforms, HERG1a and HERG1b, suggesting that heteromeric HERG1a/1b channels mediate  $I_{Kr}$  (139, 140, 152). In addition, the native channels are presumably associated with KCNE1 (175) and/or KCNE2 (4). In heterologous expression systems, HERG and KCNE1 can be coimmunoprecipitated, most likely indicating coassembly of the two subunits.

In contrast to KCNE1 effects on Kv7.1, coexpression of KCNE1 and HERG leads to a relatively mild increase in current density ( $\sim 2$ -fold), a negatively shifted voltage-conductance relation, and an increase in steady-state inactivation (175). Both effects of KCNE1, increase in HERG current density and changes in biophysical properties, were abolished when HERG was coexpressed with the KCNE1 LQT mutant D76N (34, 175). Incubation with anti-sense oligonucleotides against KCNE1 decreases the amplitude of  $I_{Kr}$  in a cell line (AT-1) derived from a mouse atrial tumor in which  $I_{Kr}$  is constitutively present (339). Although somewhat less dramatic than on Kv7.1 current, KCNE1 effects on HERG current are potentially significant in cardiac ion channel physiology.

Similarly to KCNE1, KCNE2 can be coimmunoprecipitated together with HERG following coexpression in CHO cells (4). When coexpressed in *Xenopus* oocytes, KCNE2 apparently exerts several effects on the HERG

channel. It slows activation, accelerates deactivation, shifts the activation curve by  $\sim 9$  mV to more positive membrane potentials, and decreases HERG current amplitude, presumably due to a decrease in single-channel conductance, whereas development of and recovery from inactivation remain unchanged (4). However, the results are equivocal, since they could not be reproduced in mammalian expression systems (CHO, HEK 293, GH<sub>3</sub>/B<sub>6</sub> cells) (59, 158, 169, 253, 325). Taken together, presently available data indicate association of KCNE2 and HERG, but this seems to produce only small changes in HERG biophysical properties. Also, pharmacological properties of HERG and HERG/KCNE2 channel show essentially similar sensitivities to quinidine, E-4031, and dofetilide that are identical to those of  $I_{Kr}$  measured in guinea pig myocytes (325).

In patients suffering from an inherited or a drug-induced LQT syndrome, a variety of missense mutations in KCNE2 have been detected (4, 61, 111, 267, 304). Studies with the mutant KCNE2 subunits display a clearer picture of the potential importance of KCNE2 for HERG channel activity than wild-type KCNE2. Most KCNE2 mutations reduce  $I_{Kr}$  amplitude, thereby decreasing the repolarization reserve, i.e., the ability of the HERG current to abolish the occurrence of premature action potentials or early depolarizing potentials that may then lead to torsade de points (158). For example, the mutation KCNE2-V65M induces an acceleration of HERG channel inactivation resulting in a decrease in  $I_{Kr}$  amplitude (111). The mutation KCNE2-M54T shows comparable effects on HERG channel gating (158). NH<sub>2</sub>-terminal KCNE2 mutations (T8A, Q9E) remarkably alter HERG channel drug sensitivity, which correlates with drug-induced LQT in respective mutation carriers (4, 158, 267). We can derive two important conclusions from these observations. First, the NH<sub>2</sub> terminus of KCNE2 alters HERG channel drug sensitivity. This compares with the role of the KCNE1 NH<sub>2</sub> terminus for drug sensitivity of the Kv7.1 channel. Second, pharmacology of the HERG channel in vivo is recapitulated in vitro upon coexpression with KCNE2. However, the studies cannot exclude that mutant KCNE2 subunits also affect other types of cardiac ion channels that interact with KCNE2 in vitro. Note the KCNE2 protein is more rapidly processed and transported to the cell membrane than HERG protein. This may indicate that KCNE2 is not as important for HERG channel maturation as KCNE1 is for the Kv7.1 channel (307).

KCNE2 affects HERG current modulation by cAMP (59). Binding of cAMP to a nucleotide binding domain (NBD) within the HERG channel COOH terminus induces a shift in the activation curve to more negative potentials, i.e., increases HERG activity in the physiological membrane potential range. This shift is increased when HERG is coexpressed with KCNE1 or KCNE2 (59). PKA phosphorylation also modulates HERG channel activity (59, 293). Features of this modulation are reminiscent of those



observed with the Kv7.1/KCNE1 channel, because PKA phosphorylation of HERG activity is particularly effective in the presence of the cardiac adaptor protein 14-3-3 $\epsilon$  (284), which binds to the HERG channel (121). After forming a dimer, 14-3-3 $\epsilon$  binds to PKA-phosphorylated serines (S283 in the NH<sub>2</sub> and S1137 in the COOH terminus) of HERG, thereby stabilizing the phosphorylated state of the HERG channel. This accelerates HERG channel activation and shifts the activation curve to more negative membrane potentials (51, 121). The net result is an increase in HERG channel activity at physiological membrane potentials. LQT mutations in the HERG COOH terminus abolish the 14-3-3 $\epsilon$  effect (51). If KCNE2 has an important influence in the 14-3-3 $\epsilon$ -mediated response of the HERG channel to PKA phosphorylation has not been investigated. In this context it is informative to consider that the Kv7.1 channel requires both KCNE1 and yotiao to respond to  $\beta$ -adrenergic signaling that eventually leads to Kv7.1 phosphorylation by PKA. Possibly, a similar constellation, i.e., a HERG/KCNE2 (KCNE1)/14-3-3 $\epsilon$  multiprotein complex, is necessary to ensure a proper response of  $I_{Kr}$  to  $\beta$ -adrenergic signaling. Thus sympathetic stimulation of the heart, which accelerates the heart rate, may increase both  $I_{Ks}$  and  $I_{Kr}$  activity by phosphorylation involving adaptor proteins and KCNE ancillary subunits.

The other KCNEs (KCNE3–5), which potentially could interact with the HERG channel, seem unimportant for HERG despite one report that coexpression of KCNE3 with HERG reduces HERG current amplitude in *Xenopus laevis* oocytes (257). HERG current properties were unaffected after expression of HERG with either KCNE4 in *Xenopus* oocytes (85) or KCNE5 in CHO cells (14).

#### D. Function of KCNEs In Vivo

The association of KCNE gene mutations with human diseases emphasizes the physiological role and importance of KCNEs. Mutations in KCNE1 (LQT5) and KCNE2 (LQT6) are associated with the LQT syndrome. This cardiac arrhythmia is characterized by a prolonged QT interval in the surface electrocardiogram essentially due to a delayed repolarization of the ventricular action potential. This can lead to occurrence of early afterdepolarizations, torsade de points, and ventricular fibrillation, eventually leading to sudden death (249). Electrophysiological and molecular biological studies of LQT mutations show KCNE1 and KCNE2 mutants can lead to a reduction in repolarizing current  $I_{Ks}$  (Kv7.1/KCNE1) and/or  $I_{Kr}$  (HERG/KCNE2) (34, 268, 279). The accompanying prolongation of the ventricular action potential provides a convincing explanatory basis for in vivo observed QT-interval prolongation in electrocardiograms, although many details

still await clarification. Promiscuous interactions of KCNE subunits with (cardiac) Kv channels are a major obstacle in unraveling distinctly the molecular basis of, e.g., LQT5 and LQT6 mutations. For designing potential therapies, it would be important to know if KCNE1 and KCNE2 affect only one type of cardiac current or several. Furthermore, it is unclear whether KCNE effects are the same or different in different compartments of the heart. Kv channel subunits are differentially expressed in heart tissue. Potentially, the promiscuity of KCNE subunits could give rise to interactions of KCNEs with different Kv channel types from one compartment to another.

Studies with genetically altered mice often provide deeper insights into the molecular basis and physiology of disease-causing mutations. In the case of KCNE, a significant drawback for this kind of study originates from the fact that the mouse heart, which beats  $\sim 10$  times faster, differs in its molecular physiology from the human heart. Thus action potential repolarization of mouse ventricular cardiomyocytes requires repolarizing currents with significantly faster kinetics than  $I_{Ks}$  and  $I_{Kr}$  (193). Consequently, they are not expressed in adult ventricular muscle of the mouse. This situation makes it difficult to assess the association of KCNE mutants, for example, with LQT syndrome in the mouse.

In one of the first papers describing *kcne1*<sup>-/-</sup> mice, duration of ventricular action potential was like wild type (Table 6) (48). Then it was found that action potential duration in *kcne1*<sup>-/-</sup> mice recorded from epicardium was significantly longer than the one recorded from endocardium. *kcne1*<sup>-/-</sup> mice were showing spontaneous episodes of atrial (290) and ventricular fibrillations (21). In a recent report, longer action potential duration was observed in *kcne1*<sup>-/-</sup> mice at the age of 6 mo and an increased occurrence of early afterdepolarizations and arrhythmogenesis (294). An earlier study (70) showed that *kcne1*<sup>-/-</sup> mice exhibit under bradycardic conditions a prolonged QT interval and under tachycardic conditions a shorter QT interval than wild-type mice. The data suggest that loss of KCNE1 function in the mouse impairs QT adaptability to changes in heart rates. Furthermore, *kcne1*<sup>-/-</sup> mice display shortened atrial action potentials (290). In fact, total K<sup>+</sup> currents (and those sensitive to the Kv7.1 blocker chromanol 293B) were significantly increased in atrial cells from *kcne1*<sup>-/-</sup> mice compared with controls. It is difficult to derive a coherent picture from these seemingly controversial findings. Also, synthesis of cardiac *kcne1* mRNA is significantly attenuated in newly born mouse pups (103), making it even more difficult to correlate the reported phenotypes with the *kcne1*<sup>-/-</sup> genotype. Possibly, lack of *kcne1* expression during embryogenesis influences normal heart development and K channel expression giving rise to the observed cardiac dysfunctions. For further discussion of cardiac *kcne*<sup>-/-</sup> phenotypes, see

TABLE 6. *KCNE* knockout mice

Genetic Background	Phenotype	Electrophysiology, Molecular Biology	Reference Nos.
<i>kcne1</i> <sup>-/-</sup>	Hair cell degeneration: bilateral deafness, Shaker/Waltzer movements, arrhythmogenic atrial and ventricular phenotypes of varying severity	ECG: impaired QT-RR adaptability, <i>I</i> <sub>Ks</sub> absent, <i>I</i> <sub>Kr</sub> decreased (by 50%), atrial <i>I</i> <sub>Ks</sub> increased, atrial action potentials shortened, epicardial action potentials prolonged, frequent epicardial early afterdepolarizations	21, 48, 70, 137, 290, 294, 314, 323
<i>kcne2</i> <sup>-/-</sup>	Reduced gastric proton secretion, achlorhydria, hypernatremia, gastric glandular hyperplasia	AP prolonged, <i>I</i> <sub>Kslow</sub> reduced (~50%, Kv1.5), <i>I</i> <sub>Kto,f</sub> reduced (~25%, Kv4.2), Co-IP: ventricular KCNE2 with Kv1.5 and Kv4.2, not with Kv1.4 and Kv4.3; no reduction in <i>I</i> <sub>Kr</sub> (erg) and <i>I</i> <sub>Ks</sub> (KCNQ1)	239–241
	Hypothyroidism: dwarfism, alopecia, goiter, low T <sub>4</sub> blood concentration, cardiac hypertrophy, and ventricular fibrosis	Thyroid iodide accumulation impaired	

ECG, electrocardiogram; *I*<sub>Ks</sub>, slowly activating; *I*<sub>Kr</sub>, rapidly activating K current; *I*<sub>to,f</sub>, fast component of transient outward K current; *I*<sub>Kso</sub>, sustained component of outward rectifying K current; *I*<sub>K,slow</sub>, slow component of the outward rectifying K current; AP, action potential.

below and the exciting finding that *kcne2* deficiency in the mouse affects thyroid hormone biosynthesis (240). Potentially, observed cardiac abnormalities in *kcne2*<sup>-/-</sup> mice have rather indirect causes.

In this context, it is very interesting that analysis of ventricular myocytes of *kcne2*<sup>-/-</sup> mice showed a ~50% reduction in the *I*<sub>Kslow</sub> current mediated by Kv1.5, and a ~25% reduction in the *I*<sub>to,f</sub> current, mediated by Kv4.2 (Table 6) (241). The data were supported by coimmunoprecipitation experiments indicating association of KCNE2 with na-

tive Kv1.5 and Kv4.2 subunits. Consistent with a reduced ventricular K<sup>+</sup> current was the cardiac *kcne2*<sup>-/-</sup> phenotype. Isolated, perfused intact hearts of *kcne2*<sup>-/-</sup> mice exhibited a prolonged ventricular action potential duration (Fig. 14). ECG patterns of freely running *kcne2*<sup>-/-</sup> mice remain to be investigated. Although the data appear clear-cut, one may add at this point a note of caution as an increasing number of studies show that loss of one ion channel subunit can alter expression of existing subunits or even stipulate de novo expression of novel subunits (77). In any case, the

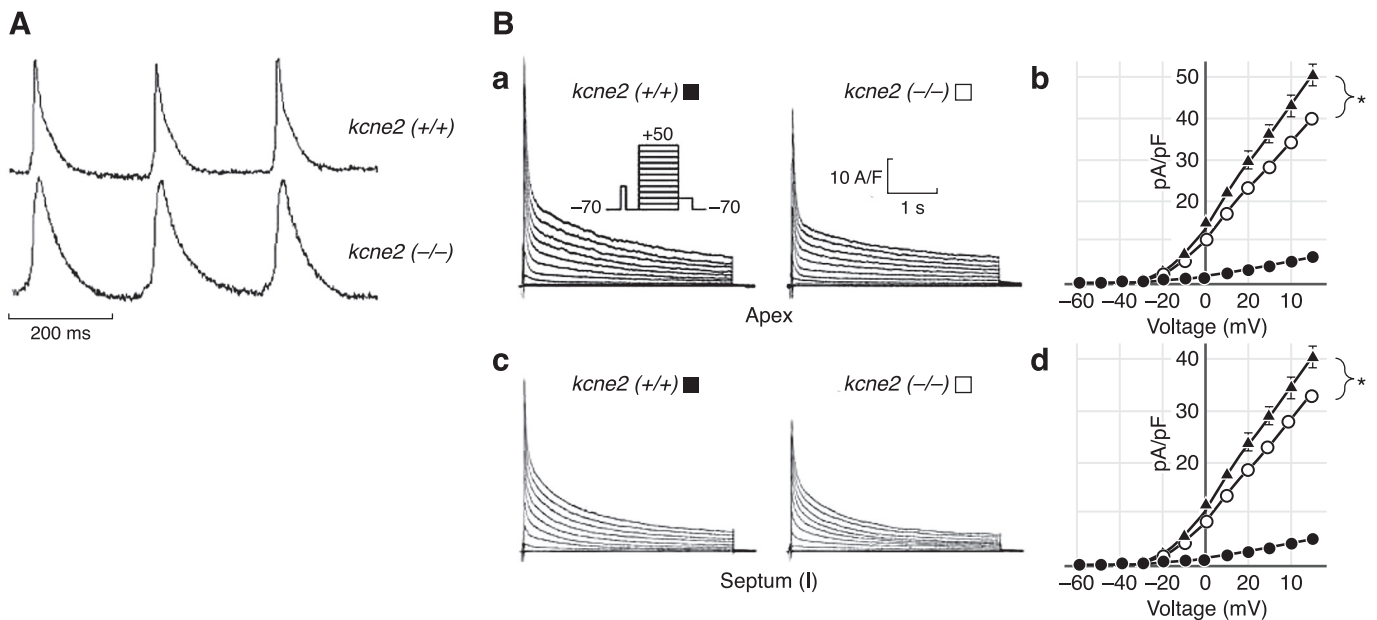


FIG. 14. Action potentials and membrane currents from a *kcne2*<sup>-/-</sup> mouse. A: ventricular myocyte action potentials in *kcne2*<sup>+/+</sup> and *kcne2*<sup>-/-</sup> mice recorded by optical mapping in isolated perfused intact hearts. B: outward currents recorded from individual myocytes isolated from apex (a and b) and septum (c and d) from *kcne2*<sup>+/+</sup> and *kcne2*<sup>-/-</sup> mice in the presence of 0.02 mM TTX. Whole cell currents were evoked by 4.5-s depolarizing potential steps (see inset for pulse diagram). b and d: Current-potential relations for peak currents (*kcne2*<sup>+/+</sup>, closed triangles; *kcne2*<sup>-/-</sup>, open circles) and steady-state currents (closed circles). [From Roepke et al. (241).]

molecular biological and electrophysiological phenotype of these mice is a warning example that extrapolations from in vitro to in vivo functions are not always as straightforward as one would wish.

Kv7.1 expression is also found in gastrointestinal epithelia, kidney, and inner ear, where Kv7.1-mediated currents have an important role in regulating transepithelial fluid and salt transport (97, 113, 194, 237). In these tissues, Kv7.1 channels may be assembled with KCNE1 and KCNE2. Accordingly, *kcne1*<sup>-/-</sup> and *kcne2*<sup>-/-</sup> mice exhibit a large variety of symptoms (reviewed in Refs. 97, 323). For example, *kcne1*<sup>-/-</sup> mice exhibit deafness and a *shaker/waltzer* behavior characterized by vestibular symptoms (bidirectional circling, head bobbing, and head tilt behavior). Apparently, defective salt and fluid transport across the *kcne1*<sup>-/-</sup> inner ear epithelium causes hair cell degeneration and structural abnormalities in cochlea and vestibular labyrinth (70, 314). Also, *kcne1*<sup>-/-</sup> mice exhibit symptoms of severe renal and gastrointestinal dysfunction, like hypokalemia, urinary and fecal salt loss, and volume depletion, consistent with a significant role of Kv7.1/KCNE1 current for transepithelial fluid and salt transport (97, 323). *kcne2*<sup>-/-</sup> mice show a defect in gastric acid secretion (239). KCNE2 is normally expressed in gastric parietal cells (64). KCNE2 deficiency leads to an abnormal distribution of the Kv7.1 channel in gastric glands. Note KCNE2 interacts in the cells with Kv7.1, but not with MERG, the mouse equivalent to HERG. In conclusion, knockout mice represent very useful animal models for the study of KCNE function in Kv7.1 channel activity related to transepithelial fluid and salt transport, whereas investigations of KCNE effects in cardiac physiology have severe limitations in the mouse.

Recently, an elegant study uncovered a crucial role for Kv7.1/KCNE channel in the thyroid. Here the Kv7.1/KCNE2 channel forms a hormone-stimulated thyrocyte K<sup>+</sup> channel required for normal thyroid tri- and tetraiodothyronine (T<sub>3</sub>, T<sub>4</sub>) hormone biosynthesis (240). Deletion of *kcne2* in the mouse impairs thyroid iodide accumulation up to eightfold, impaired maternal milk ejection, halved milk T<sub>4</sub> content, and halved litter size. The *kcne2*<sup>-/-</sup> mice had clear symptoms of hypothyroidism, including cardiac hypertrophy, alopecia, dwarfism, and goiter. Importantly, administration of T<sub>3</sub> and T<sub>4</sub> to *kcne2*<sup>-/-</sup> pups alleviates the abnormal phenotypes including the cardiac abnormalities observed with *kcne2*<sup>-/-</sup> cardiomyocytes. The data add another note of caution to conclusions drawn from correlations between genotype and phenotype. Also, the data clearly demonstrate how informative rescue experiments of abnormal phenotype(s) are to find out what might be wrong with a mouse lacking an ancillary ion channel subunit.

## E. Effects of KCNEs on Other Kv Channels In Vitro

In heterologous expression systems, KCNEs seem also to affect gating of other Kv channels. KCNE2 may serve as an example for KCNE promiscuity in in vitro expression systems and the difficulties to understand the specific details of KCNE interaction with distinct Kv channels. In addition to Kv7.1 (298) and HERG (4), KCNE2 interacts with Kv7.2 and Kv7.3 subunits forming neuronal M channels. The interaction accelerates M-current deactivation (299). KCNE2 seems also to interact with Kv4.2, Kv4.3 (350), and HCN2 (343). It is not known whether the channel complexes have counterparts in vivo. Coexpression of KCNE2 with Kv4.2 changes Kv4.2 current density and gating kinetics (350). Similar effects were observed for coexpression of KCNE1 with Kv4.3 (1).

KCNE2 as well as KCNE1 and KCNE3 also modulate Kv3.1 and Kv3.2 channels by slowing activation and deactivation and by accelerating inactivation kinetics (143). Coexpression of KCNE3 and Kv3.4, a rapidly inactivating A-type Kv channel, induces marked changes in Kv3.4 channel gating. The activation curve is shifted by -47 mV to more negative membrane potentials ( $V_{0.5} = -44$  mV) transforming this channel into an effective subthreshold channel, the single-channel conductance is increased, and recovery from inactivation is accelerated (1). For its activity, KCNE3 needs to be phosphorylated by PKC at serine-82. Ser-82 is located near or at the border between the KCNE3 transmembrane segment and KCNE3 cytoplasmic COOH terminus. Potentially, a phosphorylation at this site can influence the interaction of KCNE3 with membrane lipids. An interesting study recently discovered a KCNE3 missense mutation (KCNE3-R83H) associated with periodic paralysis in two families with members suffering from periodic paralysis, characterized by episodes of muscle weakness (1, 2). His-83 of the KCNE3 mutant is adjacent to Ser-82 and disturbs in a pH-dependent manner PKC phosphorylation of Ser-82, which is necessary for KCNE3/Kv3.4 channel activity. KCNE3-R83H, therefore, renders the KCNE3/Kv3.4 channel complex sensitive to physiological changes in intracellular pH. The mechanism may provide a molecular basis for a link between intracellular acidosis and onset of periodic paralysis (See note added in proof). Note that effects of KCNE3-R83H on Kv7.1 were not reported.

## V. ANCILLARY BK CHANNEL SUBUNITS

BK channels, K<sup>+</sup> channels with "big" conductance, are activated by both changes in membrane potential and increases in intracellular [Ca<sup>2+</sup>] (7, 42, 165, 166, 247, 313). BK channels are widely expressed in excitable tissue including neurons, where they are accumulated in axons and synaptic terminal zones (181), and in smooth muscle



cells, where they play a prominent role in the regulation of contraction (213). However, they are also expressed in nonexcitable cells, like in exocrine acinar cells where they are involved in the regulation of fluid secretion (212). Thus BK channel malfunction is associated with a variety of diseases, for example, related to hypertension, ataxia, epilepsy, or bladder contraction. BK channel activity may also be involved in the cellular mechanisms underlying cell migration, for example, in human glioma cells (252, 324). The complex voltage- and  $\text{Ca}^{2+}$ -dependent gating of the BK channel can be described by an allosteric gating model (104). In most tissues, the BK channel assembles together with ancillary BK $\beta$ -subunits markedly affecting gating behavior and pharmacology of the BK channel (157, 302).

### A. Structure of BK $\beta$ -Subunits

Comparably to Kv $\beta$ 1-subunits, which were characterized from biochemically purified Kv channel preparations, BK $\beta$ 1 was first identified in BK channel preparations purified from smooth muscle tissue, exploiting the high affinity of smooth muscle BK channel for the blocker charybdotoxin (CTX), a scorpion toxin. The isolated BK channel complex contained an octameric assembly of BK $\alpha$ - and BK $\beta$ 1-subunits in 1:1 stoichiometry (129). The BK $\beta$ 1-subunit represents a 31-kDa glycosylated peptide of 191 amino acid residues. It is a membrane integral protein comprising two transmembrane segments connected by a relatively long (~115 amino acid residues) extracellular loop and flanked by short intracellular NH<sub>2</sub> and COOH termini (202, 247, 302). Altogether, four BK $\beta$  genes (*KCNMB1*–4) were discovered, whereby the *KCNMB3* gene gives rise to four splice variants (BK  $\beta$ 3a–d) (202, 332, 333, 347). The four BK $\beta$ -subunit types display the same topology with cytoplasmic NH<sub>2</sub> and COOH termini flanking the membrane-spanning core domain consisting of two transmembrane segments and the large extracellular loop (Fig. 15). The BK $\beta$ 1-, BK $\beta$ 2-, and BK $\beta$ 3-subunits are quite similar in sequence; BK $\beta$ 4 is most divergent from the other BK $\beta$ -subunits (202).

BK $\beta$ 2- and BK $\beta$ 3-subunits have NH<sub>2</sub> termini containing a BK channel inactivating domain reminiscent of the one present at the NH<sub>2</sub> terminus of some Kv $\beta$  subunits (Fig. 15). NMR spectroscopic analysis of the structure of the BK $\beta$ 2 NH<sub>2</sub> terminus (residues 1–45) indicated two domains in the BK $\beta$ 2 NH<sub>2</sub> terminus that are connected by a flexible linker (29). The proximal domain displays a so-called ball structure that is typical for Kv channel inactivating domains and is adapted to block the intracellular pore entrance.

The extracellular loop contains four conserved cysteine residues that form disulfide bridges (93). It plays an important role in conferring toxin sensitivity to the BK channel. Exchange of the extracellular loop in BK $\beta$ 1/

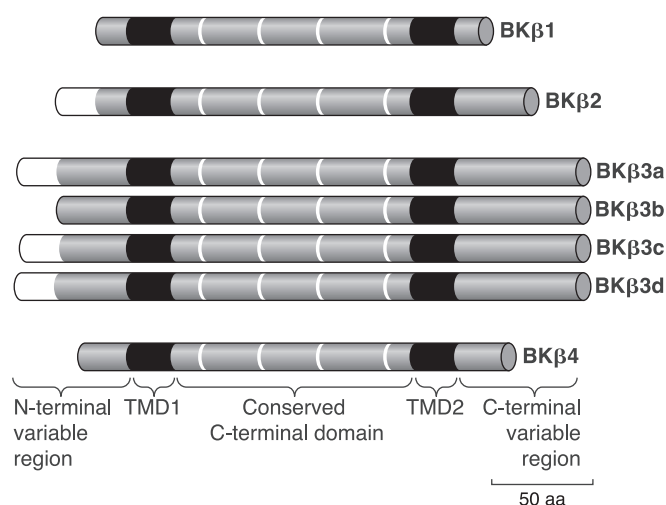


FIG. 15. Bar diagram of BK $\beta$  protein family. Human *KCNMB2* gene generates four BK $\beta$ 3 isoforms. The other *KCNMB* genes (*KCNMB1*, -2, and -4) encode each one BK $\beta$ -subunit (BK $\beta$ 1, BK $\beta$ 2, BK $\beta$ 4). Genebank (NCBI) accession numbers are as follows: NP\_004128 (BK $\beta$ 1), NP\_852006 (BK $\beta$ 2), NP\_741979 (BK $\beta$ 3a), NP\_741980 (BK $\beta$ 3b), NP\_741981 (BK $\beta$ 3c), NP\_055320 (BK $\beta$ 3d), NP\_055320 (BK $\beta$ 4). The two transmembrane domains (TMD1 and TMD2) are marked by a black box. White lines highlight conserved cysteine residues in conserved extracellular domain. Inactivating domains in NH<sub>2</sub>-terminal variable region are indicated in white. NH<sub>2</sub>- and COOH-terminal regions are located intracellularly.

BK $\beta$ 2 chimeras showed that the four cysteines of BK $\beta$ 1 are involved in transmitting BK $\beta$ 1's influence on toxin binding. Conversely, positive charges in the extracellular loop of BK $\beta$ 2 prevent CTX from approaching the channel pore leading to attenuated toxin affinity of the BK $\alpha$ /BK $\beta$ 2 channel (177, 332). Affinity-labeling experiments showed that CTX can be cross-linked to an amino acid residue in the BK $\beta$ 1 extracellular loop (130). The data suggest that part of the extracellular loop contributes to the toxin binding site near or at the extracellular pore entrance of the BK channel.

In comparison to other Kv channel  $\alpha$ -subunits, the BK channel  $\alpha$ -subunit shows NH<sub>2</sub>-terminally an extra (seventh) transmembrane segment (S0). This topology places extracellularly the NH<sub>2</sub> terminus in front of the S0 segment. Both extracellular NH<sub>2</sub> terminus and S0 segment are required for BK $\beta$ 1-subunit activity (316) and represent interaction site(s) for BK $\beta$ 1 as well as other BK $\beta$  subunits (317). Presumably, the extracellular BK $\alpha$  NH<sub>2</sub> terminus interacts with part of the extracellular BK $\beta$  loop, and the BK $\alpha$  S0 segment interacts with one or both BK $\beta$  transmembrane segments. Because the extracellular BK $\beta$  loop is responsible for BK $\beta$  effects on BK channel pharmacology and alters sensitivity to pore blocking toxins (130), it is very likely that the large extracellular loop of the BK $\beta$ 1 contributes directly or indirectly to the toxin receptor, bringing it into immediate vicinity to the outer entrance of the BK channel pore.

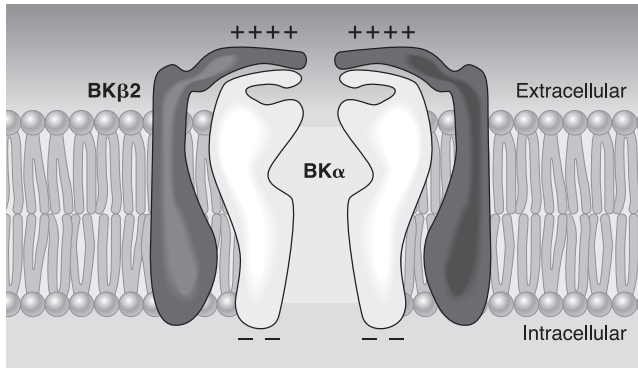


FIG. 16. Schematic side view of BK channel associated with BK $\beta$ 2-subunits. Two BK $\alpha$  (shaded in light gray) and BK $\beta$ 2-subunits (shaded in dark gray) are shown. The + signs illustrate cluster of positively charged BK $\beta$ 2 amino acid residues close to extracellular entrance of channel pore. [From Chen et al. (49).]

## B. Function of BK $\beta$ -Subunits In Vitro

Each of the four BK $\beta$ -subunits has distinct effects on BK channel gating, e.g., BK $\beta$ 1 induces high Ca<sup>2+</sup> sensitivity of BK channels, BK $\beta$ 2 and BK $\beta$ 3 produce inactivating BK channels, and BK $\beta$ 4 dramatically slows activation and deactivation of the BK channel. Also, assembly with BK $\beta$ -subunit influences the pharmacology of the BK channel. Some of these effects can be detected even if less than four BK $\beta$  subunits are bound per BK channel (146, 322).

## C. BK $\beta$ 1-Subunits

In the absence of BK $\beta$ -subunits, the BK channel exhibits low Ca<sup>2+</sup> sensitivity and activation at very positive membrane potentials (Fig. 16A) (57). Coexpression with BK $\beta$ 1 produces BK channels with increased Ca<sup>2+</sup> sensitivity, increased voltage sensitivity, slowed deactivation kinetics, increased affinity for CTX, and decreased affinity to iberiotoxin (Fig. 16B, Table 7) (71, 130, 176, 228, 315, 317, 332). Furthermore, the BK $\beta$ 1-subunit confers 17 $\beta$ -estradiol (308) and dihydrosoyasaponin (313) sensitivity to BK channels. Increased Ca<sup>2+</sup> sensitivity and shift in voltage-dependent activation to more negative membrane

potentials apparently relate to allosteric effects on the voltage sensor domain of the BK channel. It has been proposed that a ring of RCK (regulators of K conductance) domains in the BK channel COOH terminus is important for Ca<sup>2+</sup> sensitivity of BK channel gating (148, 338, 344). Potentially, BK $\beta$ 1-subunits affect RCK domain conformation, thereby modifying allosteric coupling factors operative in BK channel opening (203). However, BK channel lacking the RCK domains exhibits almost the same Ca<sup>2+</sup> sensitivity as wild-type BK channel (216).

## D. BK $\beta$ 2-Subunits

Coexpression of BK $\beta$ 2-subunits with BK $\alpha$ -subunits confers to the BK channel enhanced Ca<sup>2+</sup> sensitivity similar to BK $\beta$ 1-subunits (Fig. 16C). An important difference, however, is that BK $\beta$ 2-subunits contain an NH<sub>2</sub>-terminal inactivating domain resembling the one of Kv $\beta$  subunits (Fig. 15). Thus the BK channel rapidly inactivates when assembled with BK $\beta$ 2 (99, 317, 332, 333). BK $\beta$ 2-mediated N-type inactivation shares several features with N-type inactivation of the *Shaker* channel. The BK $\beta$ 2 inactivating domain binds to a receptor site, only accessible in the opened BK channel; recovery from inactivation is accelerated by an increase in extracellular [K<sup>+</sup>]; inactivating activity can be transferred to other BK $\beta$ -subunits, which do not have an inactivating domain by themselves (29, 317). Application of the NH<sub>2</sub>-terminal inactivating domain in the form of a peptide (residues 1–45) to the cytoplasmic side elicits complete inactivation of the BK channel; inactivating activity can be described by a “ball-and-chain” type mechanism. The association rate of the inactivating NH<sub>2</sub>-terminal BK $\beta$ 2 peptide to its BK channel receptor is similar to the one of Kv $\beta$ 1.1-mediated inactivation, whereas the dissociation rate is very slow, indicating high-affinity binding to the BK channel. The initial segment of three hydrophobic residues (residues 2–4: FIW) at the BK $\beta$ 2 NH<sub>2</sub> terminus are essential for this high affinity (331). On the other hand, no information is available about the receptor site of the BK channel which presumably is near or at the intracellular entrance to the BK channel pore. N-type inactivation locks the *Shaker*

TABLE 7. BK $\beta$ -subunit effects on BK channels in heterologous expression systems

Subunit	Ca <sup>2+</sup> Sensitivity	Activation Kinetics	Activation $V_{1/2}$	Deactivation	Inactivation	Affinity to CTX	Affinity to IBX	Reference Nos.
BK $\beta$ 1	Increased	Accelerated	Negative shift	Slowed	No	+	–	39, 71, 129, 130, 150, 176, 201, 203, 316, 317, 332
BK $\beta$ 2	Increased	Slowed	Negative shift	Slowed	Fast and complete	–	ND	99, 150, 201, 203, 317, 331, 332
BK $\beta$ 3	Low	Accelerated (f3b)	Positive shift f3a, c	±	f3a, c: fast, incomplete; f3b, d: no	±	±	39, 109, 150, 201, 306
BK $\beta$ 4	Low	Slowed	Negative shift	Slowed	No	–	–	39, 150, 177

+, Increase in parameter; –, decrease or shift to more negative potentials; ±, no effect; ND, parameter not determined.  $V_{1/2}$ , membrane potentials at which 50% of the channels are activated.

channel in an opened state allowing a transient flow of current during recovery from inactivation. In contrast, the inactivated BK channel seems to transit rapidly into an inactivated-closed state because a comparable transient flow of current is undetectable during recovery of the BK channel from inactivation (30, 331). N-type inactivation of the *Shaker* channel is well described as a first-order reaction involving an interaction of an inactivating particle with a binding site at the pore. N-type inactivation of the BK channel, however, proceeds as a two-step inactivation process (30).

The extracellular loop of BK $\beta$ 2 contains four lysines. Thus assembly of BK $\alpha$  and BK $\beta$ 2 to octamers can lead to a positively charged ring structure at the outer entrance of the channel pore (Fig. 16). The electric field formed by these charges seems to be one important component in conferring outward rectification to the BK channel (49). BK $\beta$ 1- and BK $\beta$ 4-subunits do not induce rectification in BK channels (349).

BK current properties seem to change incrementally, if the ratio of injected BK $\beta$ 2 versus BK $\alpha$  cRNA is increased in the *Xenopus laevis* oocyte expression system. The results showed that an increase in the number of bound BK $\beta$ 2-subunits induced an incremental shift in the activation curve to more negative membrane potentials as well as an incremental acceleration in the time course of inactivation. Each additional BK $\beta$ 2-subunit seems to contribute equally to the gating properties of the BK channel

(322). Similar results were obtained in coexpression studies with BK $\beta$ 1- and BK $\alpha$ -subunits. The data indicate that BK channel properties like Ca $^{2+}$  sensitivity, voltage dependence, and inactivation can be adjusted on a sliding scale by changing the fractional occupancy of the BK channel with BK $\beta$ -subunit (120, 322). Apparently, the stoichiometry of BK $\beta$ - and BK $\alpha$ -subunits is not a fixed entity for the BK channel. If cells modify BK $\beta$ /BK $\alpha$  stoichiometry to demand and thereby adapt their excitability is not known. However, BK $\beta$ /BK $\alpha$  stoichiometry can vary from one cell to another, e.g., in human coronary smooth muscle cells (288).

### E. BK $\beta$ 3-Subunits

In contrast to BK $\beta$ 1 and BK $\beta$ 2, coexpression of BK $\alpha$  with BK $\beta$ 3 isoforms has no influence on BK channel Ca $^{2+}$  sensitivity but generates outwardly rectifying BK channels. The experiments indicated that rectification is due to voltage-dependent block of the extracellular BK channel pore by the extracellular loop of the BK $\beta$ 3-subunit. Application of reducing agents like dithiothreitol (DTT) to outside-out patches attenuated BK $\beta$ 3-induced rectification, presumably due to disruption of extracellular disulfide linkages (349). The BK $\beta$ 3 gene generates four splice variants (BK $\beta$ 3a-d). They have a constant COOH terminus including the two transmembrane regions and the extra-

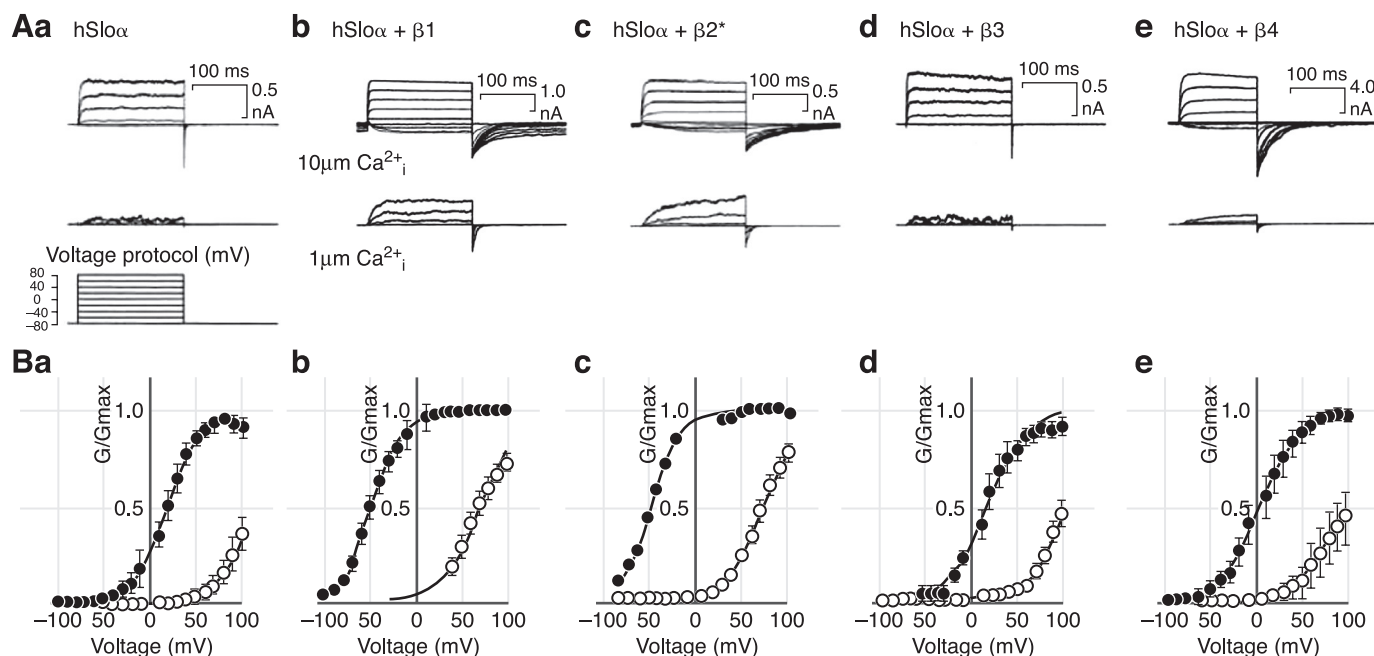


FIG. 17. Voltage- and Ca $^{2+}$ -dependent properties of hSlo $\alpha$  channels without and with one of the four BK $\beta$ -subunits. A: current traces recorded in an inside-out patch from HEK293 cells expressing hSlo $\alpha$  (a), hSlo $\alpha$  +  $\beta$ 1 (b), hSlo $\alpha$  +  $\beta$ 2 (c), hSlo $\alpha$  +  $\beta$ 3 (d), and hSlo $\alpha$  +  $\beta$ 4 (e) exposed to 1 and 10  $\mu$ M Ca $^{2+}$ . Both pipette and bath contained 140 mM K $^{+}$ . Pulse protocol was as shown in the pulse diagram. B, a–e: normalized conductance-voltage relations plotted below the corresponding panels. \*Inactivation was removed by exposing the patch to 1 mg/ml trypsin for 60 s. [Modified from Lippiat et al. (150).]



cellular loop, but varying cytoplasmic NH<sub>2</sub> termini (Fig. 15) (332). The NH<sub>2</sub> termini of BK $\beta$ 3a or BK $\beta$ 3c contain inactivating domains. Thus coexpression of BK $\alpha$  with BK $\beta$ 3a or BK $\beta$ 3c isoforms in *Xenopus laevis* oocytes leads to a rapidly inactivating BK channel. In contrast to BK $\beta$ 2, however, BK $\beta$ 3 inactivation is incomplete. Possibly, this results from a weaker affinity of the BK $\beta$ 3 inactivating domain to the BK channel receptor due to faster dissociation rates (306). Also, BK $\beta$ 3a and BK $\beta$ 3c shift the activation curve of the BK channel to more positive (unphysiological) membrane potentials, which effectively decreases BK channel open probability (201, 306). In addition, the BK $\beta$ 3a-subunit induces a slow component in BK tail currents, not seen with other BK $\beta$ 3-subunits (348).

## F. BK $\beta$ 4-Subunits

Remarkably, BK $\beta$ 4 confers to the BK channel insensitivity to block by CTX and iberiotoxin. Consistent with the view that the extracellular BK $\beta$  loop is responsible for toxin sensitivity, exchange of the extracellular BK $\beta$ 4 loop by the one of BK $\beta$ 1 restores toxin sensitivity (177). Also, the BK $\beta$ 4/BK $\alpha$  channel is characterized by slow activation and deactivation kinetics and an increased Ca<sup>2+</sup> sensitivity at intracellular Ca<sup>2+</sup> concentrations >1  $\mu$ M (38, 177). The properties of the BK $\beta$ 4/BK $\alpha$  channel resemble those of the type II BK channel described on posterior pituitary nerve terminals (35, 67) and on granular cells of hippocampal dentate gyrus (37). The slowly activating BK channel likely contributes during high-frequency action potential firing to the afterhyperpolarization amplitude (87).

## G. Function of BK $\beta$ -Subunits In Vivo

Each BK $\beta$ -subunit exhibits a distinct tissue-specific expression pattern. BK $\beta$ 1-subunits are predominantly expressed in smooth muscle cells (130). BK $\beta$ 2 is expressed in chromaffin cells, pancreatic  $\beta$ -cells, ovaries, and dorsal root ganglion cells as well as in brain (38). The BK $\beta$ 3 splice variants are prominently expressed in adrenal chromaffin cells and pancreas and also in the brain. Although the pattern of expression for each isoform of the BK $\beta$ 3-subunit is distinct, there is a considerable overlap, implying that in a particular tissue, or even in a single cell, more than one type of BK $\beta$ 3-subunit may be expressed. However, it is not known whether two or even more different types of BK $\beta$ 3-subunit associate with one BK channel. The BK $\beta$ 4-subunit, on the other hand, is predominantly expressed in the brain. The BK $\beta$ -subunit expression pattern concurs with the large variability in native BK current properties (38, 157, 313). Thus neurons express both CTX-sensitive (BK type I) and CTX-insensitive BK channels (BK type II), whereas the BK channel in smooth muscle cells, which assembled with BK $\beta$ 1, is blocked by CTX.

Antibodies against the BK $\beta$ 1-subunit were used to coimmunoprecipitate BK  $\alpha$ - and BK $\beta$ 1-subunits, demonstrating that in vivo the BK channel exists as a heteromultimer (130). The inner hair cells, tuned to respond to sounds varying in frequency  $\sim$ 20-fold, provide a striking example for variations in BK $\alpha$ /BK $\beta$  heteromultimerization in correlation to the tonotopic organization in the turtle cochlea. The tonotopic organization concurs with a gradual change in BK channel kinetics. To achieve this, two molecular mechanisms seem to operate. The first mechanism implicates a graded expression of BK $\alpha$  splice variants. The second mechanism invokes a gradual variation in the BK $\beta$ /BK $\alpha$  subunit stoichiometry for explaining the tonotopic organization in turtle cochlea (120, 228). This notion is based on in vitro coexpression studies with avian BK $\beta$ - and BK $\alpha$ -subunits necessary to obtain native-like Ca<sup>2+</sup>-sensitive BK channels. The results showed that the BK $\beta$ -subunit induced an all-or-none shift in the activation curve of a particular BK $\alpha$ -subunit isoform by  $\sim$ 100 mV and an  $\sim$ 10-fold slowing of BK channel activation. Then a gradual shift in these parameters could be achieved by varying the BK $\beta$ /BK $\alpha$  ratio (120, 228). The correlation of tonotopic organization and BK channel gating characteristics, however, needs further analysis. Note BK channel properties in mammalian cochlea are uncorrelated with the tonotopic organization of inner hair cells (224, 297).

Like other K<sup>+</sup> channels, the BK channel is in vivo part of large protein complexes. For example, analysis of BK channel preparations, immunopurified from total rat brain lysate, showed that rat brain BK $\alpha$ /BK $\beta$ 2/BK $\beta$ 4 channels are associated with several Ca<sup>2+</sup> channels as part of large protein complexes (32). Also in vascular smooth muscle cells, the BK channel appears to interact with L-, N-, and/or P/Q-type Ca<sup>2+</sup> channels,  $\beta$ 2-adrenergic receptor, PKA, and various scaffolding proteins (151). It is unclear how transient or permanent the interactions are. Potentially, BK $\beta$ 1 plays a role in localizing the BK channel to specific membrane domains at the cell surface to increase the effectiveness of a  $\beta$ -adrenergic signaling cascade and to stimulate BK channel activity by an increase in [Ca<sup>2+</sup>]<sub>i</sub> and by phosphorylation. The close vicinity of the BK channel to voltage-dependent Ca<sup>2+</sup> channels within a protein complex allows activation of BK channels within fractions of a millisecond eliciting rapid repolarization of action potentials and hyperpolarization, respectively. This negative-feedback mechanism leads to Ca<sup>2+</sup> channel deactivation and terminates Ca<sup>2+</sup> influx (31, 32). A comparable negative-feedback function was proposed for the BK channel in regulating smooth muscle tone (39, 217) and neurotransmitter release from presynaptic terminals (35). Because the BK $\beta$ -subunit regulates the Ca<sup>2+</sup> sensitivity of the BK channel, their presence is an important factor for the hyperpolarizing activity of the BK channel.

TABLE 8. *BKβ ancillary protein knockout mice*

Genetic Background	Phenotype	Electrophysiology	Reference Nos.
BKβ1 <sup>-/-</sup>	Arterial tone and blood pressure increase, increased aortic smooth muscle cell contractility in response to agonists	Ca <sup>2+</sup> sensitivity and Ca <sup>2+</sup> sparks decreased, increased open probability of BK channels, BK channel activity decreased, shift in BK channel voltage/Ca <sup>2+</sup> sensitivity	39, 198, 213, 217
	Aldosteronism resulting from renal K retention and hyperkalemia		84
BKβ4 <sup>-/-</sup>	Temporal lobe epileptic discharges	Granule cells of the dentate gyrus: gain of function of BK channels with shortening of action potentials inducing higher firing rates	37
	Decreased ethanol tolerance	Decreased ethanol tolerance at the molecular and cellular levels	164
BKβ1/4 <sup>-/-</sup>	Analysis restricted to cochlear function	Normal cochlear function (normal auditory brain stem responses)	224

This proposition found strong support in studies of BKβ function investigating BKβ1- and BKβ4-knockout mouse lines (Table 8). The data showed that the BK channel needs BKβ1-subunits for normal function in vascular smooth muscle cells (28, 191). In the absence of BKβ1, BK channel activity is shifted to more positive membrane potentials (Fig. 18) correlated with increased constriction of blood vessels and mild hypertension. In addition, vascular smooth muscle cells in BKβ1<sup>-/-</sup> mice exhibit an increased contractile response to vasoactive substances (327, 328). The importance of BKβ1-subunit for regulation of smooth muscle tone is further supported by the finding that a marked decrease in BKβ1 expression was observed in humans during acquired hypertension, like in angiotensin-induced hypertension (12). In an epidemiological study, a remarkable BKβ1 point mutation

(E65K) was found, which in vitro produces a gain-of-function in BK channel function. Individuals carrying this mutation suffer significantly less from increased diastolic blood pressure than normal individuals (75).

A single base pair deletion in exon 4 of KCNM3 (delA750) leads to truncation of the terminal 21 residues of the BKβ3b-subunit. This mutation has been associated with a form of generalized epilepsy, although it is unlikely that it can induce this disease by its own (155). Nevertheless, BKβ4<sup>-/-</sup> mice show signs of an epileptic phenotype (37). Cortical electroencephalograms of these mice exhibit increased neuronal excitability concomitant with generation of epileptic spike and waves, which first appear in the temporal lobe and subsequently generalize over the whole cortex. However, epileptic seizures display no signs of tonic-clonic component. Single-channel recordings from granule cells of hippocampal dentate gyrus show that absence of BKβ4 eliminates expression of toxin-insensitive BK type II channels. Instead, the BKβ4<sup>-/-</sup> granule cells express toxin-sensitive BK type I channels, which cause shorter durations of both action potential and afterhyperpolarization than in wild-type mice. As a result, the granule cells fire action potentials at higher frequency and undergo a decreased frequency adaptation. Recently, a very interesting correlation was made between the sensitivity of *Kcmna1*<sup>-/-</sup> mice to lolitrem B or paxilline and a neurological disorder in farm animals known as “rye grass staggers” (110). Lolitrem B belongs to a class of neurotoxic indol-terpenoids produced by the endophytic fungus *Neotyphodium lolii* (76). Animals ingesting the fungus with their food develop uncontrollable tremors and become uncoordinated in their movement. Lolitrem B and the structurally related tremor inducer paxillin both act as potent BK channel inhibitors. At higher doses, the neurotoxins are lethal. *Kcmna1*<sup>-/-</sup> mice, which exhibit a mild tremor phenotype and a moderate ataxia, are unaffected by these neurotoxins. Furthermore, when the response to lolitrem B was examined in *Kcnmb4*<sup>-/-</sup> mice, only low-level ataxia

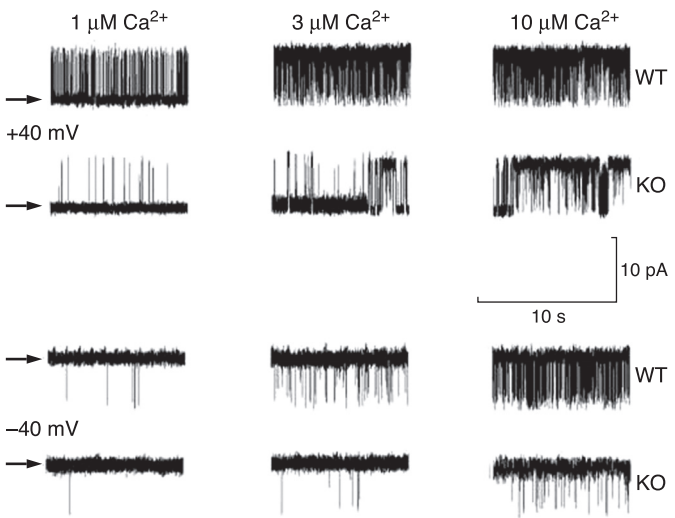


FIG. 18. Influence of BKβ1 on BK current. Single BK channel currents were recorded at indicated intracellular Ca<sup>2+</sup> concentrations and voltages on acutely isolated smooth muscle cells of the mouse aorta from control (WT) and BKβ1 knockout (KO) mice. Arrows indicate level of closed state. [Original recordings by G. Sachse and O. Pongs (see also Ref. 39).]

was observed. The data suggest that BK channels assembled with ancillary BK $\beta$ 4 subunits have an important role in the development of motor impairments induced by rye grass neurotoxins. Apparently, absence of BK $\beta$ 4 subunits renders the mouse insensitive to neurotoxins like lolitrem B and paxilline. Yet the unresolved question remains why the *Kcnma1*<sup>-/-</sup> mouse has a mild tremor and ataxia phenotype, whereas block of the BK channel by lolitrem B and paxilline exerts a very strong movement disorder.

## VI. CONCLUDING REMARKS

Kv channels are multiprotein complexes consisting of a membrane-inserted core associated with ancillary  $\beta$ -subunits. The core of Kv channels is assembled from Kv $\alpha$ -subunits and displays an essentially conserved topology with a central pore domain surrounded by the voltage sensors. In contrast,  $\beta$ -subunits come in different flavors revealing a high diversity in  $\beta$ -subunit structure and function. Yet, despite the observation of both cytoplasmic and membrane-inserted  $\beta$ -subunits, one can recognize some comparable functions and delineate general aspects of the cellular role of ancillary Kv channel subunits.

Kv channels with NH<sub>2</sub>-terminal tetramerization domains bind cytoplasmic  $\beta$ -subunits. Typical examples are the interaction of Kv $\beta$ -subunits with members of the *Shaker*-related Kv1 channel family and that of KChIPs with members of the Kv4 family. The resulting Kv-channel protein complexes potentially extend the reach with which Kv1 and Kv4 channels can communicate cellular excitability to cytoplasmic signaling pathways (and vice versa). This type of cellular communication is still largely unexplored. In the case of Kv $\beta$ -subunits, there may be a cross-talk between cellular redox status and Kv channel gating. But a satisfactory answer to this is still missing. KChIPs, on the other hand, may mediate a link to Ca<sup>2+</sup> signaling pathways or even to transcriptional activities. Many studies have shown that both Kv $\beta$  and KChIP stimulate Kv channel expression at the cell surface in *in vitro* expression systems. However, results obtained with Kv $\beta$  and, respectively, KChIP knockout mice produced contradicting data. This sets off a warning signal that data obtained *in vitro* with transiently transfected cells may not always reflect *in vivo* reality.

Seemingly simple questions like regulation of Kv $\alpha$ - and Kv $\beta$ -subunit assembly, their trafficking, and targeting are not yet well resolved. In this context, reversibility of Kv $\alpha$  and Kv $\beta$ /KChIP interaction appears as a very interesting and unresolved issue. We do not know how permanent complex formation between Kv $\alpha$ - and Kv channel  $\beta$ -subunits is. This is an important issue particularly in the light of an increasing number of examples which show that Kv channel  $\beta$ -subunits fulfill also other cellular func-

tions ranging, for example, from enzyme activities like calse-nilin (KChIP3) to transcription like DREAM (KChIP3) and CALP (KChIP4).

Another unresolved question is whether Kv $\alpha$ - and Kv channel  $\beta$ -subunits are endocytosed together or separately. Furthermore, where do we draw a line to designate a protein an ancillary subunit or a regulatory binding protein? For example, the interaction of Kv channels with proteins like calmodulin, Lgi1, ZIP, or PSD-95 can have dramatic effects on gating, cellular localization, and turnover of the Kv channel. Are they cellularly or compartmentally specific ancillary subunits? These are just a few examples to illustrate how little we know about Kv channels and their "life" *in situ*.

A common denominator for membrane-spanning Kv channel  $\beta$ -subunits can be seen in their activity to markedly modify gating of the Kv channel with which they interact. The most remarkable example represents the influence of KCNE1 and, respectively, KCNE3 on the Kv7.1 channel. The extracellular domains of membrane-spanning Kv channel  $\beta$ -subunits most likely interact with components of the extracellular matrix, yet the details of this type of interaction and their physiological consequences remain to be elucidated. Also, many open questions remain concerning regulation of assembly, trafficking, and endocytosis of membrane-spanning Kv channel  $\beta$ -subunits. Again, there are conflicting *in vitro* and *in vivo* results in the literature. In particular, the results obtained with KCNEs emphasize the need to explore Kv channel  $\beta$ -subunit function in primary cells and tissue. Here, an important aspect is that ancillary Kv channel  $\beta$ -subunits are potentially involved in the organization of large membrane protein complexes. For example, BK channel  $\beta$ -subunits are important for the association of the BK channel with L-type Ca<sup>2+</sup> channel in a multi-ion-channel protein complex. It is likely that more examples will be discovered in the future.

In landmark studies, MacKinnon and co-workers have elucidated the crystal structure of a Kv1.2-Kv $\beta$  channel complex (153, 154). Such studies are invaluable for understanding the structural basis of Kv channel  $\beta$ -subunit interaction with the pore-forming Kv $\alpha$ -subunits, the biophysical changes of the ion channel gating induced by the  $\beta$ -subunits, and their effects *in vivo*. It may be expected that the future will bring to us similarly detailed information on the structure of other Kv channel complexes, in particular on the Kv4 channel associated with KChIP and DPPL subunits, on Kv7.1-KCNE complexes, and on the BK $\alpha$ -BK $\beta$  channel complex.

## NOTE ADDED IN PROOF

After final submission of this review, a paper was published entitled "Disruption of the K<sup>+</sup> channel  $\beta$ -sub-



unit KCNE3 reveals an important role in intestinal and tracheal  $\text{Cl}^-$  transport" by Preston P, Wartosch L, Günzel D, Fromm M, Kongsuphol P, Ousingawat J, Kunzelmann K, Barhanin J, Warth R, Jentsch T (*J Biol Chem* 285: 7165–7175, 2010). The authors show that *kcne3*<sup>-/-</sup> mice lacking the KCNE3 protein were viable and fertile and did not display any sign of periodic paralysis or other skeletal-muscle abnormalities. However, *kcne3*<sup>-/-</sup> mice show a drastically reduced cAMP-stimulated electrogenic  $\text{Cl}^-$  secretion across tracheal and intestinal epithelia.

#### ACKNOWLEDGMENTS

Address for reprint requests and other correspondence: O. Pongs, Institut für Neurale Signalverarbeitung, ZMNH, Universitätsklinikum Hamburg-Eppendorf, Martinistr. 52, D-20246 Hamburg, Germany (e-mail: morin@zmnh.uni-hamburg.de).

#### GRANTS

This work was supported by grants from the Deutsche Forschungsgemeinschaft and the Fonds der Chemischen Industrie.

#### REFERENCES

- Abbott GW, Butler MH, Bendahhou S, Dalakas MC, Ptacek LJ, Goldstein SA. MiRP2 forms potassium channels in skeletal muscle with Kv3.4 and is associated with periodic paralysis. *Cell* 104: 217–231, 2001.
- Abbott GW, Butler MH, Goldstein SA. Phosphorylation and protonation of neighboring MiRP2 sites: function and pathophysiology of MiRP2-Kv3.4 potassium channels in periodic paralysis. *FASEB J* 20: 293–301, 2006.
- Abbott GW, Goldstein SA. Disease-associated mutations in KCNE potassium channel subunits (MiRPs) reveal promiscuous disruption of multiple currents and conservation of mechanism. *FASEB J* 16: 390–400, 2002.
- Abbott GW, Sesti F, Splawski I, Buck ME, Lehmann MH, Timothy KW, Keating MT, Goldstein SA. MiRP1 forms IKr potassium channels with HERG and is associated with cardiac arrhythmia. *Cell* 97: 175–187, 1999.
- Accili EA, Kiehn J, Wible BA, Brown AM. Interactions among inactivating and noninactivating Kv $\beta$  subunits, and Kv $\alpha$ 1.2, produce potassium currents with intermediate inactivation. *J Biol Chem* 272: 28232–28236, 1997.
- Accili EA, Kiehn J, Yang Q, Wang Z, Brown AM, Wible BA. Separable Kv $\beta$  subunit domains alter expression and gating of potassium channels. *J Biol Chem* 272: 25824–25831, 1997.
- Adelman JP, Shen KZ, Kavanaugh MP, Warren RA, Wu YN, Lagrutta A, Bond CT, North RA. Calcium-activated potassium channels expressed from cloned complementary DNAs. *Neuron* 9: 209–216, 1992.
- Aimond F, Kwak SP, Rhodes KJ, Nerbonne JM. Accessory Kv $\beta$ 1 subunits differentially modulate the functional expression of voltage-gated K<sup>+</sup> channels in mouse ventricular myocytes. *Circ Res* 96: 451–458, 2005.
- Alexander JC, McDermott CM, Tunur T, Rands V, Stelly C, Karhson D, Bowlby MR, An WF, Sweatt JD, Schrader LA. The role of calsenilin/DREAM/KCHIP3 in contextual fear conditioning. *Learn Mem* 16: 167–177, 2009.
- Allen D, Fakler B, Maylie J, Adelman JP. Organization and regulation of small conductance Ca<sup>2+</sup>-activated K<sup>+</sup> channel multiprotein complexes. *J Neurosci* 27: 2369–2376, 2007.
- Amarillo Y, De Santiago-Castillo JA, Dougherty K, Maffie J, Kwon E, Covarrubias M, Rudy B. Ternary Kv4.2 channels recapitulate voltage-dependent inactivation kinetics of A-type K<sup>+</sup> channels in cerebellar granule neurons. *J Physiol* 586: 2093–2106, 2008.
- Amberg GC, Bonev AD, Rossow CF, Nelson MT, Santana LF. Modulation of the molecular composition of large conductance, Ca<sup>2+</sup> activated K<sup>+</sup> channels in vascular smooth muscle during hypertension. *J Clin Invest* 112: 717–724, 2003.
- An WF, Bowlby MR, Betty M, Cao J, Ling HP, Mendoza G, Hinson JW, Mattsson KI, Strassle BW, Trimmer JS, Rhodes KJ. Modulation of A-type potassium channels by a family of calcium sensors. *Nature* 403: 553–556, 2000.
- Angelo K, Jespersen T, Grunnet M, Nielsen MS, Klaerke DA, Olesen SP. KCNE5 induces time- and voltage-dependent modulation of the KCNQ1 current. *Biophys J* 83: 1997–2006, 2002.
- Ashcroft FM. *Ion Channels and Disease*. San Diego, CA: Academic, 2000.
- Autieri MV, Belkowski SM, Constantinescu CS, Cohen JA, Prystowsky MB. Lymphocyte-specific inducible expression of potassium channel  $\beta$  subunits. *J Neuroimmunol* 77: 8–16, 1997.
- Bähring R, Boland LM, Varghese A, Gebauer M, Pongs O. Kinetic analysis of open- and closed-state inactivation transitions in human Kv4.2 A-type potassium channels. *J Physiol* 535: 65–81, 2001.
- Bähring R, Dannenberg J, Peters HC, Leicher T, Pongs O, Isbrandt D. Conserved Kv4 NH<sub>2</sub>-terminal domain critical for effects of Kv channel-interacting protein 2.2 on channel expression and gating. *J Biol Chem* 276: 23888–23894, 2001.
- Bähring R, Milligan CJ, Vardanyan V, Engeland B, Young BA, Dannenberg J, Waldschutz R, Edwards JP, Wray D, Pongs O. Coupling of voltage-dependent potassium channel inactivation and oxidoreductase active site of Kv $\beta$  subunits. *J Biol Chem* 276: 22923–22929, 2001.
- Bähring R, Vardanyan V, Pongs O. Differential modulation of Kv1 channel-mediated currents by co-expression of Kv $\beta$ 3 subunit in a mammalian cell-line. *Mol Membr Biol* 21: 19–25, 2004.
- Balasubramaniam R, Grace AA, Saumarez RC, Vandenberg JJ, Huang CL. Electrogram prolongation and nifedipine-suppressible ventricular arrhythmias in mice following targeted disruption of KCNE1. *J Physiol* 552: 535–546, 2003.
- Barghaan J, Tozakidou M, Ehmk H, Bähring R. Role of NH<sub>2</sub>-terminal domain and accessory subunits in controlling deactivation-inactivation coupling of Kv4.2 channels. *Biophys J* 94: 1276–1294, 2008.
- Barhanin J, Lesage F, Guillemare E, Fink M, Lazdunski M, Romey G. K(V)LQT1 and Isk (minK) proteins associate to form the I(Ks) cardiac potassium current. *Nature* 384: 78–80, 1996.
- Beck EJ, Bowlby M, An WF, Rhodes KJ, Covarrubias M. Remodelling inactivation gating of Kv4 channels by KCHIP1, a small-molecular-weight calcium-binding protein. *J Physiol* 538: 691–706, 2002.
- Bekkers JM. Distribution and activation of voltage-gated potassium channels in cell-attached and outside-out patches from large layer 5 cortical pyramidal neurons of the rat. *J Physiol* 525: 611–620, 2000.
- Bekkers JM. Properties of voltage-gated potassium currents in nucleated patches from large layer 5 cortical pyramidal neurons of the rat. *J Physiol* 525: 593–609, 2000.
- Bendahhou S, Marionneau C, Haurogne K, Larroque MM, Derand R, Szuts V, Escande D, Demolombe S, Barhanin J. In vitro molecular interactions and distribution of KCNE family with KCNQ1 in the human heart. *Cardiovasc Res* 67: 529–538, 2005.
- Benham CD, Bolton TB. Spontaneous transient outward currents in single visceral and vascular smooth muscle cells of the rabbit. *J Physiol* 381: 385–406, 1986.
- Bentrop D, Beyermann M, Wissmann R, Fakler B. NMR structure of the "ball-and-chain" domain of KCNMB2, the  $\beta$  2-subunit of large conductance Ca<sup>2+</sup>- and voltage-activated potassium channels. *J Biol Chem* 276: 42116–42121, 2001.
- Benzinger GR, Xia XM, Lingle CJ. Direct observation of a pre-inactivated, open state in BK channels with  $\beta$ 2 subunits. *J Gen Physiol* 127: 119–131, 2006.
- Berkefeld H, Fakler B. Repolarizing responses of BKCa-Cav complexes are distinctly shaped by their Cav subunits. *J Neurosci* 28: 8238–8245, 2008.
- Berkefeld H, Sailer CA, Bildl W, Rohde V, Thumfart JO, Eble S, Klugbauer N, Reisinger E, Bischofberger J, Oliver D, Knaus

- HG, Schulte U, Fakler B. BKCa-Cav channel complexes mediate rapid and localized Ca<sup>2+</sup>-activated K<sup>+</sup> signaling. *Science* 314: 615–620, 2006.
33. Bezanilla F. Ion channels: from conductance to structure. *Neuron* 60: 456–468, 2008.
  34. Bianchi L, Shen Z, Dennis AT, Priori SG, Napolitano C, Ronchetti E, Bryskin R, Schwartz PJ, Brown AM. Cellular dysfunction of LQT5-minK mutants: abnormalities of IKs, IKr and trafficking in long QT syndrome. *Hum Mol Genet* 8: 1499–1507, 1999.
  35. Bielefeldt K, Jackson MB. A calcium-activated potassium channel causes frequency-dependent action-potential failures in a mammalian nerve terminal. *J Neurophysiol* 70: 284–298, 1993.
  36. Birnbaum SG, Varga AW, Yuan LL, Anderson AE, Sweatt JD, Schrader LA. Structure and function of Kv4-family transient potassium channels. *Physiol Rev* 84: 803–833, 2004.
  37. Brenner R, Chen QH, Vilaythong A, Toney GM, Noebels JL, Aldrich RW. BK channel  $\beta$ 4 subunit reduces dentate gyrus excitability and protects against temporal lobe seizures. *Nat Neurosci* 8: 1752–1759, 2005.
  38. Brenner R, Jegla TJ, Wickenden A, Liu Y, Aldrich RW. Cloning and functional characterization of novel large conductance calcium-activated potassium channel  $\beta$  subunits, hKCNMB3 and hKCNMB4. *J Biol Chem* 275: 6453–6461, 2000.
  39. Brenner R, Perez GJ, Bonev AD, Eckman DM, Kosek JC, Wiler SW, Patterson AJ, Nelson MT, Aldrich RW. Vasoregulation by the  $\beta$ 1 subunit of the calcium-activated potassium channel. *Nature* 407: 870–876, 2000.
  40. Burgoyne RD. Neuronal calcium sensor proteins: generating diversity in neuronal Ca<sup>2+</sup> signalling. *Nat Rev Neurosci* 8: 182–193, 2007.
  41. Busch AE, Busch GL, Ford E, Suessbrich H, Lang HJ, Greger R, Kunzelmann K, Attali B, Stuhmer W. The role of the Isk protein in the specific pharmacological properties of the IKs channel complex. *Br J Pharmacol* 122: 187–189, 1997.
  42. Butler A, Tsunoda S, McCobb DP, Wei A, Salkoff L. mSlo, a complex mouse gene encoding “maxi” calcium-activated potassium channels. *Science* 261: 221–224, 1993.
  43. Buxbaum JD, Choi EK, Luo Y, Lilliehook C, Crowley AC, Merriam DE, Wasco W. Calsenilin: a calcium-binding protein that interacts with the presenilins and regulates the levels of a presenilin fragment. *Nat Med* 4: 1177–1181, 1998.
  44. Callsen B, Isbrandt D, Sauter K, Hartmann LS, Pongs O, Bähring R. Contribution of N and C terminal Kv4.2 channel domains to KChIP interaction. *J Physiol* 568: 397–412, 2005.
  45. Carrion AM, Link WA, Ledo F, Mellstrom B, Naranjo JR. DREAM is a Ca<sup>2+</sup>-regulated transcriptional repressor. *Nature* 398: 80–84, 1999.
  46. Castellino RC, Morales MJ, Strauss HC, Rasmuson RL. Time- and voltage-dependent modulation of a Kv1.4 channel by a  $\beta$ -subunit (Kv $\beta$ 3) cloned from ferret ventricle. *Am J Physiol Heart Circ Physiol* 269: H385–H391, 1995.
  47. Cebolla B, Fernandez-Perez A, Perea G, Araque A, Vallejo M. DREAM mediates cAMP-dependent, Ca<sup>2+</sup>-induced stimulation of GFAP gene expression and regulates cortical astroglialogenesis. *J Neurosci* 28: 6703–6713, 2008.
  48. Charpentier F, Merot J, Riochet D, Le Marec H, Escande D. Adult KCNE1-knockout mice exhibit a mild cardiac cellular phenotype. *Biochem Biophys Res Commun* 251: 806–810, 1998.
  49. Chen M, Gan G, Wu Y, Wang L, Ding J. Lysine-rich extracellular rings formed by h $\beta$ 2 subunits confer the outward rectification of BK channels. *PLoS ONE* 3: e2114, 2008.
  50. Cheng HY, Pitcher GM, Laviolette SR, Whishaw IQ, Tong KI, Kockeritz LK, Wada T, Joza NA, Crackower M, Goncalves J, Sarosi I, Woodgett JR, Oliveira-dos-Santos AJ, Ikura M, van der Kooy D, Salter MW, Penninger JM. DREAM is a critical transcriptional repressor for pain modulation. *Cell* 108: 31–43, 2002.
  51. Choe CU, Schulze-Bahr E, Neu A, Xu J, Zhu ZI, Sauter K, Bähring R, Priori S, Guicheney P, Monnig G, Napolitano C, Heidemann J, Clancy CE, Pongs O, Isbrandt D. COOH-terminal HERG (LQT2) mutations disrupt IKr channel regulation through 14–3-3 $\epsilon$ . *Hum Mol Genet* 15: 2888–2902, 2006.
  52. Chouinard SW, Wilson GF, Schlingens AK, Ganetzky B. A potassium channel  $\beta$  subunit related to the aldo-keto reductase superfamily is encoded by the *Drosophila* hyperkinetic locus. *Proc Natl Acad Sci USA* 92: 6763–6767, 1995.
  53. Clark BD, Kwon E, Maffie J, Jeong HY, Nadal M, Strop P, Rudy B. DPP6 localization in brain supports function as a Kv4 channel associated protein. *Front Mol Neurosci* 1: 8, 2008.
  54. Cohen JA, Arai M, Prak EL, Brooks SA, Young LH, Prystowsky MB. Characterization of a novel mRNA expressed by neurons in mature brain. *J Neurosci Res* 31: 273–284, 1992.
  55. Conforti L, Bodi I, Nisbet JW, Millhorn DE. O<sub>2</sub>-sensitive K<sup>+</sup> channels: role of the Kv1.2 subunit in mediating the hypoxic response. *J Physiol* 524: 783–793, 2000.
  56. Connor JX, McCormack K, Pletsch A, Gaeta S, Ganetzky B, Chiu SY, Messing A. Genetic modifiers of the Kv $\beta$ 2-null phenotype in mice. *Genes Brain Behav* 4: 77–88, 2005.
  57. Cox DH, Cui J, Aldrich RW. Allosteric gating of a large conductance Ca-activated K<sup>+</sup> channel. *J Gen Physiol* 110: 257–281, 1997.
  58. Cronin S, Berger S, Ding J, Schymick JC, Washecka N, Hernandez DG, Greenway MJ, Bradley DG, Traynor BJ, Hardiman O. A genome-wide association study of sporadic ALS in a homogenous Irish population. *Hum Mol Genet* 17: 768–774, 2008.
  59. Cui J, Kagan A, Qin D, Mathew J, Melman YF, McDonald TV. Analysis of the cyclic nucleotide binding domain of the HERG potassium channel and interactions with KCNE2. *J Biol Chem* 276: 17244–17251, 2001.
  60. Cui J, Yang H, Lee US. Molecular mechanisms of BK channel activation. *Cell Mol Life Sci* 66: 852–875, 2009.
  61. Curran ME, Splawski I, Timothy KW, Vincent GM, Green ED, Keating MT. A molecular basis for cardiac arrhythmia: HERG mutations cause long QT syndrome. *Cell* 80: 795–803, 1995.
  62. Decher N, Gonzalez T, Streit AK, Sachse FB, Renigunta V, Soom M, Heinemann SH, Daut J, Sanguinetti MC. Structural determinants of Kv $\beta$ 1.3-induced channel inactivation: a hairpin modulated by PIP<sub>2</sub>. *EMBO J* 27: 3164–3174, 2008.
  63. Decher N, Kumar P, Gonzalez T, Renigunta V, Sanguinetti MC. Structural basis for competition between drug binding and Kv $\beta$ 1.3 accessory subunit-induced N-type inactivation of Kv1.5 channels. *Mol Pharmacol* 68: 995–1005, 2005.
  64. Dedek K, Waldegger S. Colocalization of KCNQ1/KCNE channel subunits in the mouse gastrointestinal tract. *Pflügers Arch* 442: 896–902, 2001.
  65. Deschenes I, Tomaselli GF. Modulation of Kv4 current by accessory subunits. *FEBS Lett* 528: 183–188, 2002.
  66. Deutsch C. Potassium channel ontogeny. *Annu Rev Physiol* 64: 19–46, 2002.
  67. Dopico AM, Widmer H, Wang G, Lemos JR, Treistman SN. Rat supraoptic magnocellular neurones show distinct large conductance, Ca<sup>2+</sup>-activated K<sup>+</sup> channel subtypes in cell bodies versus nerve endings. *J Physiol* 519: 101–114, 1999.
  68. Dougherty K, Covarrubias M. A dipeptidyl aminopeptidase-like protein remodels gating charge dynamics in Kv4.2 channels. *J Gen Physiol* 128: 745–753, 2006.
  69. Doyle DA, Morais Cabral J, Pfuetschner RA, Kuo A, Gulbis JM, Cohen SL, Chait BT, MacKinnon R. The structure of the potassium channel: molecular basis of K<sup>+</sup> conduction and selectivity. *Science* 280: 69–77, 1998.
  70. Drici MD, Arrighi I, Chouabe C, Mann JR, Lazdunski M, Romey G, Barhanin J. Involvement of Isk-associated K<sup>+</sup> channel in heart rate control of repolarization in a murine engineered model of Jervell and Lange-Nielsen syndrome. *Circ Res* 83: 95–102, 1998.
  71. Dworetzky SI, Boissard CG, Lum-Ragan JT, McKay MC, Post-Munson DJ, Trojnecki JT, Chang CP, Gribkoff VK. Phenotypic alteration of a human BK (hSlo) channel by hSlo $\beta$  subunit coexpression: changes in blocker sensitivity, activation/relaxation and inactivation kinetics, and protein kinase A modulation. *J Neurosci* 16: 4543–4550, 1996.
  72. England SK, Uebele VN, Kodali J, Bennett PB, Tamkun MM. A novel K<sup>+</sup> channel  $\beta$ -subunit (hKv $\beta$ 1.3) is produced via alternative mRNA splicing. *J Biol Chem* 270: 28531–28534, 1995.
  73. Fedida D, Zhang S, Kwan DC, Eduljee C, Kehl SJ. Synergistic inhibition of the maximum conductance of Kv1.5 channels by



- extracellular  $K^+$  reduction and acidification. *Cell Biochem Biophys* 43: 231–242, 2005.
74. **Feng G, Tintrop H, Kirsch J, Nichol MC, Kuhse J, Betz H, Sanes JR.** Dual requirement for gephyrin in glycine receptor clustering and molybdoenzyme activity. *Science* 282: 1321–1324, 1998.
  75. **Fernandez-Fernandez JM, Tomas M, Vazquez E, Orio P, Latorre R, Senti M, Marrugat J, Valverde MA.** Gain-of-function mutation in the KCNMB1 potassium channel subunit is associated with low prevalence of diastolic hypertension. *J Clin Invest* 113: 1032–1039, 2004.
  76. **Fletcher LR, Harvey IC.** An association of a *Lolium* endophyte with ryegrass staggers. *N Z Vet J* 29: 185–186, 1981.
  77. **Foehring RC.** Who needs A current? Functional remodelling in the  $Kv4.2^{-/-}$  mouse. *J Physiol* 586: 1461, 2008.
  78. **Fontan-Lozano A, Romero-Granados R, del-Pozo-Martin Y, Suarez-Pereira I, Delgado-Garcia JM, Penninger JM, Carrion AM.** Lack of DREAM protein enhances learning and memory and slows brain aging. *Curr Biol* 19: 54–60, 2009.
  79. **Gage SD, Kobertz WR.** KCNE3 truncation mutants reveal a bipartite modulation of KCNQ1  $K^+$  channels. *J Gen Physiol* 124: 759–771, 2004.
  80. **Gebauer M, Isbrandt D, Sauter K, Callsen B, Nolting A, Pongs O, Bähring R.** N-type inactivation features of  $Kv4.2$  channel gating. *Biophys J* 86: 210–223, 2004.
  81. **Geiger JR, Jonas P.** Dynamic control of presynaptic  $Ca^{2+}$  inflow by fast-inactivating  $K^+$  channels in hippocampal mossy fiber boutons. *Neuron* 28: 927–939, 2000.
  82. **Giese KP, Storm JF, Reuter D, Fedorov NB, Shao LR, Leicher T, Pongs O, Silva AJ.** Reduced  $K^+$  channel inactivation, spike broadening, and after-hyperpolarization in  $Kv\beta 1.1$ -deficient mice with impaired learning. *Learn Mem* 5: 257–273, 1998.
  83. **Gong J, Xu J, Bezanilla M, van Huizen R, Derin R, Li M.** Differential stimulation of PKC phosphorylation of potassium channels by ZIP1 and ZIP2. *Science* 285: 1565–1569, 1999.
  84. **Grimm PR, Irsik DL, Settles DC, Holtzclaw JD, Sansom SC.** Hypertension of  $Kcnmb1^{-/-}$  is linked to deficient K secretion and aldosteronism. *Proc Natl Acad Sci USA* 106: 11800–11805, 2009.
  85. **Grunnet M, Jespersen T, Rasmussen HB, Ljungstrom T, Jorgensen NK, Olesen SP, Klaerke DA.** KCNE4 is an inhibitory subunit to the KCNQ1 channel. *J Physiol* 542: 119–130, 2002.
  86. **Gu C, Zhou W, Puthenveedu MA, Xu M, Jan YN, Jan LY.** The microtubule plus-end tracking protein EB1 is required for  $Kv1$  voltage-gated  $K^+$  channel axonal targeting. *Neuron* 52: 803–816, 2006.
  87. **Gu N, Vervaeke K, Storm JF.** BK potassium channels facilitate high-frequency firing and cause early spike frequency adaptation in rat CA1 hippocampal pyramidal cells. *J Physiol* 580: 859–882, 2007.
  88. **Gulbis JM, Mann S, MacKinnon R.** Structure of a voltage-dependent  $K^+$  channel  $\beta$  subunit. *Cell* 97: 943–952, 1999.
  89. **Gulbis JM, Zhou M, Mann S, MacKinnon R.** Structure of the cytoplasmic  $\beta$  subunit-T1 assembly of voltage-dependent  $K^+$  channels. *Science* 289: 123–127, 2000.
  90. **Guo W, Jung WE, Marionneau C, Aimond F, Xu H, Yamada KA, Schwarz TL, Demolombe S, Nerbonne JM.** Targeted deletion of  $Kv4.2$  eliminates I(to,f) and results in electrical and molecular remodeling, with no evidence of ventricular hypertrophy or myocardial dysfunction. *Circ Res* 97: 1342–1350, 2005.
  91. **Haitin Y, Attali B.** The COOH-terminus of  $Kv7$  channels: a multifunctional module. *J Physiol* 586: 1803–1810, 2008.
  92. **Han W, Nattel S, Noguchi T, Shrier A.** COOH-terminal domain of  $Kv4.2$  and associated KChIP2 interactions regulate functional expression and gating of  $Kv4.2$ . *J Biol Chem* 281: 27134–27144, 2006.
  93. **Hanner M, Vianna-Jorge R, Kamassah A, Schmalhofer WA, Knaus HG, Kaczorowski GJ, Garcia ML.** The  $\beta$  subunit of the high conductance calcium-activated potassium channel. Identification of residues involved in charybdotoxin binding. *J Biol Chem* 273: 16289–16296, 1998.
  94. **Heinemann S, Rettig J, Scott V, Parcej DN, Lorra C, Dolly J, Pongs O.** The inactivation behaviour of voltage-gated K-channels may be determined by association of  $\alpha$ - and  $\beta$ -subunits. *J Physiol* 88: 173–180, 1994.
  95. **Heinemann SH, Rettig J, Graack HR, Pongs O.** Functional characterization of  $Kv$  channel  $\beta$ -subunits from rat brain. *J Physiol* 493: 625–633, 1996.
  96. **Heinemann SH, Rettig J, Wunder F, Pongs O.** Molecular and functional characterization of a rat brain  $Kv\beta 3$  potassium channel subunit. *FEBS Lett* 377: 383–389, 1995.
  97. **Heitzmann D, Warth R.** Physiology and pathophysiology of potassium channels in gastrointestinal epithelia. *Physiol Rev* 88: 1119–1182, 2008.
  98. **Hernandez CC, Zaika O, Tolstykh GP, Shapiro MS.** Regulation of neural KCNQ channels: signalling pathways, structural motifs and functional implications. *J Physiol* 586: 1811–1821, 2008.
  99. **Hicks GA, Marrion NV.**  $Ca^{2+}$ -dependent inactivation of large conductance  $Ca^{2+}$ -activated  $K^+$  (BK) channels in rat hippocampal neurones produced by pore block from an associated particle. *J Physiol* 508: 721–734, 1998.
  100. **Hoffman DA, Magee JC, Colbert CM, Johnston D.**  $K^+$  channel regulation of signal propagation in dendrites of hippocampal pyramidal neurons. *Nature* 387: 869–875, 1997.
  101. **Holmqvist MH, Cao J, Hernandez-Pineda R, Jacobson MD, Carroll KI, Sung MA, Betty M, Ge P, Gilbride KJ, Brown ME, Jurman ME, Lawson D, Silos-Santiago I, Xie Y, Covarrubias M, Rhodes KJ, Distefano PS, An WF.** Elimination of fast inactivation in  $Kv4$  A-type potassium channels by an auxiliary subunit domain. *Proc Natl Acad Sci USA* 99: 1035–1040, 2002.
  102. **Holmqvist MH, Cao J, Knoppers MH, Jurman ME, Distefano PS, Rhodes KJ, Xie Y, An WF.** Kinetic modulation of  $Kv4$ -mediated A-current by arachidonic acid is dependent on potassium channel interacting proteins. *J Neurosci* 21: 4154–4161, 2001.
  103. **Honore E, Attali B, Romey G, Heurteaux C, Ricard P, Lesage F, Lazdunski M, Barhanin J.** Cloning, expression, pharmacology and regulation of a delayed rectifier  $K^+$  channel in mouse heart. *EMBO J* 10: 2805–2811, 1991.
  104. **Horrigan FT, Aldrich RW.** Coupling between voltage sensor activation,  $Ca^{2+}$  binding and channel opening in large conductance (BK) potassium channels. *J Gen Physiol* 120: 267–305, 2002.
  105. **Hotta Y, Benzer S.** Mapping of behaviour in *Drosophila* mosaics. *Nature* 240: 527–535, 1972.
  106. **Hough RB, Lengeling A, Bedian V, Lo C, Bucan M.** Rump white inversion in the mouse disrupts dipeptidyl aminopeptidase-like protein 6 and causes dysregulation of Kit expression. *Proc Natl Acad Sci USA* 95: 13800–13805, 1998.
  107. **Howard RJ, Clark KA, Holton JM, Minor DL Jr.** Structural insight into KCNQ ( $Kv7$ ) channel assembly and channelopathy. *Neuron* 53: 663–675, 2007.
  108. **Hu HJ, Carrasquillo Y, Karim F, Jung WE, Nerbonne JM, Schwarz TL, Gereau RW.** The  $Kv4.2$  potassium channel subunit is required for pain plasticity. *Neuron* 50: 89–100, 2006.
  109. **Hu S, Labuda MZ, Pandolfo M, Goss GG, McDermid HE, Ali DW.** Variants of the KCNMB3 regulatory subunit of maxi BK channels affect channel inactivation. *Physiol Genomics* 15: 191–198, 2003.
  110. **Imlach WL, Finch SC, Dunlop J, Meredith AL, Aldrich RW, Dalziel JE.** The molecular mechanism of “ryegrass staggers,” a neurological disorder of  $K^+$  channels. *J Pharmacol Exp Ther* 327: 657–664, 2008.
  111. **Isbrandt D, Friederich P, Solth A, Haverkamp W, Ebner A, Borggrete M, Funke H, Sauter K, Breithardt G, Pongs O, Schulze-Bahr E.** Identification and functional characterization of a novel KCNE2 (MiRP1) mutation that alters HERG channel kinetics. *J Mol Med* 80: 524–532, 2002.
  112. **Jackson MB, Konnerth A, Augustine GJ.** Action potential broadening and frequency-dependent facilitation of calcium signals in pituitary nerve terminals. *Proc Natl Acad Sci USA* 88: 380–384, 1991.
  113. **Jentsch TJ.** Neuronal KCNQ potassium channels: physiology and role in disease. *Nat Rev Neurosci* 1: 21–30, 2000.
  114. **Jerng HH, Kunjilwar K, Pfaffinger PJ.** Multiprotein assembly of  $Kv4.2$ , KChIP3 and DPP10 produces ternary channel complexes with ISA-like properties. *J Physiol* 568: 767–788, 2005.
  115. **Jerng HH, Lauver AD, Pfaffinger PJ.** DPP10 splice variants are localized in distinct neuronal populations and act to differentially



- regulate the inactivation properties of Kv4-based ion channels. *Mol Cell Neurosci* 35: 604–624, 2007.
116. **Jerng HH, Pfaffinger PJ.** Multiple Kv channel-interacting proteins contain an NH<sub>2</sub>-terminal transmembrane domain that regulates Kv4 channel trafficking and gating. *J Biol Chem* 283: 36046–36059, 2008.
  117. **Jerng HH, Pfaffinger PJ, Covarrubias M.** Molecular physiology and modulation of somatodendritic A-type potassium channels. *Mol Cell Neurosci* 27: 343–369, 2004.
  118. **Jerng HH, Shahidullah M, Covarrubias M.** Inactivation gating of Kv4 potassium channels: molecular interactions involving the inner vestibule of the pore. *J Gen Physiol* 113: 641–660, 1999.
  119. **Johnston D, Hoffman DA, Colbert CM, Magee JC.** Regulation of back-propagating action potentials in hippocampal neurons. *Curr Opin Neurobiol* 9: 288–292, 1999.
  120. **Jones EM, Gray-Keller M, Fettiplace R.** The role of Ca<sup>2+</sup>-activated K<sup>+</sup> channel spliced variants in the tonotopic organization of the turtle cochlea. *J Physiol* 518: 653–665, 1999.
  121. **Kagan A, Melman YF, Krumerman A, McDonald TV.** 14–3–3 amplifies and prolongs adrenergic stimulation of HERG K<sup>+</sup> channel activity. *EMBO J* 21: 1889–1898, 2002.
  122. **Kamb A, Tseng-Crank J, Tanouye MA.** Multiple products of the *Drosophila Shaker* gene may contribute to potassium channel diversity. *Neuron* 1: 421–430, 1988.
  123. **Kang C, Tian C, Sonnichsen FD, Smith JA, Meiler J, George AL Jr, Vanoye CG, Kim HJ, Sanders CR.** Structure of KCNE1 and implications for how it modulates the KCNQ1 potassium channel. *Biochemistry* 47: 7999–8006, 2008.
  124. **Kaulin YA, De Santiago-Castillo JA, Rocha CA, Covarrubias M.** Mechanism of the modulation of Kv4:KChIP-1 channels by external K<sup>+</sup>. *Biophys J* 94: 1241–1251, 2008.
  125. **Kaulin YA, De Santiago-Castillo JA, Rocha CA, Nadal MS, Rudy B, Covarrubias M.** The dipeptidyl-peptidase-like protein DPP6 determines the unitary conductance of neuronal Kv4.2 channels. *J Neurosci* 29: 3242–3251, 2009.
  126. **Kim J, Nadal MS, Clemens AM, Baron M, Jung SC, Misumi Y, Rudy B, Hoffman DA.** Kv4 accessory protein DPPX (DPP6) is a critical regulator of membrane excitability in hippocampal CA1 pyramidal neurons. *J Neurophysiol* 100: 1835–1847, 2008.
  127. **Kim LA, Furst J, Gutierrez D, Butler MH, Xu S, Goldstein SA, Grigorieff N.** Three-dimensional structure of I(to); Kv4.2-KChIP2 ion channels by electron microscopy at 21 Å resolution. *Neuron* 41: 513–519, 2004.
  128. **Kim Y, Park MK, Uhm DY, Shin J, Chung S.** Modulation of delayed rectifier potassium channels by  $\alpha$ 1-adrenergic activation via protein kinase C zeta and p62 in PC12 cells. *Neurosci Lett* 387: 43–48, 2005.
  129. **Knaus HG, Eberhart A, Kaczorowski GJ, Garcia ML.** Covalent attachment of charybdotoxin to the  $\beta$ -subunit of the high conductance Ca<sup>2+</sup>-activated K<sup>+</sup> channel. Identification of the site of incorporation and implications for channel topology. *J Biol Chem* 269: 23336–23341, 1994.
  130. **Knaus HG, Folander K, Garcia-Calvo M, Garcia ML, Kaczorowski GJ, Smith M, Swanson R.** Primary sequence and immunological characterization of  $\beta$ -subunit of high conductance Ca<sup>2+</sup>-activated K<sup>+</sup> channel from smooth muscle. *J Biol Chem* 269: 17274–17278, 1994.
  131. **Kole MH, Letzkus JJ, Stuart GJ.** Axon initial segment Kv1 channels control axonal action potential waveform and synaptic efficacy. *Neuron* 55: 633–647, 2007.
  132. **Korngreen A, Sakmann B.** Voltage-gated K<sup>+</sup> channels in layer 5 neocortical pyramidal neurones from young rats: subtypes and gradients. *J Physiol* 525: 621–639, 2000.
  133. **Kreusch A, Pfaffinger PJ, Stevens CF, Choe S.** Crystal structure of the tetramerization domain of the *Shaker* potassium channel. *Nature* 392: 945–948, 1998.
  134. **Krumerman A, Gao X, Bian JS, Melman YF, Kagan A, McDonald TV.** An LQT mutant minK alters KvLQT1 trafficking. *Am J Physiol Cell Physiol* 286: C1453–C1463, 2004.
  135. **Kunjilwar K, Strang C, DeRubeis D, Pfaffinger PJ.** KChIP3 rescues the functional expression of Shal channel tetramerization mutants. *J Biol Chem* 279: 54542–54551, 2004.
  136. **Kuo HC, Cheng CF, Clark RB, Lin JJ, Lin JL, Hoshijima M, Nguyen-Tran VT, Gu Y, Ikeda Y, Chu PH, Ross J, Giles WR, Chien KR.** A defect in the Kv channel-interacting protein 2 (KChIP2) gene leads to a complete loss of I(to) and confers susceptibility to ventricular tachycardia. *Cell* 107: 801–813, 2001.
  137. **Kupersmidt S, Yang T, Anderson ME, Wessels A, Niswender KD, Magnuson MA, Roden DM.** Replacement by homologous recombination of the minK gene with lacZ reveals restriction of minK expression to the mouse cardiac conduction system. *Circ Res* 84: 146–152, 1999.
  138. **Kurokawa J, Motoike HK, Rao J, Kass RS.** Regulatory actions of the A-kinase anchoring protein Yotiao on a heart potassium channel downstream of PKA phosphorylation. *Proc Natl Acad Sci USA* 101: 16374–16378, 2004.
  139. **Larsen AP, Olesen SP, Grunnet M, Jespersen T.** Characterization of hERG1a and hERG1b potassium channels—a possible role for hERG1b in the I (Kr) current. *Pflügers Arch* 456: 1137–1148, 2008.
  140. **Lees-Miller JP, Kondo C, Wang L, Duff HJ.** Electrophysiological characterization of an alternatively processed ERG K<sup>+</sup> channel in mouse and human hearts. *Circ Res* 81: 719–726, 1997.
  141. **Leicher T, Bähring R, Isbrandt D, Pongs O.** Coexpression of the KCNA3B gene product with Kv1.5 leads to a novel A-type potassium channel. *J Biol Chem* 273: 35095–35101, 1998.
  142. **Leicher T, Roeper J, Weber K, Wang X, Pongs O.** Structural and functional characterization of human potassium channel subunit  $\beta$  1 (KCNA1B). *Neuropharmacology* 35: 787–795, 1996.
  143. **Lewis A, McCrossan ZA, Abbott GW.** MinK, MiRP1, and MiRP2 diversify Kv3.1 and Kv3.2 potassium channel gating. *J Biol Chem* 279: 7884–7892, 2004.
  144. **Li H, Guo W, Mellor RL, Nerbonne JM.** KChIP2 modulates the cell surface expression of Kv 1.5-encoded K(+) channels. *J Mol Cell Cardiol* 39: 121–132, 2005.
  145. **Li HL, Qu YJ, Lu YC, Bondarenko VE, Wang S, Skerrett IM, Morales MJ.** DPP10 is an inactivation modulatory protein of Kv4.3 and Kv1.4. *Am J Physiol Cell Physiol* 291: C966–C976, 2006.
  146. **Li W, Gao SB, Lv CX, Wu Y, Guo ZH, Ding JP, Xu T.** Characterization of voltage- and Ca<sup>2+</sup>-activated K<sup>+</sup> channels in rat dorsal root ganglion neurons. *J Cell Physiol* 212: 348–357, 2007.
  147. **Lilliehook C, Bozdagi O, Yao J, Gomez-Ramirez M, Zaidi NF, Wasco W, Gandy S, Santucci AC, Haroutunian V, Huntley GW, Buxbaum JD.** Altered A $\beta$  formation and long-term potentiation in a calenilin knock-out. *J Neurosci* 23: 9097–9106, 2003.
  148. **Lingle CJ.** Gating rings formed by RCK domains: keys to gate opening. *J Gen Physiol* 129: 101–107, 2007.
  149. **Link WA, Ledo F, Torres B, Palczewska M, Madsen TM, Savignac M, Albar JP, Mellstrom B, Naranjo JR.** Day-night changes in downstream regulatory element antagonist modulator/potassium channel interacting protein activity contribute to circadian gene expression in pineal gland. *J Neurosci* 24: 5346–5355, 2004.
  150. **Lippiat JD, Standen NB, Harrow ID, Phillips SC, Davies NW.** Properties of BK(Ca) channels formed by bicistronic expression of hSlo $\alpha$  and  $\beta$ 1–4 subunits in HEK293 cells. *J Membr Biol* 192: 141–148, 2003.
  151. **Liu G, Shi J, Yang L, Cao L, Park SM, Cui J, Marx SO.** Assembly of a Ca<sup>2+</sup>-dependent BK channel signaling complex by binding to  $\beta$ 2 adrenergic receptor. *EMBO J* 23: 2196–2205, 2004.
  152. **London B, Trudeau MC, Newton KP, Beyer AK, Copeland NG, Gilbert DJ, Jenkins NA, Satler CA, Robertson GA.** Two isoforms of the mouse ether-a-go-go-related gene coassemble to form channels with properties similar to the rapidly activating component of the cardiac delayed rectifier K<sup>+</sup> current. *Circ Res* 81: 870–878, 1997.
  153. **Long SB, Campbell EB, Mackinnon R.** Crystal structure of a mammalian voltage-dependent *Shaker* family K<sup>+</sup> channel. *Science* 309: 897–903, 2005.
  154. **Long SB, Campbell EB, Mackinnon R.** Voltage sensor of Kv1.2: structural basis of electromechanical coupling. *Science* 309: 903–908, 2005.
  155. **Lorenz S, Heils A, Kasper JM, Sander T.** Allelic association of a truncation mutation of the KCNMB3 gene with idiopathic generalized epilepsy. *Am J Med Genet B Neuropsychiatr Genet* 144: 10–13, 2007.

156. **Lorincz A, Nusser Z.** Cell-type-dependent molecular composition of the axon initial segment. *J Neurosci* 28: 14329–14340, 2008.
157. **Lu R, Alioua A, Kumar Y, Eghbali M, Stefani E, Toro L.** MaxiK channel partners: physiological impact. *J Physiol* 570: 65–72, 2006.
158. **Lu Y, Mahaut-Smith MP, Huang CL, Vandenberg JI.** Mutant MiRP1 subunits modulate HERG K<sup>+</sup> channel gating: a mechanism for pro-arrhythmia in long QT syndrome type 6. *J Physiol* 551: 253–262, 2003.
159. **Lundby A, Ravn LS, Svendsen JH, Hauns S, Olesen SP, Schmitt N.** KCNE3 mutation V17M identified in a patient with lone atrial fibrillation. *Cell Physiol Biochem* 21: 47–54, 2008.
160. **Maffie J, Blenkinsop T, Rudy B.** A novel DPP6 isoform (DPP6-E) can account for differences between neuronal and reconstituted A-type K<sup>+</sup> channels. *Neurosci Lett* 449: 189–194, 2009.
161. **Maffie J, Rudy B.** Weighing the evidence for a ternary protein complex mediating A-type K<sup>+</sup> currents in neurons. *J Physiol* 586: 5609–5623, 2008.
162. **Manderfield LJ, Daniels MA, Vanoye CG, George AL Jr.** KCNE4 domains required for inhibition of KCNQ1. *J Physiol* 587: 303–314, 2009.
163. **Marshall CR, Noor A, Vincent JB, Lionel AC, Feuk L, Skaug J, Shago M, Moessner R, Pinto D, Ren Y, Thiruvahindrapaduran B, Fiebig A, Schreiber S, Friedman J, Ketelaars CE, Vos YJ, Ficcioglu C, Kirkpatrick S, Nicolson R, Sloman L, Summers A, Gibbons CA, Teebi A, Chitayat D, Weksberg R, Thompson A, Vardy C, Crosbie V, Luscombe S, Baatjes R, Zwaigenbaum L, Roberts W, Fernandez B, Szatmari P, Scherer SW.** Structural variation of chromosomes in autism spectrum disorder. *Am J Hum Genet* 82: 477–488, 2008.
164. **Martin GE, Hendrickson LM, Penta KL, Friesen RM, Pietrzykowski AZ, Tapper AR, Treistman SN.** Identification of a BK channel auxiliary protein controlling molecular and behavioral tolerance to alcohol. *Proc Natl Acad Sci USA* 105: 17543–17548, 2008.
165. **Marty A.** Ca-dependent K channels with large unitary conductance in chromaffin cell membranes. *Nature* 291: 497–500, 1981.
166. **Marty A.** The physiological role of calcium-dependent channels. *Trends Neurosci* 12: 420–424, 1989.
167. **Marx SO, Kurokawa J, Reiken S, Motoike H, D'Armiento J, Marks AR, Kass RS.** Requirement of a macromolecular signaling complex for  $\beta$  adrenergic receptor modulation of the KCNQ1-KCNE1 potassium channel. *Science* 295: 496–499, 2002.
168. **Maylie J, Bond CT, Herson PS, Lee WS, Adelman JP.** Small conductance Ca<sup>2+</sup>-activated K<sup>+</sup> channels and calmodulin. *J Physiol* 554: 255–261, 2004.
169. **Mazhari R, Greenstein JL, Winslow RL, Marban E, Nuss HB.** Molecular interactions between two long-QT syndrome gene products, HERG and KCNE2, rationalized by in vitro and in silico analysis. *Circ Res* 89: 33–38, 2001.
170. **McCormack K, Connor JX, Zhou L, Ho LL, Ganetzky B, Chiu SY, Messing A.** Genetic analysis of the mammalian K<sup>+</sup> channel  $\beta$  subunit Kv $\beta$ 2 (Kcnab2). *J Biol Chem* 277: 13219–13228, 2002.
171. **McCormack K, McCormack T, Tanouye M, Rudy B, Stuhmer W.** Alternative splicing of the human *Shaker* K<sup>+</sup> channel  $\beta$  1 gene and functional expression of the  $\beta$  2 gene product. *FEBS Lett* 370: 32–36, 1995.
172. **McCormack T, McCormack K.** *Shaker* K<sup>+</sup> channel  $\beta$  subunits belong to an NAD(P)H-dependent oxidoreductase superfamily. *Cell* 79: 1133–1135, 1994.
173. **McCormack T, McCormack K, Nadal MS, Vieira E, Ozaita A, Rudy B.** The effects of *Shaker*  $\beta$ -subunits on the human lymphocyte K<sup>+</sup> channel Kv1.3. *J Biol Chem* 274: 20123–20126, 1999.
174. **McCrossan ZA, Abbott GW.** The Mink-related peptides. *Neuropharmacology* 47: 787–821, 2004.
175. **McDonald TV, Yu Z, Ming Z, Palma E, Meyers MB, Wang KW, Goldstein SA, Fishman GI.** A minK-HERG complex regulates the cardiac potassium current I(Kr). *Nature* 388: 289–292, 1997.
176. **Meera P, Wallner M, Jiang Z, Toro L.** A calcium switch for the functional coupling between  $\alpha$  (hsl $\alpha$ ) and  $\beta$  subunits (Kv,ca $\beta$ ) of maxi K channels. *FEBS Lett* 385: 127–128, 1996.
177. **Meera P, Wallner M, Toro L.** A neuronal  $\beta$  subunit (KCNMB4) makes the large conductance, voltage- and Ca<sup>2+</sup>-activated K<sup>+</sup> channel resistant to charybdotoxin and iberitoxin. *Proc Natl Acad Sci USA* 97: 5562–5567, 2000.
178. **Melman YF, Domenech A, de la Luna S, McDonald TV.** Structural determinants of KvLQT1 control by the KCNE family of proteins. *J Biol Chem* 276: 6439–6444, 2001.
179. **Melman YF, Krummnerman A, McDonald TV.** KCNE regulation of KvLQT1 channels: structure-function correlates. *Trends Cardiovasc Med* 12: 182–187, 2002.
180. **Menegola M, Trimmer JS.** Unanticipated region- and cell-specific downregulation of individual KChIP auxiliary subunit isoforms in Kv4.2 knock-out mouse brain. *J Neurosci* 26: 12137–12142, 2006.
181. **Misonou H, Menegola M, Buchwalder L, Park EW, Meredith A, Rhodes KJ, Aldrich RW, Trimmer JS.** Immunolocalization of the Ca<sup>2+</sup>-activated K<sup>+</sup> channel Slo1 in axons and nerve terminals of mammalian brain and cultured neurons. *J Comp Neurol* 496: 289–302, 2006.
182. **Morales MJ, Castellino RC, Crews AL, Rasmusson RL, Strauss HC.** A novel  $\beta$  subunit increases rate of inactivation of specific voltage-gated potassium channel  $\alpha$  subunits. *J Biol Chem* 270: 6272–6277, 1995.
183. **Morin TJ, Kobertz WR.** Counting membrane-embedded KCNE  $\beta$ -subunits in functioning K<sup>+</sup> channel complexes. *Proc Natl Acad Sci USA* 105: 1478–1482, 2008.
184. **Morohashi Y, Hatano N, Ohya S, Takikawa R, Watabiki T, Takasugi N, Imaizumi Y, Tomita T, Iwatsubo T.** Molecular cloning and characterization of CALP/KChIP4, a novel EF-hand protein interacting with presenilin 2 and voltage-gated potassium channel subunit Kv4. *J Biol Chem* 277: 14965–14975, 2002.
185. **Murphy GG, Fedorov NB, Giese KP, Ohno M, Friedman E, Chen R, Silva AJ.** Increased neuronal excitability, synaptic plasticity, and learning in aged Kv $\beta$ 1.1 knockout mice. *Curr Biol* 14: 1907–1915, 2004.
186. **Nadal MS, Amarillo Y, Vega-Saenz de Miera E, Rudy B.** Differential characterization of three alternative spliced isoforms of DPPX. *Brain Res* 1094: 1–12, 2006.
187. **Nadal MS, Ozaita A, Amarillo Y, Vega-Saenz de Miera E, Ma Y, Mo W, Goldberg EM, Misumi Y, Ikehara Y, Neubert TA, Rudy B.** The CD26-related dipeptidyl aminopeptidase-like protein DPPX is a critical component of neuronal A-type K<sup>+</sup> channels. *Neuron* 37: 449–461, 2003.
188. **Nagaya N, Papazian DM.** Potassium channel  $\alpha$  and  $\beta$  subunits assemble in the endoplasmic reticulum. *J Biol Chem* 272: 3022–3027, 1997.
189. **Nakamura TY, Nandi S, Pountney DJ, Artman M, Rudy B, Coetzee WA.** Different effects of the Ca<sup>2+</sup>-binding protein, KChIP1, on two Kv4 subfamily members, Kv4.1 and Kv4.2. *FEBS Lett* 499: 205–209, 2001.
190. **Need AC, Irvine EE, Giese KP.** Learning and memory impairments in Kv $\beta$ 1.1-null mutants are rescued by environmental enrichment or aging. *Eur J Neurosci* 18: 1640–1644, 2003.
191. **Nelson MT, Bonev AD.** The  $\beta$ 1 subunit of the Ca<sup>2+</sup>-sensitive K<sup>+</sup> channel protects against hypertension. *J Clin Invest* 113: 955–957, 2004.
192. **Nerbonne JM, Gerber BR, Norris A, Burkhalter A.** Electrical remodelling maintains firing properties in cortical pyramidal neurons lacking KCND2-encoded A-type K<sup>+</sup> currents. *J Physiol* 586: 1565–1579, 2008.
193. **Nerbonne JM, Kass RS.** Molecular physiology of cardiac repolarization. *Physiol Rev* 85: 1205–1253, 2005.
194. **Neyroud N, Tesson F, Denjoy I, Leibovici M, Donger C, Barhanin J, Faure S, Gary F, Coumel P, Petit C, Schwartz K, Guicheney P.** A novel mutation in the potassium channel gene KVLQT1 causes the Jervell and Lange-Nielsen cardioauditory syndrome. *Nat Genet* 15: 186–189, 1997.
195. **Nicolas CS, Park KH, El Harchi A, Camonis J, Kass RS, Escande D, Merot J, Loussouarn G, Le Bouffant F, Baro I.** IKs response to protein kinase A-dependent KCNQ1 phosphorylation requires direct interaction with microtubules. *Cardiovasc Res* 79: 427–435, 2008.
196. **Niwa N, Wang W, Sha Q, Marionneau C, Nerbonne JM.** Kv4.3 is not required for the generation of functional I<sub>to,f</sub> channels in adult mouse ventricles. *J Mol Cell Cardiol* 44: 95–104, 2008.
197. **O'Callaghan DW, Hasdemir B, Leighton M, Burgoyne RD.** Residues within the myristoylation motif determine intracellular targeting of the neuronal Ca<sup>2+</sup> sensor protein KChIP1 to post-ER



- transport vesicles and traffic of Kv4 K<sup>+</sup> channels. *J Cell Sci* 116: 4833–4845, 2003.
198. **Oelze M, Warnholtz A, Faulhaber J, Wenzel P, Kleschyov AL, Coldewey M, Hink U, Pongs O, Fleming I, Wassmann S, Meinertz T, Ehmke H, Daiber A, Munzel T.** NADPH oxidase accounts for enhanced superoxide production and impaired endothelium-dependent smooth muscle relaxation in BK $\beta$ 1<sup>-/-</sup> mice. *Arterioscler Thromb Vasc Biol* 26: 1753–1759, 2006.
  199. **Ogawa Y, Rasband MN.** The functional organization and assembly of the axon initial segment. *Curr Opin Neurobiol* 18: 307–313, 2008.
  200. **Oliver D, Lien CC, Soom M, Baukrowitz T, Jonas P, Fakler B.** Functional conversion between A-type and delayed rectifier K<sup>+</sup> channels by membrane lipids. *Science* 304: 265–270, 2004.
  201. **Orio P, Latorre R.** Differential effects of  $\beta$ 1 and  $\beta$ 2 subunits on BK channel activity. *J Gen Physiol* 125: 395–411, 2005.
  202. **Orio P, Rojas P, Ferreira G, Latorre R.** New disguises for an old channel: MaxiK channel  $\beta$ -subunits. *News Physiol Sci* 17: 156–161, 2002.
  203. **Orio P, Torres Y, Rojas P, Carvacho I, Garcia ML, Toro L, Valverde MA, Latorre R.** Structural determinants for functional coupling between the  $\beta$  and  $\alpha$  subunits in the Ca<sup>2+</sup>-activated K<sup>+</sup> (BK) channel. *J Gen Physiol* 127: 191–204, 2006.
  204. **Pan Y, Weng J, Cao Y, Boshes RC, Zhou M.** Functional coupling between the Kv1.1 channel and aldoketoreductase Kv $\beta$ 1. *J Biol Chem* 283: 8634–8642, 2008.
  205. **Panaghi G, Tai KK, Abbott GW.** Interaction of KCNE subunits with the KCNQ1 K<sup>+</sup> channel pore. *J Physiol* 570: 455–467, 2006.
  206. **Parcej DN, Dolly JO.** Dendrotoxin acceptor from bovine synaptic plasma membranes. Binding properties, purification and subunit composition of a putative constituent of certain voltage-activated K<sup>+</sup> channels. *Biochem J* 257: 899–903, 1989.
  207. **Parcej DN, Scott VE, Dolly JO.** Oligomeric properties of  $\alpha$ -dendrotoxin-sensitive potassium ion channels purified from bovine brain. *Biochemistry* 31: 11084–11088, 1992.
  208. **Patel AJ, Lazdunski M, Honore E.** Kv2.1/Kv9.3, a novel ATP-dependent delayed-rectifier K<sup>+</sup> channel in oxygen-sensitive pulmonary artery myocytes. *EMBO J* 16: 6615–6625, 1997.
  209. **Patel SP, Campbell DL.** Transient outward potassium current, “I<sub>to</sub>,” phenotypes in the mammalian left ventricle: underlying molecular, cellular and biophysical mechanisms. *J Physiol* 569: 7–39, 2005.
  210. **Perez-Garcia MT, Lopez-Lopez JR, Gonzalez C.** Kv $\beta$ 1.2 subunit coexpression in HEK293 cells confers O<sub>2</sub> sensitivity to Kv4.2 but not to Shaker channels. *J Gen Physiol* 113: 897–907, 1999.
  211. **Peters CJ, Vaid M, Horne AJ, Fedida D, Accili EA.** The molecular basis for the actions of K(V) $\beta$ 1.2 on the opening and closing of the K(V)1.2 delayed rectifier channel. *Channels* 3: 314–322, 2009.
  212. **Petersen OH.** Stimulus-secretion coupling: cytoplasmic calcium signals and the control of ion channels in exocrine acinar cells. *J Physiol* 448: 1–51, 1992.
  213. **Petkov GV, Bonev AD, Heppner TJ, Brenner R, Aldrich RW, Nelson MT.**  $\beta$ 1-Subunit of the Ca<sup>2+</sup>-activated K<sup>+</sup> channel regulates contractile activity of mouse urinary bladder smooth muscle. *J Physiol* 537: 443–452, 2001.
  214. **Piccini M, Casari G, Zhou J, Bruttini M, Volti SL, Ballabio A, Renieri A.** Evidence for genetic heterogeneity in benign familial hematuria. *Am J Nephrol* 19: 464–467, 1999.
  215. **Pioletti M, Findeisen F, Hura GL, Minor DL Jr.** Three-dimensional structure of the KChIP1-Kv4.3 T1 complex reveals a cross-shaped octamer. *Nat Struct Mol Biol* 13: 987–995, 2006.
  216. **Piskowski R, Aldrich RW.** Calcium activation of BK(Ca) potassium channels lacking the calcium bowl and RCK domains. *Nature* 420: 499–502, 2002.
  217. **Pluger S, Faulhaber J, Furstenu M, Lohn M, Waldschutz R, Gollasch M, Haller H, Luft FC, Ehmke H, Pongs O.** Mice with disrupted BK channel  $\beta$ 1 subunit gene feature abnormal Ca<sup>2+</sup> spark/STOC coupling and elevated blood pressure. *Circ Res* 87: E53–60, 2000.
  218. **Poliak S, Gollan L, Martinez R, Custer A, Einheber S, Salzer JL, Trimmer JS, Shrager P, Peles E.** Caspr2, a new member of the neuroligin superfamily, is localized at the juxtaparanodes of myelinated axons and associates with K<sup>+</sup> channels. *Neuron* 24: 1037–1047, 1999.
  219. **Pongs O.** Molecular biology of voltage-dependent potassium channels. *Physiol Rev* 72 Suppl: S69–S88, 1992.
  220. **Pongs O.** Regulation of the activity of voltage-gated potassium channel by  $\beta$  subunits. *The Neurosciences* 7: 137–146, 1995.
  221. **Pongs O, Kecskemethy N, Muller R, Krah-Jentgens I, Baumann A, Kiltz HH, Canal I, Llamazares S, Ferrus A.** Shaker encodes a family of putative potassium channel proteins in the nervous system of *Drosophila*. *EMBO J* 7: 1087–1096, 1988.
  222. **Pongs O, Leicher T, Berger M, Roeper J, Bähring R, Wray D, Giese KP, Silva AJ, Storm JF.** Functional and molecular aspects of voltage-gated K<sup>+</sup> channel  $\beta$  subunits. *Ann NY Acad Sci* 868: 344–355, 1999.
  223. **Pusch M.** Increase of the single-channel conductance of KvLQT1 potassium channels induced by the association with minK. *Pflügers Arch* 437: 172–174, 1998.
  224. **Pyott SJ, Meredith AL, Fodor AA, Vazquez AE, Yamoah EN, Aldrich RW.** Cochlear function in mice lacking the BK channel  $\alpha$ ,  $\beta$ 1, or  $\beta$ 4 subunits. *J Biol Chem* 282: 3312–3324, 2007.
  225. **Qi SY, Riviere PJ, Trojnar J, Junien JL, Akinsanya KO.** Cloning and characterization of dipeptidyl peptidase 10, a new member of an emerging subgroup of serine proteases. *Biochem J* 373: 179–189, 2003.
  226. **Raab-Graham KF, Haddick PC, Jan YN, Jan LY.** Activity- and mTOR-dependent suppression of Kv1.1 channel mRNA translation in dendrites. *Science* 314: 144–148, 2006.
  227. **Radick S, Cotella D, Graf EM, Ravens U, Wettwer E.** Expression and function of dipeptidyl-aminopeptidase-like protein 6 as a putative  $\beta$ -subunit of human cardiac transient outward current encoded by Kv4.3. *J Physiol* 565: 751–756, 2005.
  228. **Ramanathan K, Michael TH, Jiang GJ, Hiel H, Fuchs PA.** A molecular mechanism for electrical tuning of cochlear hair cells. *Science* 283: 215–217, 1999.
  229. **Ramu Y, Xu Y, Lu Z.** Enzymatic activation of voltage-gated potassium channels. *Nature* 442: 696–699, 2006.
  230. **Rehm H, Lazdunski M.** Purification and subunit structure of a putative K<sup>+</sup>-channel protein identified by its binding properties for dendrotoxin I. *Proc Natl Acad Sci USA* 85: 4919–4923, 1988.
  231. **Ren X, Hayashi Y, Yoshimura N, Takimoto K.** Transmembrane interaction mediates complex formation between peptidase homologues and Kv4 channels. *Mol Cell Neurosci* 29: 320–332, 2005.
  232. **Rettig J, Heinemann SH, Wunder F, Lorra C, Parcej DN, Dolly JO, Pongs O.** Inactivation properties of voltage-gated K<sup>+</sup> channels altered by presence of  $\beta$ -subunit. *Nature* 369: 289–294, 1994.
  233. **Rhodes KJ, Carroll KI, Sung MA, Doliveira LC, Monaghan MM, Burke SL, Strassle BW, Buchwalder L, Menegola M, Cao J, An WF, Trimmer JS.** KChIPs and Kv4  $\alpha$  subunits as integral components of A-type potassium channels in mammalian brain. *J Neurosci* 24: 7903–7915, 2004.
  234. **Rhodes KJ, Keilbaugh SA, Barrezueta NX, Lopez KL, Trimmer JS.** Association and colocalization of K<sup>+</sup> channel  $\alpha$ - and  $\beta$ -subunit polypeptides in rat brain. *J Neurosci* 15: 5360–5371, 1995.
  235. **Rhodes KJ, Monaghan MM, Barrezueta NX, Nawoschik S, Bekele-Arcuri Z, Matos MF, Nakahira K, Schechter LE, Trimmer JS.** Voltage-gated K<sup>+</sup> channel  $\beta$  subunits: expression and distribution of Kv $\beta$ 1 and Kv $\beta$ 2 in adult rat brain. *J Neurosci* 16: 4846–4860, 1996.
  236. **Rhodes KJ, Strassle BW, Monaghan MM, Bekele-Arcuri Z, Matos MF, Trimmer JS.** Association and colocalization of the Kv $\beta$ 1 and Kv $\beta$ 2  $\beta$ -subunits with Kv1  $\alpha$ -subunits in mammalian brain K<sup>+</sup> channel complexes. *J Neurosci* 17: 8246–8258, 1997.
  237. **Robbins J.** KCNQ potassium channels: physiology, pathophysiology, and pharmacology. *Pharmacol Ther* 90: 1–19, 2001.
  238. **Rocheleau JM, Kobertz WR.** KCNE peptides differentially affect voltage sensor equilibrium and equilibration rates in KCNQ1 K<sup>+</sup> channels. *J Gen Physiol* 131: 59–68, 2008.
  239. **Roepke TK, Anantharam A, Kirchhoff P, Busque SM, Young JB, Geibel JP, Lerner DJ, Abbott GW.** The KCNE2 potassium channel ancillary subunit is essential for gastric acid secretion. *J Biol Chem* 281: 23740–23747, 2006.
  240. **Roepke TK, King EC, Reyna-Neyra A, Paroder M, Purtell K, Koba W, Fine E, Lerner DJ, Carrasco N, Abbott GW.** Kcne2 deletion uncovers its crucial role in thyroid hormone biosynthesis. *Nat Med* 15: 1186–1194, 2009.



241. Roepke TK, Kontogeorgis A, Ovanez C, Xu X, Young JB, Purtell K, Goldstein PA, Christini DJ, Peters NS, Akar FG, Gutstein DE, Lerner DJ, Abbott GW. Targeted deletion of *kcne2* impairs ventricular repolarization via disruption of *I(K<sub>s</sub>slow1)* and *I(to,f)*. *FASEB J* 22: 3648–3660, 2008.
242. Roper J, Schwarz JR. Heterogeneous distribution of fast and slow potassium channels in myelinated rat nerve fibres. *J Physiol* 416: 93–110, 1989.
243. Rosati B, Grau F, Rodriguez S, Li H, Nerbonne JM, McKinnon D. Concordant expression of KChIP2 mRNA, protein and transient outward current throughout the canine ventricle. *J Physiol* 548: 815–822, 2003.
244. Rosati B, McKinnon D. Regulation of ion channel expression. *Circ Res* 94: 874–883, 2004.
245. Rosati B, Pan Z, Lypen S, Wang HS, Cohen I, Dixon JE, McKinnon D. Regulation of KChIP2 potassium channel  $\beta$  subunit gene expression underlies the gradient of transient outward current in canine and human ventricle. *J Physiol* 533: 119–125, 2001.
246. Ruppersberg JP, Schroter KH, Sakmann B, Stocker M, Sewing S, Pongs O. Heteromultimeric channels formed by rat brain potassium-channel proteins. *Nature* 345: 535–537, 1990.
247. Salkoff L, Butler A, Ferreira G, Santi C, Wei A. High-conductance potassium channels of the SLO family. *Nat Rev Neurosci* 7: 921–931, 2006.
248. Sanguinetti MC, Curran ME, Zou A, Shen J, Spector PS, Atkinson DL, Keating MT. Coassembly of K(V)LQT1 and minK (IsK) proteins to form cardiac I(Ks) potassium channel. *Nature* 384: 80–83, 1996.
249. Sanguinetti MC, Jiang C, Curran ME, Keating MT. A mechanistic link between an inherited and an acquired cardiac arrhythmia: HERG encodes the IKr potassium channel. *Cell* 81: 299–307, 1995.
250. Sanguinetti MC, Jurkiewicz NK. Two components of cardiac delayed rectifier K<sup>+</sup> current. Differential sensitivity to block by class III antiarrhythmic agents. *J Gen Physiol* 96: 195–215, 1990.
251. Scannevin RH, Wang K, Jow F, Megules J, Kopsco DC, Edris W, Carroll KC, Lu Q, Xu W, Xu Z, Katz AH, Olland S, Lin L, Taylor M, Stahl M, Malakian K, Somers W, Mosyak L, Bowlby MR, Chanda P, Rhodes KJ. Two NH<sub>2</sub>-terminal domains of Kv4 K<sup>+</sup> channels regulate binding to and modulation by KChIP1. *Neuron* 41: 587–598, 2004.
252. Schilling T, Stock C, Schwab A, Eder C. Functional importance of Ca<sup>2+</sup>-activated K<sup>+</sup> channels for lysophosphatidic acid-induced microglial migration. *Eur J Neurosci* 19: 1469–1474, 2004.
253. Schledermann W, Wulfen I, Schwarz JR, Bauer CK. Modulation of rat *erg1*, *erg2*, *erg3* and HERG K<sup>+</sup> currents by thyrotropin-releasing hormone in anterior pituitary cells via the native signal cascade. *J Physiol* 532: 143–163, 2001.
254. Schmidt D, Jiang QX, MacKinnon R. Phospholipids and the origin of cationic gating charges in voltage sensors. *Nature* 444: 775–779, 2006.
255. Schmidt D, MacKinnon R. Voltage-dependent K<sup>+</sup> channel gating and voltage sensor toxin sensitivity depend on the mechanical state of the lipid membrane. *Proc Natl Acad Sci USA* 105: 19276–19281, 2008.
256. Schmitt N, Schwarz M, Peretz A, Abitbol I, Attali B, Pongs O. A recessive COOH-terminal Jervell and Lange-Nielsen mutation of the KCNQ1 channel impairs subunit assembly. *EMBO J* 19: 332–340, 2000.
257. Schroeder BC, Waldegger S, Fehr S, Bleich M, Warth R, Greger R, Jentsch TJ. A constitutively open potassium channel formed by KCNQ1 and KCNE3. *Nature* 403: 196–199, 2000.
258. Schulte U, Thumfart JO, Klocker N, Sailer CA, Bildl W, Biniossek M, Dehn D, Deller T, Eble S, Abbass K, Wangler T, Knaus HG, Fakler B. The epilepsy-linked Lgi1 protein assembles into presynaptic Kv1 channels and inhibits inactivation by Kv $\beta$ 1. *Neuron* 49: 697–706, 2006.
259. Schultz D, Litt M, Smith L, Thayer M, McCormack K. Localization of two potassium channel  $\beta$  subunit genes, *KCNA1B* and *KCNA2B*. *Genomics* 31: 389–391, 1996.
260. Schwarz JR, Eikhof G. Na currents and action potentials in rat myelinated nerve fibres at 20 and 37 degrees C. *Pflügers Arch* 409: 569–577, 1987.
261. Schwarz JR, Reid G, Bostock H. Action potentials and membrane currents in the human node of Ranvier. *Pflügers Arch* 430: 283–292, 1995.
262. Schwarz TL, Tempel BL, Papazian DM, Jan YN, Jan LY. Multiple potassium-channel components are produced by alternative splicing at the *Shaker* locus in *Drosophila*. *Nature* 331: 137–142, 1988.
263. Schwenk J, Zolles G, Kandias NG, Neubauer I, Kalbacher H, Covarrubias M, Fakler B, Bentrop D. NMR analysis of KChIP4a reveals structural basis for control of surface expression of Kv4 channel complexes. *J Biol Chem* 283: 18937–18946, 2008.
264. Scott VE, Parcej DN, Keen JN, Findlay JB, Dolly JO.  $\alpha$ -Dendrotoxin acceptor from bovine brain is a K<sup>+</sup> channel protein. Evidence from the NH<sub>2</sub>-terminal sequence of its larger subunit. *J Biol Chem* 265: 20094–20097, 1990.
265. Scott VE, Rettig J, Parcej DN, Keen JN, Findlay JB, Pongs O, Dolly JO. Primary structure of a  $\beta$  subunit of  $\alpha$ -dendrotoxin-sensitive K<sup>+</sup> channels from bovine brain. *Proc Natl Acad Sci USA* 91: 1637–1641, 1994.
266. Serodio P, Vega-Saenz de Miera E, Rudy B. Cloning of a novel component of A-type K<sup>+</sup> channels operating at subthreshold potentials with unique expression in heart and brain. *J Neurophysiol* 75: 2174–2179, 1996.
267. Sesti F, Abbott GW, Wei J, Murray KT, Saksena S, Schwartz PJ, Priori SG, Roden DM, George AL Jr, Goldstein SA. A common polymorphism associated with antibiotic-induced cardiac arrhythmia. *Proc Natl Acad Sci USA* 97: 10613–10618, 2000.
268. Sesti F, Goldstein SA. Single-channel characteristics of wild-type IKs channels and channels formed with two minK mutants that cause long QT syndrome. *J Gen Physiol* 112: 651–663, 1998.
269. Shamgar L, Haitin Y, Yishare I, Malka E, Schottelndreier H, Peretz A, Paas Y, Attali B. KCNE1 constrains the voltage sensor of Kv7.1 K<sup>+</sup> channels. *PLoS ONE* 3: e1943, 2008.
270. Shamgar L, Ma L, Schmitt N, Haitin Y, Peretz A, Wiener R, Hirsch J, Pongs O, Attali B. Calmodulin is essential for cardiac IKs channel gating and assembly: impaired function in long-QT mutations. *Circ Res* 98: 1055–1063, 2006.
271. Shamotienko OG, Parcej DN, Dolly JO. Subunit combinations defined for K<sup>+</sup> channel Kv1 subtypes in synaptic membranes from bovine brain. *Biochemistry* 36: 8195–8201, 1997.
272. Shi G, Nakahira K, Hammond S, Rhodes KJ, Schechter LE, Trimmer JS.  $\beta$  Subunits promote K<sup>+</sup> channel surface expression through effects early in biosynthesis. *Neuron* 16: 843–852, 1996.
273. Shibasaki T. Conductance and kinetics of delayed rectifier potassium channels in nodal cells of the rabbit heart. *J Physiol* 387: 227–250, 1987.
274. Shibata R, Misonou H, Campomanes CR, Anderson AE, Schrader LA, Doliveira LC, Carroll KI, Sweatt JD, Rhodes KJ, Trimmer JS. A fundamental role for KChIPs in determining the molecular properties and trafficking of Kv4.2 potassium channels. *J Biol Chem* 278: 36445–36454, 2003.
275. Soh H, Goldstein SA. I SA channel complexes include four subunits each of DPP6 and Kv4.2. *J Biol Chem* 283: 15072–15077, 2008.
276. Sokolova O, Accardi A, Gutierrez D, Lau A, Rigney M, Grigorieff N. Conformational changes in the C terminus of *Shaker* K<sup>+</sup> channel bound to the rat Kv $\beta$ 2-subunit. *Proc Natl Acad Sci USA* 100: 12607–12612, 2003.
277. Sokolova O, Kolmakova-Partensky L, Grigorieff N. Three-dimensional structure of a voltage-gated potassium channel at 2.5 nm resolution. *Structure* 9: 215–220, 2001.
278. Sole L, Roura-Ferrer M, Perez-Verdaguer M, Oliveras A, Calvo M, Fernandez-Fernandez JM, Felipe A. KCNE4 suppresses Kv1.3 currents by modulating trafficking, surface expression and channel gating. *J Cell Sci* 122: 3738–3748, 2009.
279. Splawski I, Tristani-Firouzi M, Lehmann MH, Sanguinetti MC, Keating MT. Mutations in the hminK gene cause long QT syndrome and suppress IKs function. *Nat Genet* 17: 338–340, 1997.
280. Spreafico F, Barski JJ, Farina C, Meyer M. Mouse DREAM/calnexin/KChIP3: gene structure, coding potential, and expression. *Mol Cell Neurosci* 17: 1–16, 2001.
281. Strop P, Bankovich AJ, Hansen KC, Garcia KC, Brunger AT. Structure of a human A-type potassium channel interacting protein

- DPPX, a member of the dipeptidyl aminopeptidase family. *J Mol Biol* 343: 1055–1065, 2004.
282. **Swartz KJ.** Sensing voltage across lipid membranes. *Nature* 456: 891–897, 2008.
  283. **Swartz KJ.** Towards a structural view of gating in potassium channels. *Nat Rev Neurosci* 5: 905–916, 2004.
  284. **Takahashi Y.** The 14–3–3 proteins: gene, gene expression, and function. *Neurochem Res* 28: 1265–1273, 2003.
  285. **Takimoto K, Hayashi Y, Ren X, Yoshimura N.** Species and tissue differences in the expression of DPPY splicing variants. *Biochem Biophys Res Commun* 348: 1094–1100, 2006.
  286. **Takimoto K, Yang EK, Conforti L.** Palmitoylation of KChIP splicing variants is required for efficient cell surface expression of Kv4.3 channels. *J Biol Chem* 277: 26904–26911, 2002.
  287. **Takumi T, Ohkubo H, Nakanishi S.** Cloning of a membrane protein that induces a slow voltage-gated potassium current. *Science* 242: 1042–1045, 1988.
  288. **Tanaka Y, Meera P, Song M, Knaus HG, Toro L.** Molecular constituents of maxi KCa channels in human coronary smooth muscle: predominant  $\alpha + \beta$  subunit complexes. *J Physiol* 502: 545–557, 1997.
  289. **Tapper AR, George AL Jr.** MinK subdomains that mediate modulation of and association with KvLQT1. *J Gen Physiol* 116: 379–390, 2000.
  290. **Temple J, Frias P, Rottman J, Yang T, Wu Y, Verheijck EE, Zhang W, Siprachanh C, Kanki H, Atkinson JB, King P, Anderson ME, Kupersmidt S, Roden DM.** Atrial fibrillation in KCNE1-null mice. *Circ Res* 97: 62–69, 2005.
  291. **Teng S, Ma L, Zhen Y, Lin C, Bahringer R, Vardanyan V, Pongs O, Hui R.** Novel gene hKCNE4 slows the activation of the KCNQ1 channel. *Biochem Biophys Res Commun* 303: 808–813, 2003.
  292. **Teutsch C, Kondo RP, Dederko DA, Chrast J, Chien KR, Giles WR.** Spatial distributions of Kv4 channels and KChIP2 isoforms in the murine heart based on laser capture microdissection. *Cardiovasc Res* 73: 739–749, 2007.
  293. **Thomas D, Zhang W, Karle CA, Kathofer S, Schols W, Kubler W, Kiehn J.** Deletion of protein kinase A phosphorylation sites in the HERG potassium channel inhibits activation shift by protein kinase A. *J Biol Chem* 274: 27457–27462, 1999.
  294. **Thomas G, Killeen MJ, Gurung IS, Hakim P, Balasubramanian R, Goddard CA, Grace AA, Huang CL.** Mechanisms of ventricular arrhythmogenesis in mice following targeted disruption of KCNE1 modelling long QT syndrome 5. *J Physiol* 578: 99–114, 2007.
  295. **Thomsen MB, Sosunov EA, Anyukhovsky EP, Ozgen N, Boyden PA, Rosen MR.** Deleting the accessory subunit KChIP2 results in loss of  $I_{(to,f)}$  and increased  $I_{(K,slow)}$  that maintains normal action potential configuration. *Heart Rhythm* 6: 370–377, 2009.
  296. **Thomsen MB, Wang C, Ozgen N, Wang HG, Rosen MR, Pitt GS.** Accessory subunit KChIP2 modulates the cardiac L-type calcium current. *Circ Res* 104: 1382–1389, 2009.
  297. **Thurm H, Fakler B, Oliver D.**  $Ca^{2+}$ -independent activation of BKCa channels at negative potentials in mammalian inner hair cells. *J Physiol* 569: 137–151, 2005.
  298. **Tinel N, Diochot S, Borsotto M, Lazdunski M, Barhanin J.** KCNE2 confers background current characteristics to the cardiac KCNQ1 potassium channel. *EMBO J* 19: 6326–6330, 2000.
  299. **Tinel N, Diochot S, Lauritzen I, Barhanin J, Lazdunski M, Borsotto M.** M-type KCNQ2-KCNQ3 potassium channels are modulated by the KCNE2 subunit. *FEBS Lett* 480: 137–141, 2000.
  300. **Tipparaju SM, Liu SQ, Barski OA, Bhatnagar A.** NADPH binding to  $\beta$ -subunit regulates inactivation of voltage-gated  $K^+$  channels. *Biochem Biophys Res Commun* 359: 269–276, 2007.
  301. **Tipparaju SM, Saxena N, Liu SQ, Kumar R, Bhatnagar A.** Differential regulation of voltage-gated  $K^+$  channels by oxidized and reduced pyridine nucleotide coenzymes. *Am J Physiol Cell Physiol* 288: C366–C376, 2005.
  302. **Torres YP, Morera FJ, Carvacho I, Latorre R.** A marriage of convenience:  $\beta$ -subunits and voltage-dependent  $K^+$  channels. *J Biol Chem* 282: 24485–24489, 2007.
  303. **Tristani-Firouzi M, Sanguinetti MC.** Voltage-dependent inactivation of the human  $K^+$  channel KvLQT1 is eliminated by association with minimal  $K^+$  channel (minK) subunits. *J Physiol* 510: 37–45, 1998.
  304. **Trudeau MC, Warmke JW, Ganetzky B, Robertson GA.** HERG, a human inward rectifier in the voltage-gated potassium channel family. *Science* 269: 92–95, 1995.
  305. **Uebele VN, England SK, Gallagher DJ, Snyders DJ, Bennett PB, Tamkun MM.** Distinct domains of the voltage-gated  $K^+$  channel Kv $\beta$ 1.3  $\beta$ -subunit affect voltage-dependent gating. *Am J Physiol Cell Physiol* 274: C1485–C1495, 1998.
  306. **Uebele VN, Lagrutta A, Wade T, Figueroa DJ, Liu Y, McKenna E, Austin CP, Bennett PB, Swanson R.** Cloning and functional expression of two families of  $\beta$ -subunits of the large conductance calcium-activated  $K^+$  channel. *J Biol Chem* 275: 23211–23218, 2000.
  307. **Um SY, McDonald TV.** Differential association between HERG and KCNE1 or KCNE2. *PLoS ONE* 2: e933, 2007.
  308. **Valverde MA, Rojas P, Amigo J, Cosmelli D, Orio P, Bahamonde MI, Mann GE, Vergara C, Latorre R.** Acute activation of Maxi-K channels (hSlo) by estradiol binding to the  $\beta$  subunit. *Science* 285: 1929–1931, 1999.
  309. **Van Es MA, van Vught PW, Blauw HM, Franke L, Saris CG, Van den Bosch L, de Jong SW, de Jong V, Baas F, van't Slot R, Lemmens R, Schelhaas HJ, Birve A, Slegers K, Van Broeckhoven C, Schymick JC, Traynor BJ, Wokke JH, Wijmenga C, Robberecht W, Andersen PM, Veldink JH, Ophoff RA, van den Berg LH.** Genetic variation in DPP6 is associated with susceptibility to amyotrophic lateral sclerosis. *Nat Genet* 40: 29–31, 2008.
  310. **Van Huizen R, Czajkowsky DM, Shi D, Shao Z, Li M.** Images of oligomeric Kv $\beta$ 2, a modulatory subunit of potassium channels. *FEBS Lett* 457: 107–111, 1999.
  311. **Veh RW, Lichtinghagen R, Sewing S, Wunder F, Grumbach IM, Pongs O.** Immunohistochemical localization of five members of the Kv1 channel subunits: contrasting subcellular locations and neuron-specific co-localizations in rat brain. *Eur J Neurosci* 7: 2189–2205, 1995.
  312. **Venn N, Haynes LP, Burgoyne RD.** Specific effects of KChIP3/calsenilin/DREAM, but not KChIPs 1, 2 and 4, on calcium signalling and regulated secretion in PC12 cells. *Biochem J* 413: 71–80, 2008.
  313. **Vergara C, Latorre R, Marrion NV, Adelman JP.** Calcium-activated potassium channels. *Curr Opin Neurobiol* 8: 321–329, 1998.
  314. **Vetter DE, Mann JR, Wangemann P, Liu J, McLaughlin KJ, Lesage F, Marcus DC, Lazdunski M, Heinemann SF, Barhanin J.** Inner ear defects induced by null mutation of the *isk* gene. *Neuron* 17: 1251–1264, 1996.
  315. **Wallner M, Meera P, Ottolia M, Kaczorowski GJ, Latorre R, Garcia ML, Stefani E, Toro L.** Characterization of and modulation by a  $\beta$ -subunit of a human maxi KCa channel cloned from myometrium. *Receptors Channels* 3: 185–199, 1995.
  316. **Wallner M, Meera P, Toro L.** Determinant for  $\beta$ -subunit regulation in high-conductance voltage-activated and  $Ca^{2+}$ -sensitive  $K^+$  channels: an additional transmembrane region at the N terminus. *Proc Natl Acad Sci USA* 93: 14922–14927, 1996.
  317. **Wallner M, Meera P, Toro L.** Molecular basis of fast inactivation in voltage and  $Ca^{2+}$ -activated  $K^+$  channels: a transmembrane  $\beta$ -subunit homolog. *Proc Natl Acad Sci USA* 96: 4137–4142, 1999.
  318. **Wang FC, Bell N, Reid P, Smith LA, McIntosh P, Robertson B, Dolly JO.** Identification of residues in dendrotoxin K responsible for its discrimination between neuronal  $K^+$  channels containing Kv1.1 and 1.2  $\alpha$  subunits. *Eur J Biochem* 263: 222–229, 1999.
  319. **Wang H, Yan Y, Liu Q, Huang Y, Shen Y, Chen L, Chen Y, Yang Q, Hao Q, Wang K, Chai J.** Structural basis for modulation of Kv4  $K^+$  channels by auxiliary KChIP subunits. *Nat Neurosci* 10: 32–39, 2007.
  320. **Wang HS, Brown BS, McKinnon D, Cohen IS.** Molecular basis for differential sensitivity of KCNQ and IKs channels to the cognitive enhancer XE991. *Mol Pharmacol* 57: 1218–1223, 2000.
  321. **Wang L, Takimoto K, Levitan ES.** Differential association of the auxiliary subunit Kv $\beta$ 2 with Kv1.4 and Kv4.3  $K^+$  channels. *FEBS Lett* 547: 162–164, 2003.
  322. **Wang YW, Ding JP, Xia XM, Lingle CJ.** Consequences of the stoichiometry of Slo1  $\alpha$  and auxiliary  $\beta$  subunits on functional properties of large-conductance  $Ca^{2+}$ -activated  $K^+$  channels. *J Neurosci* 22: 1550–1561, 2002.

323. Warth R, Barhanin J. The multifaceted phenotype of the knock-out mouse for the KCNE1 potassium channel gene. *Am J Physiol Regul Integr Comp Physiol* 282: R639–R648, 2002.
324. Weaver AK, Bomben VC, Sontheimer H. Expression and function of calcium-activated potassium channels in human glioma cells. *Glia* 54: 223–233, 2006.
325. Weerapura M, Nattel S, Chartier D, Caballero R, Hebert TE. A comparison of currents carried by HERG, with and without coexpression of MiRP1, the native rapid delayed rectifier current. Is MiRP1 the missing link? *J Physiol* 540: 15–27, 2002.
326. Weng J, Cao Y, Moss N, Zhou M. Modulation of voltage-dependent *Shaker* family potassium channels by an aldo-keto reductase. *J Biol Chem* 281: 15194–15200, 2006.
327. Werner ME, Knorn AM, Meredith AL, Aldrich RW, Nelson MT. Frequency encoding of cholinergic- and purinergic-mediated signaling to mouse urinary bladder smooth muscle: modulation by BK channels. *Am J Physiol Regul Integr Comp Physiol* 292: R616–R624, 2007.
328. Werner ME, Meredith AL, Aldrich RW, Nelson MT. Hypercontractility and impaired sildenafil relaxations in the BKCa channel deletion model of erectile dysfunction. *Am J Physiol Regul Integr Comp Physiol* 295: R181–R188, 2008.
329. Wible BA, Wang L, Kuryshv YA, Basu A, Haldar S, Brown AM. Increased K<sup>+</sup> efflux and apoptosis induced by the potassium channel modulatory protein KChAP/PIAS3 $\beta$  in prostate cancer cells. *J Biol Chem* 277: 17852–17862, 2002.
330. Wiener R, Haitin Y, Shamgar L, Fernandez-Alonso MC, Martos A, Chomsky-Hecht O, Rivas G, Attali B, Hirsch JA. The KCNQ1 (Kv7.1) COOH terminus, a multitiered scaffold for subunit assembly and protein interaction. *J Biol Chem* 283: 5815–5830, 2008.
331. Xia XM, Ding JP, Lingle CJ. Inactivation of BK channels by the NH<sub>2</sub> terminus of the  $\beta$ 2 auxiliary subunit: an essential role of a terminal peptide segment of three hydrophobic residues. *J Gen Physiol* 121: 125–148, 2003.
332. Xia XM, Ding JP, Lingle CJ. Molecular basis for the inactivation of Ca<sup>2+</sup>- and voltage-dependent BK channels in adrenal chromaffin cells and rat insulinoma tumor cells. *J Neurosci* 19: 5255–5264, 1999.
333. Xia XM, Ding JP, Zeng XH, Duan KL, Lingle CJ. Rectification and rapid activation at low Ca<sup>2+</sup> of Ca<sup>2+</sup>-activated, voltage-dependent BK currents: consequences of rapid inactivation by a novel  $\beta$  subunit. *J Neurosci* 20: 4890–4903, 2000.
334. Xiong H, Xia K, Li B, Zhao G, Zhang Z. KChIP1: a potential modulator to GABAergic system. *Acta Biochim Biophys Sin* 41: 295–300, 2009.
335. Xu X, Jiang M, Hsu KL, Zhang M, Tseng GN. KCNQ1 and KCNE1 in the IKs channel complex make state-dependent contacts in their extracellular domains. *J Gen Physiol* 131: 589–603, 2008.
336. Xu Y, Ramu Y, Lu Z. Removal of phospho-head groups of membrane lipids immobilizes voltage sensors of K<sup>+</sup> channels. *Nature* 451: 826–829, 2008.
337. Yang EK, Alvira MR, Levitan ES, Takimoto K. Kv $\beta$  subunits increase expression of Kv4.3 channels by interacting with their C termini. *J Biol Chem* 276: 4839–4844, 2001.
338. Yang H, Zhang G, Shi J, Lee U, Delaloye K, Cui J. Subunit-specific effect of the voltage sensor domain on Ca<sup>2+</sup> sensitivity of BK channels. *Biophys J* 94: 4678–4687, 2008.
339. Yang T, Kupersmidt S, Roden DM. Anti-minK antisense decreases the amplitude of the rapidly activating cardiac delayed rectifier K<sup>+</sup> current. *Circ Res* 77: 1246–1253, 1995.
340. Yang Y, Sigworth FJ. Single-channel properties of IKs potassium channels. *J Gen Physiol* 112: 665–678, 1998.
341. Yang Y, Xia M, Jin Q, Bendahhou S, Shi J, Chen Y, Liang B, Lin J, Liu Y, Liu B, Zhou Q, Zhang D, Wang R, Ma N, Su X, Niu K, Pei Y, Xu W, Chen Z, Wan H, Cui J, Barhanin J. Identification of a KCNE2 gain-of-function mutation in patients with familial atrial fibrillation. *Am J Hum Genet* 75: 899–905, 2004.
342. Yellen G. The voltage-gated potassium channels and their relatives. *Nature* 419: 35–42, 2002.
343. Yu H, Wu J, Potapova I, Wymore RT, Holmes B, Zuckerman J, Pan Z, Wang H, Shi W, Robinson RB, El-Maghrabi MR, Benjamin W, Dixon J, McKinnon D, Cohen IS, Wymore R. MinK-related peptide 1: a  $\beta$  subunit for the HCN ion channel subunit family enhances expression and speeds activation. *Circ Res* 88: E84–87, 2001.
344. Yusifov T, Savalli N, Gandhi CS, Ottolia M, Olcese R. The RCK2 domain of the human BKCa channel is a calcium sensor. *Proc Natl Acad Sci USA* 105: 376–381, 2008.
345. Zagha E, Lang EJ, Rudy B. Kv3.3 channels at the Purkinje cell soma are necessary for generation of the classical complex spike waveform. *J Neurosci* 28: 1291–1300, 2008.
346. Zagha E, Ozaita A, Chang SY, Nadal MS, Lin U, Saganich MJ, McCormack T, Akinsanya KO, Qi SY, Rudy B. DPP10 modulates Kv4-mediated A-type potassium channels. *J Biol Chem* 280: 18853–18861, 2005.
347. Zeng X, Xia XM, Lingle CJ. Species-specific differences among KCNMB3 BK  $\beta$ 3 auxiliary subunits: some  $\beta$ 3 NH<sub>2</sub>-terminal variants may be primate-specific subunits. *J Gen Physiol* 132: 115–129, 2008.
348. Zeng XH, Benzinger GR, Xia XM, Lingle CJ. BK channels with  $\beta$ 3a subunits generate use-dependent slow afterhyperpolarizing currents by an inactivation-coupled mechanism. *J Neurosci* 27: 4707–4715, 2007.
349. Zeng XH, Xia XM, Lingle CJ. Redox-sensitive extracellular gates formed by auxiliary  $\beta$  subunits of calcium-activated potassium channels. *Nat Struct Biol* 10: 448–454, 2003.
350. Zhang M, Jiang M, Tseng GN. minK-related peptide 1 associates with Kv4.2 and modulates its gating function: potential role as  $\beta$  subunit of cardiac transient outward channel? *Circ Res* 88: 1012–1019, 2001.
351. Zhou W, Qian Y, Kunjilwar K, Pfaffinger PJ, Choe S. Structural insights into the functional interaction of KChIP1 with Shal-type K<sup>+</sup> channels. *Neuron* 41: 573–586, 2004.